

**FIRE RESISTANCE ANALYSIS OF BEAMS IN
MULTI-STOREY REINFORCED CONCRETE
INSTITUTIONAL BUILDING**

LOH CIAO XIN

UNIVERSITI TUNKU ABDUL RAHMAN

**FIRE RESISTANCE ANALYSIS OF BEAMS IN MULTI-STOREY
REINFORCED CONCRETE INSTITUTIONAL BUILDING**

LOH CIAO XIN

**A project report submitted in partial fulfillment of the requirements for the
award of Bachelor of Engineering (Hons.) Environmental Engineering**

**Faculty of Engineering and Green Technology
Universiti Tunku Abdul Rahman**

APRIL 2018

DECLARATION

I hereby declare that this project is based on my original work except for citations and quotations which have been duly acknowledged. I also declare that it had not been previously and concurrently submitted for any other degree or award at UTAR or other institutions.

Signature : _____

Name : _____

ID No. : _____

Date : _____

APPROVAL OF SUBMISSION

I certify that this project report entitled “**FIRE RESISTANCE ANALYSIS OF BEAMS IN MULTI-STOREY REINFORCED CONCRETE INSTITUTIONAL BUILDING**” was prepared by **LOH CIAO XIN** has met the required standard for submission in partial fulfillment of the requirements for the award of Bachelor of Engineering (Hons.) Environmental Engineering at Universiti Tunku Abdul Rahman.

Approved by,

Signature : _____

Supervisor : Dr. Zafarullah Nizamani

Date : _____

The copyright of this report belongs to the author under the terms of the copyright Act 1987 as qualified by Intellectual Property Policy of Universiti Tunku Abdul Rahman. Due acknowledgement shall always be made of the use of any material contained in, or derived from, this report.

© 2019, Loh Ciao Xin. All rights reserved.

ACKNOWLEDGEMENTS

I am grateful to the God for the good health and wellbeing that were necessary to complete this book.

I wish express my gratitude to my research supervisor, Dr. Zafarullah Nizamani for his patient guidance, enthusiastic encouragement and useful critiques of this research work. I am also grateful to everyone for their contribution to the successful completion of this project.

Finally, I wish to thank my loveliest parents for their financially and mentally supports and encouragement throughout the completion of this paper.

FIRE RESISTANCE ANALYSIS OF BEAMS IN MULTI-STOREY REINFORCED CONCRETE INSTITUTIONAL BUILDING

ABSTRACT

Fire analysis is currently incorporated into building modelling practice to evaluate the performance of a high-rise building against fire. Before that, most of the buildings did not incorporate these practices into account as they think that fire accident will never be happened on them as the probability of fire accident to take place is too low. However, they have started to focus in this topic since the incident 911 had occurred. Following by that, the researchers pointed out that there is a must to incorporate fire practices into the construction of buildings. Thus, this study is carried out to evaluate the effect of fire on beams of fire room during different fire duration. The model designed is a 4 stories tall institutional building in UTAR Kampar, Perak. Throughout this study, Eurocode is followed in the structural and fire design of building and suggested a target reliability index, β_{target} of 3.8 as a guidelines of structural safety for 50 years design period. Two methods of structure reliability analysis methods are proposed to evaluate the reliability index of structure under fire.

TABLE OF CONTENTS

DECLARATION	ii
APPROVAL FOR SUBMISSION	iii
ACKNOWLEDGEMENTS	v
ABSTRACT	vi
TABLE OF CONTENTS	vii
LIST OF TABLES	xi
LIST OF FIGURES	xiii
LIST OF SYMBOLS	xvi
LIST OF ABBREVIATIONS	xvii
LIST OF APPENDICE	xviii

CHAPTER

1	INTRODUCTION	
	1.1 Overview	1
	1.2 Background	2

1.3 Problem Statement	4
1.4 Aims and Objectives	8
1.5 Analysis if Structure	9
1.6 Reliability of Structure	9
1.7 Scope of Work	10
1.8 Outline of Thesis	11

2 LITERRATURE REVIEW

2.1 Introduction	12
2.1.2 Fire Active Measures	13
2.3 Design Code	16
2.3.1 EN 1990	16
2.3.2 EN 1992-1-2	16
2.3.3 ISO 834	17
2.4 Uncertain Parameters in Fire Design	19
2.4.1 Concrete compressive strength, f_{ck}	19
2.4.2 Reinforcement yield strength, f_{yk}	21
2.4.3 Concrete cover, c	23
2.4.4 Model Uncertainty, K	28
2.4.5 Load Uncertainty	29
2.5 Bending Moment Resistance	32

2.5.1 Eurocode	32
2.5.2 ACI Code	33
2.6 Limit State Equation	35
2.7 Methods of Reliability	37
2.7.1 Monte Carlo Simulation	37
2.7.2 First-Order Reliability Method (FORM)	39
2.7.3 Second-Order Reliability Method (SORM)	40
2.8 Reliability Index or Probability Failure	41
 3 METHODOLOGY	
3.1 Structural Model	44
3.1.1 Buildings Layout	44
3.1.2 On-site Measurements	47
3.2 ETABS 2016 Modeling	49
3.3 Fire Resistance Analysis Process	57
3.3.1 Limit State Equation	61
3.3.2 Uncertainties in Limit State Equation	62
3.3.3 Reliability index manual calculation	68
3.3.4 Reliability index Matlab calculation	69

4	RESULTS AND DISCUSSIONS	
4.0	Fire Resistance Analysis	70
4.1	Design Fire	69
4.1.1	Eurocode Parametric Fire	69
4.1.2	Opening Factor	71
4.2	Fire & Material Temperature Analysis	73
4.2.1	Fire Load in Compartments	73
4.2.2	Maximum Compartment Temperature	76
4.2.3	Realistic Temperature-Time Curve	79
4.2.4	Concrete and Steel Temperature Increases	83
4.2.5	Cross Section Reduction/ Spalling	86
4.3	Structural Behavior Analysis	88
4.3.1	Fire Severity	91
4.3.2	Fire Resistance	94
4.4	Reliability Analysis	105
4.4.1	FORM	110
4.4.2	FOSM	115

5	CONCLUSION	
	5.1 Conclusion	119
	APPENDICES	121
	REFERENCES	146

LIST OF TABLES

TABLES	TITLE	PAGE
1.1	Malaysia fire loss variation over 10 years.	7
2.1	Differences between localized and fully developed fire.	13
2.2	Fire temperature, T at ISO 834 fire duration, R.	18
2.3	Reinforcement yield strength reduction factor, $k_{fy,T}$ at elevated temperature, T.	23
2.4	Summary on results in Test 1 and Test 2.	26
2.5	Probabilistic Model of Load parameters.	32
2.6	Probabilistic Model of Resistance Parameters.	34
2.7	Limit state equations by other publications.	38
3.1	Dimension of beams and columns.	48
3.2	Block e building materials properties.	50
3.3	Variable loads Defined in ETABS 2016.	52
3.4	Characteristics of 4 fire compartments subjected to fire.	54
3.5	Limit state load combination equation at fire situation by different codes.	60

3.6	Input data of beam width, b and depth, d in EasyFit.	64
3.7	Results of beam width, b and beam depth, d of four beams type from EasyFit.	67
3.8	Probabilistic model of load and resistance uncertain parameters.	67
4.1	Thermal properties of room boundary material.	72
4.2	Opening factor of four fire rooms.	74
4.3	Total mass of fuel presence in different fire compartment.	76
4.4	Total fire load in different fire compartment.	77
4.5	Fire load, Q_{fi} and time to reach maximum fire temperature, t_{max} in fire rooms.	79
4.6	Temperature time relation at different fire room.	81
4.7	Temperature of Eurocode parametric fire and ISO 834 fire at different fire duration.	84
4.8	Concrete and steel reinforcement temperature and strength during 4 hours fire.	87
4.9	The reduced cross section of beams after spalling.	90
4.10	Design moment, M_D at ambient condition and at fire.	92
4.11	Area of compression and tension steel reinforcement in different beam type.	96
4.12	Moment of resistance, M_R at ambient condition and at fire.	98
4.13	Moment resistance at maximum fire temperature, $M_{R,fi}$ at different fire duration.	103

4.14	Comparison of moment resistance at fire, $M_{R,fi}$ with the design moment at fire, $M_{D, fi}$.	104
4.15	Reliability index, β of beams using FORM method.	112
4.16	Reliability index, β of beams using FOSM method.	116

LIST OF FIGURES

FIGURES	TITLE	PAGE
1.1	Fire triangle for fire to take place.	2
1.2	Number of fire calls in different types of fire.	3
1.3	Fire cases of institute in 2014.	3
1.4	Statistics of fire occurrence in different types of premise.	6
1.5	Source of fire ignition in different types of premise.	6
1.6	Linear regression analysis of fire loss percentage from year 1994 to 2003.	8
2.1	Distance between UTAR FEGT Block E to the Kampar Fire and escue Station.	15
2.2	Timeline of fire event from the fire ignition to the fire suppression.	15
2.3	Stress-strain relationship of concrete under fire.	17

2.4	The ISO 834 standard temperature-time curve.	19
2.5	Concrete compressive strength reduction factor at T °C, $k_{fck,T}$ decrease with elevated temperature, T .	20
2.6	Concrete compressive strength, f_c at elevated temperature, T .	21
2.7	Reinforcement yield strength reduction factor, $k_{fy,T}$ at elevated temperature, T of Class N steel.	22
2.8	Cross section of slab and reinforcement steel bar.	24
2.9	Cross section of beam.	25
2.10	Temperature at different part of beam varies with fire exposure time.	25
2.11	The reliability vs. concrete cover relationship of Test 1.	27
2.12	The reliability vs. concrete cover relationship of Test 2.	28
2.13	Relationship of bending moment resistance, $M_{R,fi,t}$ and concrete cover, c	28
2.14	Histogram of fire spread against the number of occurrence.	40
2.15	Failure probability using FORM.	41
2.16	Characteristic of a system performance function, G .	43
3.1	AutoCAD drawing of Block E ground floor.	45
3.2	AutoCAD drawing of Block E first floor.	45
3.3	AutoCAD drawing of Block E second floor.	46
3.4	The area of study in Block E.	46

3.5	A laser range meter is used to measure the dimension of structure.	47
3.6	Shape definition of frame section.	51
3.7	Material and dimension definition of frame section.	51
3.8	Side section view of building in ETABS 2016.	52
3.9	Elevation section view of building first floor in ETABS 2016.	53
3.10	3-dimensional schematic drawing of building in ETABS 2016.	53
3.11	Beams location in computer room.	55
3.12	Beams location in office.	55
3.13	Beams location in laboratory.	56
3.14	Beams location in classroom.	56
3.15	Flowchart of methodology for fire assessment of structural element's load bearing capacity.	57
3.16	The value for combination factor for variable loads, Ψ_1 .	59
3.17	Permanent action and variable action in design accidental situation.	59
3.18	Thermal properties of building materials.	61
3.19	Fitting analysis result Beam 1 width, b.	64
3.20	Graph of probability density function of Beam 1 width, b.	65
3.21	Fitting analysis result Beam 1 depth, d.	65

3.22	Graph of probability density function of Beam 1 depth, d. Steps for the analysis of building's fire resistance.	66
4.1	Steps for the analysis of building's fire resistance.	70
4.2	AutoCad drawing of multiple vertical openings presence in fire room for opening factor calculation.	73
4.3	Temperature-time curve of different opening factor of fire room.	84
4.4	The reduced cross section of beam after spalling.	89
4.5	Fire exposure on three sides of the beam.	89
4.6	Design moment, M_D of classroom beam 3 at ambient.	93
4.7	Design moment, M_D of classroom beam 3 at fire.	93
4.8	Section, stress and strain block diagram of a doubly reinforced beam.	95
4.9	Table of reinforcement areas and perimeters.	95
4.10	Moment resistance at fire, $M_{R,fi}$ of beams during different fire duration, R in classroom.	100
4.11	Moment resistance at fire, $M_{R,fi}$ of beams during different fire duration, R in office.	100
4.12	Moment resistance at fire, $M_{R,fi}$ of beams during different fire duration, R in laboratory.	100
4.13	Moment resistance at fire, $M_{R,fi}$ of beams during different fire duration, R in computer room.	101
4.14	Fire temperature, T (°C) reached by fire rooms in 4 hours	106

	fire duration.	
4.15	Moment Resistance at fire, $M_{Rd,fi}$ in classroom.	108
4.16	Moment Resistance at fire, $M_{Rd,fi}$ in office.	108
4.17	Moment Resistance at fire, $M_{Rd,fi}$ in laboratory.	109
4.18	Moment Resistance at fire, $M_{Rd,fi}$ in computer room.	109
4.19	Reliability index, β of beams in classroom using FORM methods.	113
4.20	Reliability index, β of beams in office using FORM methods.	113
4.21	Reliability index, β of beams in laboratory using FORM methods.	114
4.22	Reliability index, β of beams in computer room using FORM methods.	114
4.23	Reliability index, β of beams in classroom using FOSM methods.	117
4.24	Reliability index, β of beams in office using FOSM methods.	117
4.25	Reliability index, β of beams in laboratory using FOSM methods.	118
4.26	Reliability index, β of beams in computer room using FOSM methods.	118

LIST OF ABBREVIATIONS

Symbol	Description
a	Distance from the center of main steel reinforcement to the nearest concrete surface
a_b	Bottom reinforcement axis distance from slab surface
a_t	Top reinforcement axis distance from slab surface
A_s	Area of compression reinforcement
A_s'	Area of tension reinforcement
A_{sb}	Bottom Reinforcement area
A_{st}	Top Reinforcement area
A_t	Total enclosure area
A_v	Total area of vertical opening
b	Beam width
b_{fi}	New beam width after fire
b	Thermal inertia
c	Concrete cover
d	Beam depth
d_{fi}	New beam depth after fire

d'	Beam effective depth
e_f	Fire load density
E	Energy contained value
E_c	Concrete modulus of elasticity at 20 °C
$f_{c,20}^{\circ C}$	Concrete compressive strength at 20 °C
$f_{y,20}^{\circ C}$	Reinforcement yield strength at 20 °C
F_{cc}	Concrete compressive force
F_{st}	Reinforcement tensile force
$G(X)$	Limit state function as a function of random vector
g	Uniformly distributed permanent load
h	Slab thickness
H_v	Average height of vertical opening
i_{500}	Depth of the 500 °C isotherm
$k_{fc(t)}$	Concrete compressive strength reduction factor at t °C
$k_{fy(t)}$	Reinforcement yield strength reduction factor at t °C
K	Model uncertainty
K_E	Model uncertainty for load
K_R	Model uncertainty for resistance
K_T	Total model uncertainty
l	Slab free span

$L(X)$	Load effect
M	Weight combustible material
M_{Ed}	Design moment induced by design load
M_{Gk}	Bending moment induced by permanent load.
M_n	Nominal moment of resistance
M_{Qk}	Bending moment induced by imposed load.
M_D	Design moment
$M_{D,fi}$	Design moment during fire
M_{Ed}	Design Load
$M_{E,fi}$	Design load during fire
$M_{R,ambient}$	Moment resistance at ambient
M_{Rd}	Design moment of resistance
$M_{R,fi}$	Moment resistance during fire/ Moment capacity
O	Opening factor
q	Uniformly distributed imposed load
Q_f	Fire load
Q_k	Characteristic value of a single variable action
R	Fire duration
R^2	Coefficient of determination
$R(X)$	Resistance effect

s	Reinforcement axis spacing
t	Time of fire exposure
t_{\max}	Time to reach the maximum fire temperature
t^*	Fictitious time
t^*_{\max}	Maximum fictitious time
T_{decay}	Fire temperature at decay phase
T_g	Fire temperature
T_{\max}	Fire temperature at maximum temperature
T_c	Temperature of concrete
T_s	Temperature of steel reinforcement
Z	Distance from the centroid of F_{cc} to F_{st}
Z_l	Distance from the centroid of F_{sc} to F_{st}
ACI	American Concrete Institute
BOMBA	Malaysia Department of Fire and Rescue
C50	Concrete class grade 50
EC 0	Eurocode 0
EC 1	Eurocode 1
EC 2	Eurocode 2
HSC	High strength concrete
ISO	International Organization for Standardization
FORM	First Order Reliability Method

FOSM	First Order Secondary Method
SORM	Second Order Reliability Method

LIST OF ABBREVIATIONS

β	Reliability index
β_{target}	Target reliability index
μ	Mean
μ_{K_T}	Mean value of total model uncertainty
μ_{K_R}	Mean value of model uncertainty for resistance
μ_{K_E}	Mean value of model uncertainty for load
μ_{K_M}	Mean value of additional model uncertainty
σ	Standard deviation
σ^2	variance
$(\sigma_{K_T})^2$	Variance of total model uncertainty
$(\sigma_{K_R})^2$	Variance of model uncertainty for resistance
$(\sigma_{K_E})^2$	Variance of model uncertainty for load

$(\sigma_{\mathbf{K}_M})^2$	Variance of additional model uncertainty
Ψ_0	Factor for combination value of a variable action
Ψ_1	Factor for frequent value of a variable action
Ψ_2	Factor for quasi-permanent value of a variable action
γ_G	Partial factor for permanent actions
γ_Q	Partial factor for imposed actions
ξ	Reduction factor
Φ	Main reinforcement steel bar diameter
c_p	Heat capacity
ρ	Density
λ	Thermal conductivity
Γ	Γ factor
ΔH_c	Calorific value

LIST OF APPENDICES

A (i)	Location of classroom in AutoCad drawing.
A (ii)	Location of office in AutoCad drawing.
A (iii)	Location of laboratory in AutoCad drawing.
A (iv)	Location of computer room in AutoCad drawing.
B	On-site pictures of fire rooms with types of fuel load available.
C	Calculation of time and fire temperature in classroom at heating phase and decay phase.
D	Example Calculation of concrete temperature, T_c and steel reinforcement temperature, T_s in Classroom at 4 hours fire duration.
E	Example Calculation of Moment Resistance, $M_{R,fi}$ at different fire duration of Beam No. 3 in Classroom.
F	Table of concrete compressive strength, f_{ck} and reinforcement yield strength, f_{yk} of different fire room at different fire duration, R.
G	Table of Concrete compressive strength, f_{ck} and reinforcement yield strength, f_{yk} of different fire room at different fire duration, R during continuous fire growth.
H	FORM reliability analysis in classroom beam no 1 at 1 hour fire duration.
I	FOSM reliability analysis in classroom beam no 1 at 1 hour fire duration.

CHAPTER 1

INTRODUCTION

1.1 Overview

In today's world of the twenty-first century, the demand of people towards a safe and healthy building to stay has increased. Due to the urbanization, the safety of the structure under fire has gained attention nowadays. Fire is one of the main consideration in structure among the load conditions because the damages caused by the fire is relatively high. Elements in structure can experience failure due to fire exposure. The risk of losses with respect to the economy and human safety should be reduced to a minimum. Different fire scenarios should be used to get the best condition for the design. A recent case of blaze in Grenfell Tower, London on 14th June 2017 had caused a total of 72 casualties which had aroused public concern as well as the significance of fire safety in the building structural design. In addition, in 2003 Hengyang City, China an eight stories building of reinforced concrete went through a huge fire which leads to the collapsed of the building. The data from test showed that the over 46% of the parts of building have experienced 1300 °C of high temperature. (Li et al., 2015) The building structure eventually collapsed due to the large fire load which weakened and subsequently damaged the major columns. Hence, the development of building structure should

follow the current standards and codes which relate to fire design for human safety and protection.

1.2 Background

Fire is a process of rapid oxidation of a substance with the presence of oxygen, heat and fuel. These three basic elements that must be present in order for fire combustion to take place, it was symbolized by the “fire triangle” showed in Figure 1.1. In Malaysia, the fire behavior of building material was evaluated by several testing methods indicated in British standard BS 476 in accordance to the laws and regulations in Uniform Building By-Law (UBBL), the result from the test will categorize the materials according to their respective level of resistance to fire. (Anon, 2018) According to the annual report of Malaysia Department of Fire and Rescue in 2014, there was a total of 54,540 fire calls obtained. Among the fire calls, the type of fire in a building and its property received the third highest cases of fire, 5,677 calls as showed in Figure 1.2. On the other hand, the type of building affected by fire was categorized according to the UBBL standard, among the categories of building fire, institute building had 182 fire cases out of total 2,712 cases in 2014. (Figure 1.3)

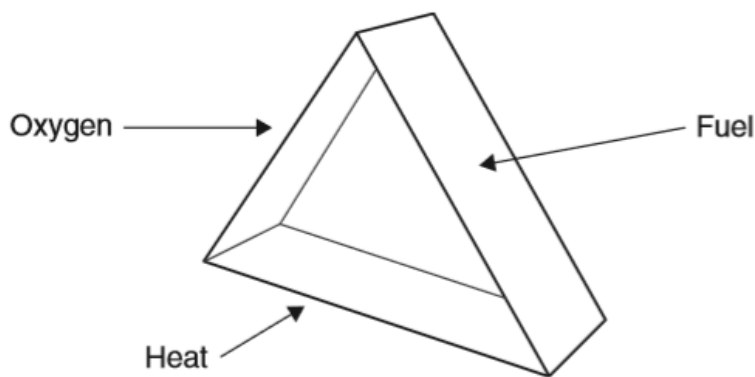


Figure 1.1: Fire triangle for a fire to take place. (Hasofer, A. M., 2012)

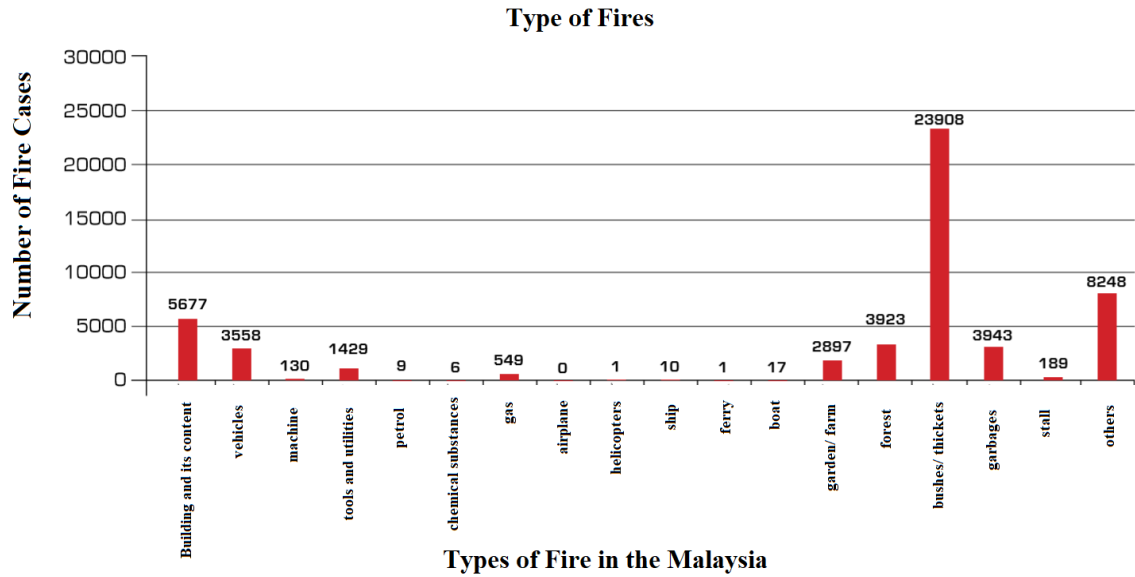


Figure 1.2: Number of fire calls in different types of fire. (Bomba, 2018)

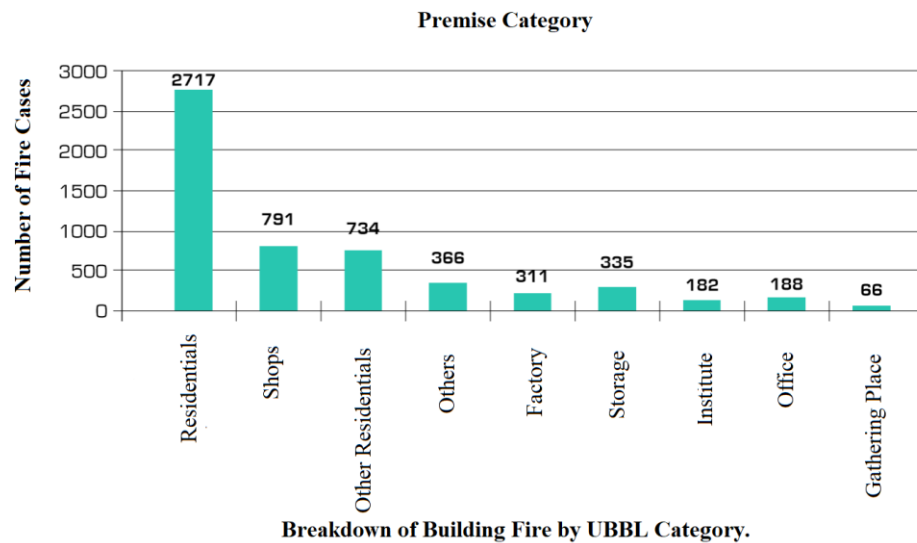


Figure 1.3: Fire cases of the institute in 2014. (Bomba, 2018)

1.3 Problem Statement

The past approach of structural fire design was focused solely on the prescriptive way of the adequate steel member insulation for fire resistance. This type of approach was unsuccessful in representing the actual performance of structure subject to fire given that the reliability of structure during the case of uncertainty was excluded. (Guo. Q. R., 2015) Information on the performance of building in term of fire safety was limited and hence the building performance-based reliability assessment need to be carried out. Fire safety in institutional or university is one of the main safety management to focus on in order to safeguard the risk of students and properties in university. Fire in a multi-story building like in the institutional building are more difficult to control due to a large number of students occupied the building and the occupied compartment are confined space. The occurrence of fire and human safety are subjected to wide varying of factors from chemical, building design, construction, safety codes, standards and design of safety and emergency equipment.

Factors such as the collapse of previous structure, loads complexity, competition, economic profit and society demand had led to the involvement of the reliability factor to be included in the design of buildings. Fire resistance analysis is carried out in order to predict the performance of building structure when subjects to sudden heating and cooling due to fire. A more systematic method on the structural fire design of safety and protection needs to be developed with a strong fundamental knowledge on the fire. The fire structural analysis is taken into consideration of various issues into account which includes the material characteristics, support condition, thermal condition and loading type. The results obtained from the analysis later adopted into the fire protection system of a building.

Fire consideration of most of the buildings is necessary to reduce the risk of fire damage to personnel, society and property as well as the environment. The construction products directive 89/106/EEC mentioned in EN 1992-1-2 state the limit of fire risks that cannot be valid during the design and construction phase of building. Among the limitations in fire risks are the structure should have high load bearing resistance, the generation and spread of fire should be controlled within the construction area without affecting the nearby area, the escaping time for the occupants should be sufficient and lastly the safety of fire brigade personnel should be put into consideration. In structural fire parts of the Eurocodes, the passive fire protection is discussed to ensure the load bearing resistance of structure and fire spread are within the safety limit. The design considerations of the structure adopted in the study are the characteristic of construction materials, the behavior of structures under fire as well as the general engineering structure rules. (ACI 216, 1994)

1.3.1 Malaysia Fire Loss Statistics

The occurrence of fires in Malaysia is due to many reasons such as natural, accidental, incendiary and undetermined provide by the statistics from the Fire and Rescue Department of Malaysia (BOMBA). The reasons for the occurrence of fire in Malaysia's higher education institution are mainly due to accidental and incendiary. Statistics of fire according to different types of premises in Figure 1.4 showed that an institution of higher education has a total of 25 fire cases in the Year 2004. Among the total 25 fire cases, accidental and incendiary have 24 and 1 fire cases in the year 2013 respectively. Furthermore, the main source of fire ignition which triggered the fires is from electrical such as arcs, resistance heating, overload, sparks or short circuit. Figure 1.4 showed the fire ignition from electrical problems accounted for 22 fire cases out of the total 25 fire cases and a percentage of 88%. The fire caused by electrical is mainly due to the faulty

in the electrical wiring system in higher education institutions whereby old wiring system that lack of regular maintenance can initiated short circuit easily. On the other hand, apart from the electricity problems, the fire ignited by lighter, growing fire and explosive have 12 % or 3 fire cases among the 25 total fire cases in higher education institutions.

Jenis Premis (Premises)	Semulajadi (Natural)	Kemalangan (Accidental)	Sengaja Dibakar (Incendiary)	Tidak Dapat Dipastikan (Undetermined)	Jumlah (Total)
Kediaman (Residential)	28	3,747	173	14	3,962
Pangsapuri/Kondominium/ (Condo)	2	554	34	0	590
Hotel (Hotel)	1	41	2	0	44
Asrama/Hostel (Boarding/Hostel)	2	50	7	0	59
Sekolah (School)	5	107	10	0	122
Institusi Pengajian Tinggi (Higher Education Institution)	0	24	1	0	25
Hospital (Hospital)	0	18	1	0	19
Klinik (Clinic)	0	23	2	0	25
Pejabat (Office)	3	280	14	0	297
Kedai (Shop)	1	665	65	4	735
Pusat Membeli Belah (Shopping Complex)	0	34	1	0	35
Dewan Perhimpunan (Place of Assembly)	3	35	1	0	39
Stor/Gudang (Store)	1	231	33	3	268
Kilang/Bengkel (Factory)	5	363	26	4	398
Stesen Minyak (Petrol Station)	0	15	0	0	15
Struktur Khas (Special Structure)	0	28	0	1	29
Lain-lain Bangunan (Others Building)	3	451	15	3	472
Jumlah (Total)	54	6,666	385	29	7,134

Figure 1.4: Statistics of fire occurrence in different types of the premise. (BOMBA Malaysia, 2014)

PREMIS Premises	Mancis / Lighter (SN)	Pelita / Lin / Door (SN2) Candle / Torch	Objek Permukaan Panas / Kimpalan (SN3) Hot Surface	Geseran / Hentaman (SN4) Friction	Tindokbalas Kmal (SN5) Chemical Reaction	Peralatan Gas (SN6) Gas Equipment	Arcs (SN7A)	Sparks / Short Circuit (SN7B)	Overcurrent / Overload (SN7C)	Resistance Heating (SN7D)	Air Berbaras (SN8) Glowing Fire	Bunga Api / Mercun (SN9) Fireworks	Kilat (SN10) Lightning	Kebakaran Spontan (SN11) Spontaneous Burning	Letupan (SN12) Explosive	Larian (SN13) Others	Tidak Dapat Dipastikan Undetermined	JUMLAH Total
Kediaman/ Residential	357	192	74	16	3	1,011	620	1,000	268	149	169	10	25	3	5	46	14	3,962
Pangsapuri / Kondominium Condo	52	27	12	8	0	209	83	94	5	52	38	4	2	0	1	3	0	590
Hotel/ Hotel	0	3	5	0	0	7	2	18	2	3	3	0	1	0	0	0	0	44
Asrama / Hostel Boarding/Hostel	10	0	0	0	0	9	3	15	10	5	4	0	2	0	0	1	0	59
Sekolah/ School	14	0	1	0	0	9	20	37	11	12	11	2	4	1	0	0	0	122
Institusi Pengajian Tinggi (Higher Education Institution)	1	0	0	0	0	0	7	11	3	1	1	0	0	0	1	0	0	25

Figure 1.5: Source of fire ignition in different types of the premise. (BOMBA Malaysia, 2014)

Table 1.1 represented the fire loss in Malaysia varies from the year 1994 to 2003. From the fire loss data in Malaysia over the 10 years, a linear regression analysis which suggested in Hasofer, A. M. study of the risk analysis in building fire safety engineering and a graph is plotted to represent the relationship between the fire loss data in Figure x. The percentage of fire loss is represented as y whereas year is represented as x. The constant c in equation x reflected the uncertainty in variable y. The trend of linear regression equation of variable y on variable x is expressed in Eq. (1.1).

$$y = m x + c \quad (1.1)$$

The coefficient of determination, R^2 from the linear regression analysis in Figure 1.6 is 0.4273. The $R^2 < 0$ indicated that the relationship between the fire loss data and the regression line are in good agreement. (Hasofer,A.M., 2012)

Table 1.1: Malaysia fire loss variation over 10 years. (BOMBA, 2014)

Year	1994	1995	1996	1997	1998	1999	2000	2001	2002	2003
Number of Fire cases	2491	2486	2186	2368	3011	2625	2737	2489	2887	3061
Percentage of Fire cases (%)	9.46	9.40	8.30	9.00	11.43	9.97	10.39	9.45	10.96	11.62

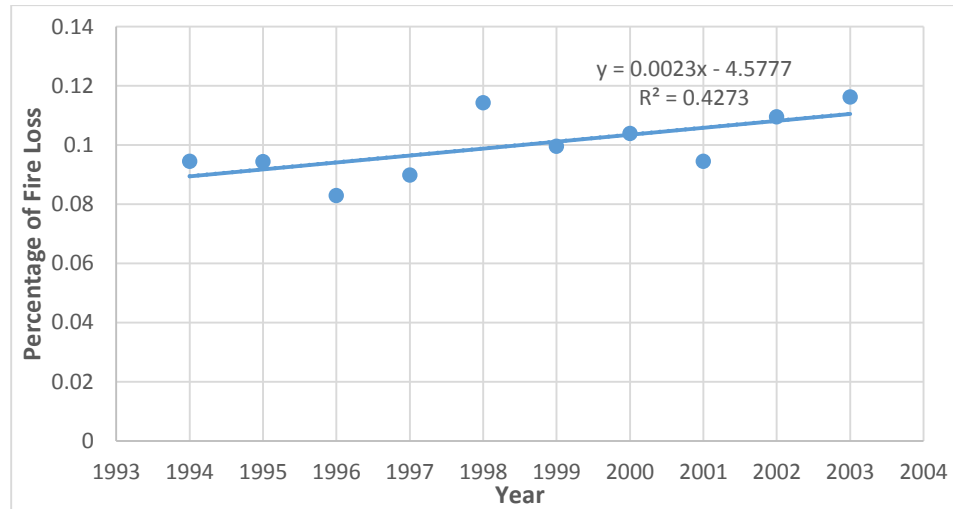


Figure 1.6: Linear regression analysis of fire loss percentage from the year 1994 to 2003.

1.4 Aims and Objectives

The 3 main objectives of the study are shown as following:

- I. To analyze and design the building based on EC 2 and ISO 834.
- II. To evaluate the performance of structural elements with or without fire conditions.
- III. To determine the reliability index, β of the structural beams using 2 methods.

1.5 Analysis of Structure

The design of structure can exist in a wide range of design situations and should incorporate the standards and suggestions in the design codes for the purposes of reducing the fire-related risks and as an ethical practice of engineering profession. The design codes that functioned as a reference document in the concrete design and structural fire design are Eurocode EN 1990, EN 1991, EN 1992 and International Organization for Standardization ISO 834 respectively. The Eurocode 1 to Eurocode 2 provided guidelines on the actions, materials and structural behaviors on the concrete structure in terms of safety, serviceability and durability. Besides, ISO 834 provided test data on the structural element's fire resistance during standard fire exposure situations. On the other hand, these codes of engineering are updated with the changed in societal, political and economic considerations. Hence, it is feasible to obey the design code to maintain the design within the acceptable range of the considerations and regulate safety issues at the national level.

1.6 Reliability of Structure.

Every structural design is different in aspects of their components and system due to their materials used, structural dimensions, loading types and degree of exposure. The differences in structure failure mechanism contributed to the lack of failure frequency data available and hence analyzation of structural reliability is necessary to minimize the effects of structural failure due to the extreme event like a fire. The structural reliability is defined as the resistance of the structure to the extreme loading and the load carrying capacity. The methods of reliability used are the Monte Carlo simulation, First Order Reliability Method (FORM) and Second Order Reliability Method (SORM). Monte

Carlo simulation solved the integrals in a random sample with a smaller number of trials that needed to evaluate the reliability. FORM and SORM are two types of methods both developed to estimate the probability integration of reliability of structure. FORM performed by approximation of Taylor first order expansion whereas SORM approximate the failure surface by Taylor second order expansion.

1.7 Scope of Work

The scopes of work include the modeling and analysis of an institutional building. Besides, the reliability analysis of structure is determined in accordance with European code and ACI standard. The objective of this study is to carry out the structural reliability of the building under the exposure of fire.

1.8 Outline of Thesis

This thesis is organized as follows:

- Chapter 1 presents an introduction to this study and its significance.
- Chapter 2 presents the study of design codes used for fire, probabilistic model of parameters affecting the fire and limit state equation from published work.
- Chapter 3 presents the methodology of the reinforced concrete building fire analysis which in accordance with the Eurocode 2 and ISO 834. In this chapter, the methods and equations used for fire design and analysis are defined.
- Chapter 4 deals with the design moment and resistance of structural beams under different fire duration at two conditions of fire development. A comparison of the fire severity and fire resistance is made to evaluate the structural safety under fire. The results of the reliability index are generated by two methods which are the First Order Reliability Method (FORM) and First Order Secondary Method (FOSM).
- Chapter 5 presents the conclusion of this study.

CHAPTER 2

LITERATURE REVIEW

2.1 Type of Fire

The amount of fire during the real case of fire does not remain constant over time. The fire ignites at a certain point is known as localized fire where the fire load occurred at a part of the fire compartment. The localized fire is trapped at the upper part of the compartment which is the layer under the ceiling when hot air rises and contributed to the formation of two-zone model in the compartment.

After a period of time, the localized fire will slowly grow into a fully developed fire where the fire load is uniformly distributed in the entire fire compartment. Besides, the gas temperature at a compartment with fully developed fire has a constant gas temperature because of the complete combustion of fuel and oxygen in the whole compartment. The good mixing of the gas gave an equivalent temperature in the compartment and this is called a one-zone model. The differences between the two types of fire stated above are summarized in Table 2.1. (Veljkovic et al., 2015)

Table 2.1: Differences between localized and fully developed fire.
(Veljkovic et al., 2015)

Types of Fire	Fire Load	Gas temperature
Localized fire	Only a part of the compartment is in fire	Two zones (two temperature-time curves)
Fully developed fire	The fire load uniformly distributed in the whole compartment is in fire	One zones (one temperature-time curves)

2.1.2 Fire Active Measures

The fire detection system is installed in every compartment which intends to perform their purpose on give an early warning to the people. During the system operation, the system first needs to be activated by detecting the fire and triggered the fire alarm as notification to the public. The fire detection system is assumed to fail if it is unable to achieve both the detection and notification during an actual fire scenario. This type of failure situation is extremely dangerous and needs to be avoided.

Since automated fire extinguishing system such as sprinkler is absence in the building, the fire is solely controlled by the operation of manual fire-fighting such as the reel hose and the off-site fire department. In order to successfully control the fire, the fire extinguisher must be able to function and the reel hose must enable to deliver the required amount of water to the fire scene to extinguish the fire. Therefore, fire brigade, in this case, played an important role to support the existing active fire measure in

reducing the risk of fire to a minimum and prevent the fire spread to other compartments. Hence, without an early detection of the fire, the fire department will never inform on the fire and this situation will further delay the time for effective fire suppression. Other than putting off the fire, fire brigade also responsible in assisting the evacuation of building's occupants in the case of fire.

There are several uncertainties occurred during the fire that encountered by the fire brigade such as the notification of fire alarm, the traveling time to site, equipment setting time, and the size of fire growth. If manual fire suppression is attempted, the action of reel hose needed to be taken within 3 minutes right after the notification of fire with the condition that the growth of fire still within a manageable size. In the study of Tillander and Rahkonen. K., the total mean time required by the fire brigade to be notified on the fire and arrived at the fire scene is 10 minutes. This required period of time for fire brigade intervention is known as the response time, t_r . The probability of fire brigade to successfully put out the fire is considered small when compared to the other 3 active measures. The efficiency of fire brigade largely depends on the operation of the sprinkler system because the sprinkler system will control the fire before the arrival of the fire brigade. The failure in fire brigade occurred when the fire is unsuccessfully extinguished by the fire brigade within 15 minutes. It is assumed that the fire brigade reacted to the fire call at the right time and the potential time needed is identified as the time taken to reach the fire site. The time for the fire brigade to reach the fire site is mainly varied due to the factors of the distance between the fire building and the nearest fire department, traffic condition and weather. From the information provided in Figure 2.1, the distance between UTAR FEGT Block E to the Kampar Fire and Rescue Station was 4.9 km and the estimated arrival time is 11 minutes.

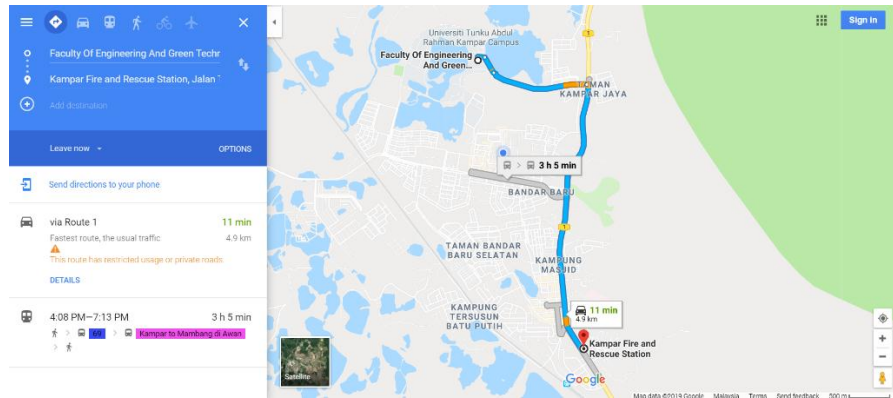


Figure 2.1: Distance between UTAR FEGT Block E to the Kampar Fire and Rescue Station.

In Molken, T., et.al. study on the damage and residual load-bearing capacity of a concrete slab after fire suggested the time duration from the fire ignition to the successful fire suppression approximately took 19 to 44 minutes. The time for the fire brigade to start the fire extinguishing operation until the fire been extinguished was estimated between a half to an hour based on the experience of firefighters from their past fire events. A timeline of fire event from the fire ignition to the fire been extinguished was represented in Figure 2.2.

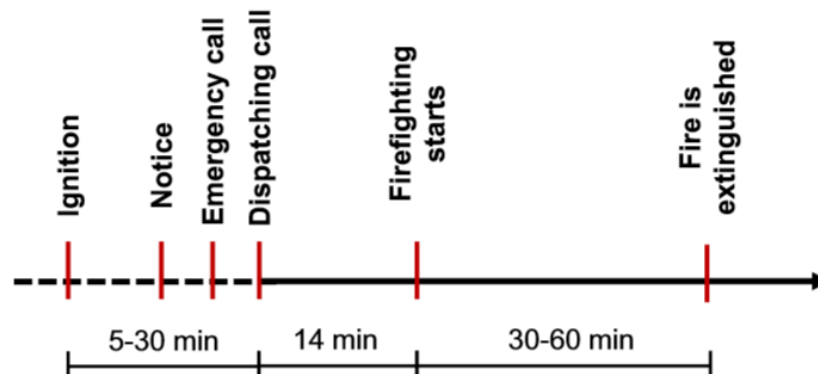


Figure 2.2: Timeline of fire event from the fire ignition to the fire suppression.
(Molken, T., et.al., 2017)

2.3 Design Code

2.3.1. EN 1990

Eurocode EN 1990 was the basis of structural design which provides extra information for the structural design and works cooperatively with Eurocode 2. This code evaluates the mechanical actions, load combinations, material behavior as well as the structural behavior and reliability design. The numerical values for partial safety factors and parameters of reliability are given in EN 1990 which act as a fundamental base of reference for all others Eurocode.

2.3.2 EN 1992-1-2

The concrete elements in the structural fire design are governed by the Eurocode EN 1992-1-2 which is the Design of concrete structure- Part 1-2 General rules- Structural fire design. This code explains the importance and regulations of concrete structure design when exposed to accidental fire. The main subjects covered by this code include the safety conditions and steps of design. EN1992-1-2 is widely used by people such as designers, contractors and pertinent authorities.

On the other hand, this code solely provides information on the passive practices of fire protection, active measures are not taken into account. The formulas given in EN 1992-1-2 are suitable to concrete class less than of C90/105, furthermore, for concrete class more than C50 and above is considered high strength concrete (HSC) and should refer to section 6 in the code. Eurocode 2 use the ISO 834 standard fire curve in Figure 2.4 as a standard fire curve and predicted the concrete and steel properties under increased temperature. The deformation of concrete properties under compression in

term of compressive strength, $f_{c,\theta}$ and strain, ϵ during the fire is represented in the stress-strain relationship which is represented in Figure 2.3.

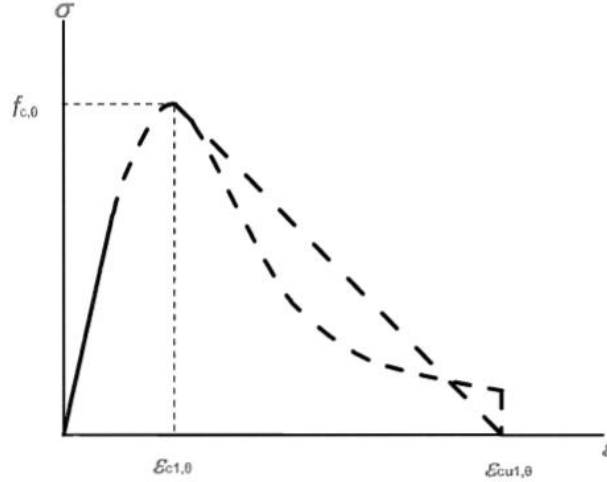


Figure 2.3: Stress-strain relationship of concrete under fire.

2.4.3 ISO 834

ISO 834: Fire-resistance tests- Elements of building construction was the fire design code under the International Organization for Standardization (ISO). A standard test procedure is stated in ISO 834 to evaluate the fire resistance of structure subjected to standard fire exposure. The fire design is based on the natural fire curve whereby the elements such as the fire load, room ventilation and the room property are taken into consideration. ISO 834 is important in fire design because the information on the fire design of a structure is not stated clearly in Eurocodes because the performance of fire in concrete structures is unrealistic compared to the ISO 834 standard fire.

The formula of ISO 834 defines temperature ($^{\circ}\text{C}$) by the Eq. (2.1) where T is the temperature and t is the time of fire exposure.

$$T = 345 \log_{10}(8t + 1) + 20 \quad (2.1)$$

ISO 834 temperature- time curve represents a small-scale test of the full- scale tests of fire resistance in order to evaluate the performance of structural elements in the fire. The tests include the assessing of thermal expansion, thermal shrinkage and deformation due to load. The time of fire resistance start from 0 min of ISO 834 standard fire curve and continue to increase until the element has exceeded its design resistance capacity. Table 2.2 represents the fire temperature from ISO 834 fire duration, R zero to 4 hours using Eq. (2.1). The temperature at different fire duration is later plotted into ISO 834 temperature- time curve of the effect of the rectangular reinforced concrete beam under fire is shown in Figure 2.4.

Table 2.2: Fire temperature, T at ISO834 fire duration, R.

Fire Duration, R (hr)	Fire Temperature, T (°C)
0	0
1	945.3
1.5	1006
2	1049
2.5	1082.4
3	1109.7
4	1152.8



Figure 2.4: The ISO 834 standard temperature-time curve.

2.4 Uncertain Parameters in Fire Design

2.4.1 Concrete compressive strength, f_{ck}

When concrete is subjected to high temperature, the concrete compressive strength will eventually decrease. Hence, the concrete compressive strength reduction factor at the elevated temperature at T °C, $k_{fc,T}$ has to be taken into account. The uncertainty of concrete compressive strength has a lognormal probability distribution and the mean and variance are given in Table 2.7.

Concrete compressive strength at an elevated temperature T , $f_{ck,T}$ is based on the concrete compressive strength at normal temperature 20 °C, $f_{ck,20^\circ C}$ and the concrete compressive strength reduction factor at T °C, $k_{fc,T}$. The $k_{fc,T}$ is temperature dependent represented by the formula given in EN 1992 as shown in Eq. (2.2).

$$k_{fc,T} = \frac{f_{ck,T}}{f_{ck,20^\circ C}} \quad (2.2)$$

EN 1992-1-2 explains the graphical relationship between $k_{fc,T}$ to the elevated temperature, T as shown in Figure 2.6. The graph in Figure 2.6 allows the values of reduction factor, $k_{fc,T}$ to be determined with that change in temperature. The reduction in values of reduction factor, $k_{fc,T}$ with the increased temperature directly represented the reduction of concrete compressive strength, f_{ck} when referring back to Eq (2.2). When $k_{fc,T}$ increase with temperature, the $f_{c,T}$ increase, their relationship is directly proportional to each other. In Figure 2.5, curve 2 increase more in $k_{fc,T}$ than the one in curve 2 during temperature increase. Furthermore, the curve 1 and 2 from Figure 2.5 was further tabulated into a table of the concrete compressive strength as a function of the temperature represents by column 2 and column 5 for siliceous aggregates and calcareous aggregates respectively highlighted in Figure 2.6. (EN 1992-1-2)

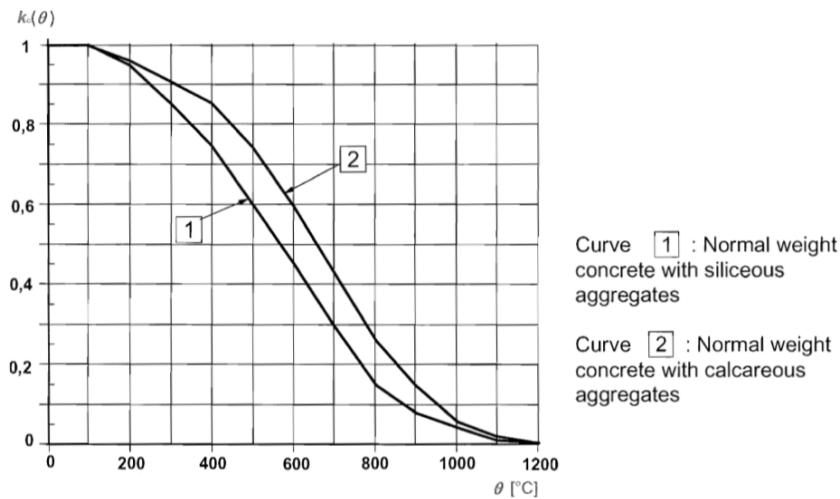


Figure 2.5: Concrete compressive strength reduction factor at T °C, $k_{fc,T}$ decrease with elevated temperature, T . (EN 1992-1-2 section 4.2.4.2)

Concrete	Siliceous aggregates			Calcareous aggregates		
temp. θ	$f_{c,\theta} / f_{ck}$	$\varepsilon_{c1,\theta}$	$\varepsilon_{cu1,\theta}$	$f_{c,\theta} / f_{ck}$	$\varepsilon_{c1,\theta}$	$\varepsilon_{cu1,\theta}$
[°C]	[-]	[-]	[-]	[-]	[-]	[-]
1	2	3	4	5	6	7
20	1,00	0,0025	0,0200	1,00	0,0025	0,0200
100	1,00	0,0040	0,0225	1,00	0,0040	0,0225
200	0,95	0,0055	0,0250	0,97	0,0055	0,0250
300	0,85	0,0070	0,0275	0,91	0,0070	0,0275
400	0,75	0,0100	0,0300	0,85	0,0100	0,0300
500	0,60	0,0150	0,0325	0,74	0,0150	0,0325
600	0,45	0,0250	0,0350	0,60	0,0250	0,0350
700	0,30	0,0250	0,0375	0,43	0,0250	0,0375
800	0,15	0,0250	0,0400	0,27	0,0250	0,0400
900	0,08	0,0250	0,0425	0,15	0,0250	0,0425
1000	0,04	0,0250	0,0450	0,06	0,0250	0,0450
1100	0,01	0,0250	0,0475	0,02	0,0250	0,0475
1200	0,00	-	-	0,00	-	-

Figure 2.6: Concrete compressive strength, f_c at elevated temperature, T. (EN 1992-1-2)

2.4.2 Reinforcement yield strength, f_{yk}

Reinforcement yield strength at an elevated temperature T, $f_{yk,T}$ is based on the reinforcement yield strength at 20 °C, $f_{yk,20^\circ C}$ and the reinforcement yield strength reduction factor at T°C, $k_{fy,T}$. The uncertainty of reinforcement yield strength has a lognormal probability distribution and the mean and variance are given in Table 2.7. The relationship between them was represented by the formula $k_{fy,T}$ in Eq. (2.3).

$$k_{fy,T} = \frac{f_{yk,T}}{f_{yk,20^\circ C}} \quad (2.3)$$

EN 1992-1-2 shows the graphical relationship between $k_{fy,T}$ to the elevated temperature, T in Figure 2.7. The graph in Figure 2.7 allowed values of reduction factor, $k_{fy,T}$ to be determined with the change in temperature. The reduction in values of reduction factor, $k_{fy,T}$ with the increased temperature directly represented the reduction of reinforcement yield strength, $f_{yk,T}$ when referring back to Eq. (2.3). When $k_{fy,T}$ increase with temperature, the $f_{yk,T}$ increase, their relationship is directly proportional to each other. The tension reinforcement for hot-rolled, cold worked reinforcement steel and strain value less than 2% are represented by curve 1, 2 and 3 respectively in Figure 2.7. In Figure 2.7, the ascending order of $k_{fy,T}$ increase during temperature increase is curve 3, curve 2 and curve 1 respectively. The equation used to calculate reinforcement yield strength reduction factor at T °C, $k_{fy,T}$ at elevated temperature, T in given in Table 2.3.

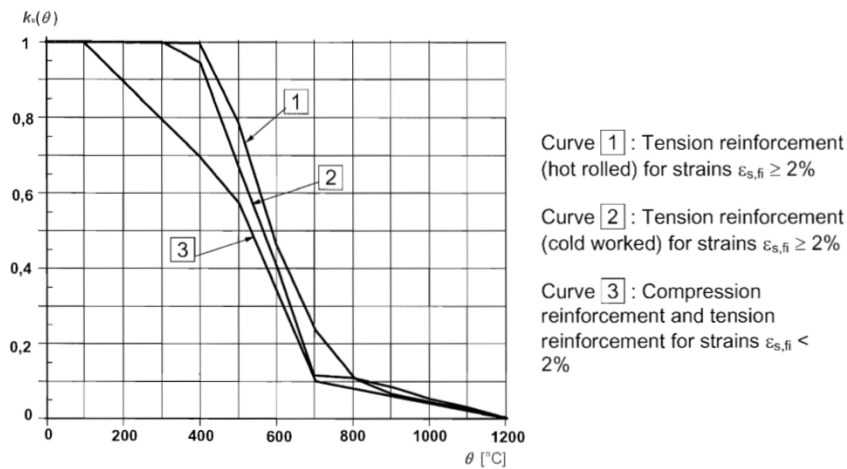


Figure 2.7: Reinforcement yield strength reduction factor, $k_{fy,T}$ at elevated temperature, T of Class N steel. (EN 1992-1-2 section 4.2.4.2)

Table 2.3: Reinforcement yield strength reduction factor, $k_{fy,T}$ at elevated temperature, T. (EN 1992-1-2)

Reinforcement yield strength reduction factor, k_{fy} ,	Fire Temperature, T (°C)
1.0	20°C T 100°C
$0.7 - 0.3 (T - 400) / 300$	100°C 400°C
$0.57 - 0.13 (T - 500) / 100$	400°C T 500°C
$0.1 - 0.47 (T - 700) / 200$	500°C T 700°C
$0.1 (1200 - T) / 500$	700°C T 1200°C

2.4.3 Concrete Cover, c

According to EN1992-1-1 concrete cover is significant to provide in concrete for the efficient forces transfer, as a protection to the embedded steel from corrosion and also provide fire resistance to the building structure. The concrete cover is represented by “c”, which is the distance from the concrete surface to the center of the main steel reinforcement. Figure 2.8 shows the cross section of slab and reinforcement steel bar where s is the horizontal reinforcement spacing, a is the distance from the reinforcement to the nearest concrete surface, h is the slab thickness and ϕ is the reinforcement bar diameter.

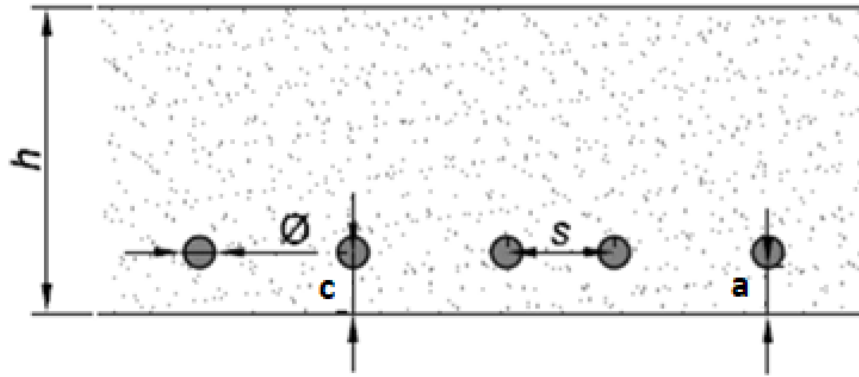


Table 2.8: Cross section of slab and reinforcement steel bar. (Van Coile, R., 2015)

The uncertainty of concrete cover has a continuous Beta probability distribution $[\mu \pm 3\sigma]$ and the mean and variance are given in Table 2.7. The changes in concrete cover have an important role in the changes of bending moment of resistance, $M_{R,fi,t}$. During a fire scene where a slab with a small c value, the heat from fire accelerated at a higher rate in the reinforcement and subsequently decreased the value of $M_{R,fi,t}$. (Coile, Taewe and Caspeelee, 2013)

In Kodur and Dwaikat, 2008 study on RC beam subjected to fire at 3 sides, the temperature varies at different concrete depth over the time of fire exposure. The cross section of the beam with the location of rebar, link and cover is represented by Figure 2.9. Figure 2.10 represented the different concrete parts at various fire exposure time starting from the rebar located at the corner, the rebar at center, the concrete at 125mm from the bottom, the center of the beam depth, 375mm from the bottom and the top side which is not exposed to fire.

The temperature in the concrete beam increase when the concrete depth from fire exposure surface decrease. The side of concrete which does not expose to fire has a constant temperature from 0 to 60 minutes as shown in Figure 2.10. The properties of

concrete with low thermal conductivity made the heat transmission in concrete to be very slow. Hence, the thickness of concrete cover affects the penetration of heat to the inner part of the concrete and will subsequently lower the strength of rebar. The ASTM E119 standard fire curve is used in this study whereby the strength and failure criteria are evaluated in fire resistance. Hence, the ASTM E119 curve has the largest temperature increase during fire exposure.

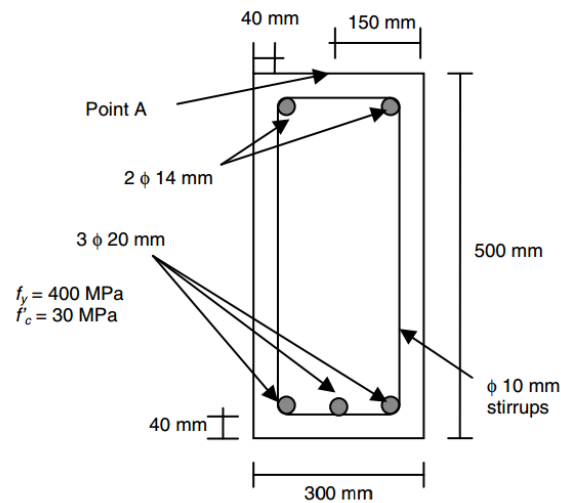


Figure 2.9: Cross section of the beam. (Kodur and Dwaikat, 2008)

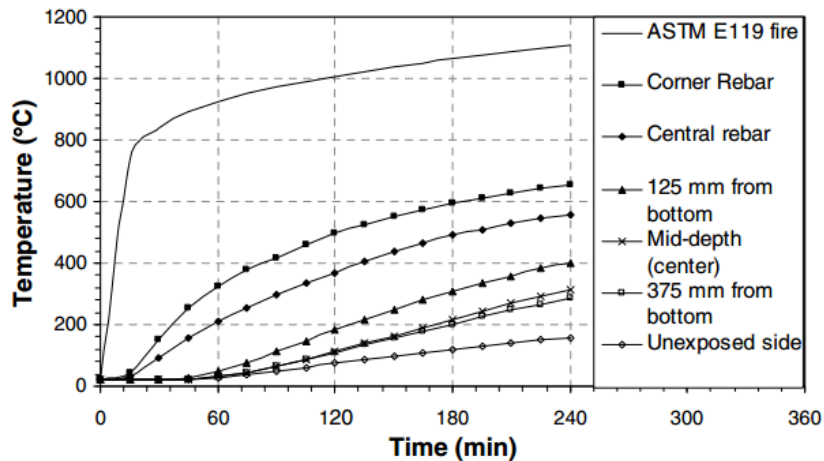


Figure 2.10: Temperature at the different part of the beam varies with fire exposure time. (Kodur and Dwaikat, 2008)

Two tests are cited in Coile, Taewe and Caspee, (2013) on the relationship between the nominal concrete cover and the reliability index. The reliability vs. concrete cover relationship of Test 1 and Test 2 are represented respectively in Figure 2.11 and Figure 2.12. In example 1, the reliability index of the lognormal approximation (LN) has high reliability from the observed histogram (A) during the fire exposure time of 30 to 90 minutes. On the other hand, the mixed-lognormal approximation (mixed-LN) falls slightly below the observed histogram (A) and has reduced reliability. The observation on LN and mixed-LN approximations in Figure 2.11 similar to example 1 whereby the LN approximation deviated more than the one in Test 1. A summary of Test 1 and Test 2 is shown in Table 2.4.

Table 2.4: Summary of results in Test 1 and Test 2.

Test	1		2	
Distribution	Lognormal (LN)	Mixed- lognormal (Mixed LN)	Lognormal (LN)	Mixed- lognormal (Mixed LN)
Concrete cover, c (mm)	15	15	35	35
Standard deviation, σ (mm)	5	5	10	10
σ_c (mm)	5	5	10	10
Reliability Index	Overestimated	Slightly underestimated	Overestimated	Small Deviation

Coile, Taewe and Caspee, (2013) had made a conclusion on their research based on Test 1 and 2 and stated that mixed-LN approximation represents the bending moment resistance, $M_{R,fi,t}$ more accurate than LN approximation. Moreover, Erdem, H., (2008) results also showed that with a greater concrete cover thickness, c the bending moment resistance, $M_{R,fi,t}$ tends to increase. The relationship of RC beam bending moment resistance, $M_{R,fi,t}$ and concrete, c is represented in Figure 2.13 over the fire duration from 0, 5, 60 to 120 minutes. Hence, due to the reason on concrete cover variability has a huge effect on the bending moment of resistance, the concrete cover must be taken into consideration at the fire exposure condition. This step can further prevent a large divergence in the lognormal distribution from happening.

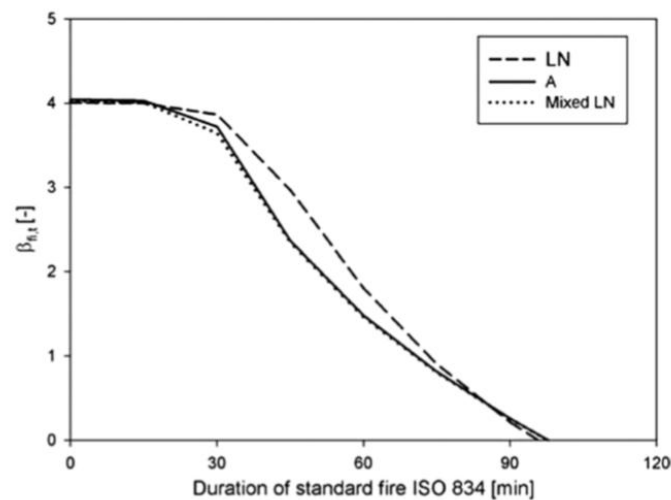


Figure 2.11: The reliability vs. concrete cover relationship of Test 1. (Coile, Taewe and Caspee, 2013)

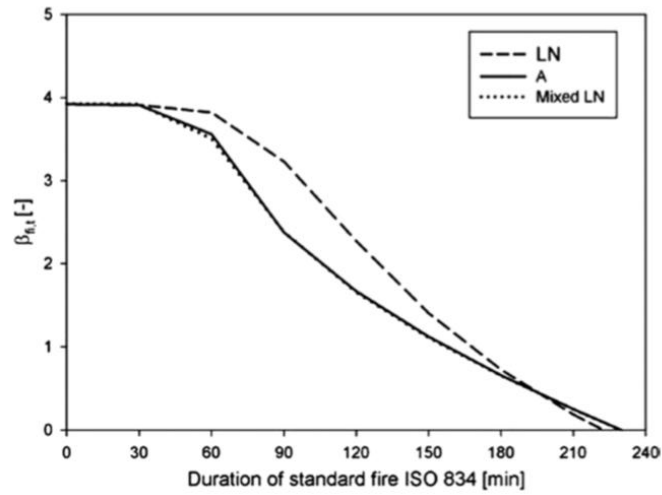


Figure 2.12: The reliability vs. concrete cover relationship of Test 2. (Coile, Taewe and Caspeelee, 2013)

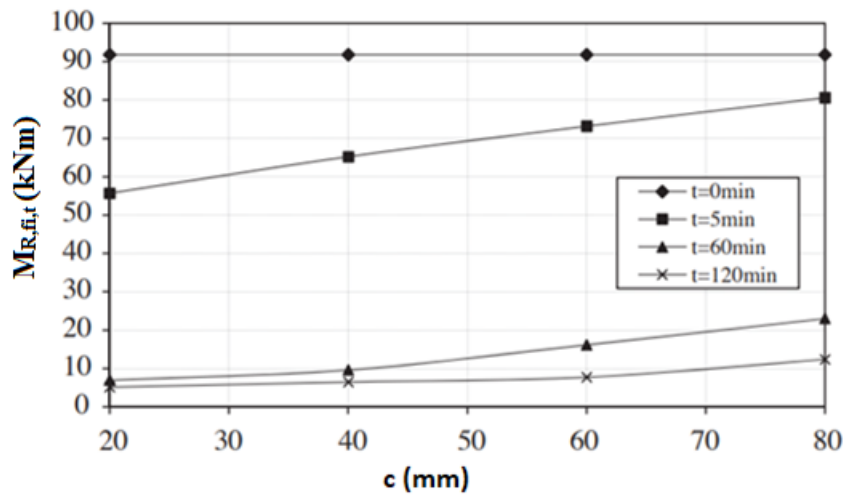


Table 2.13: Relationship of bending moment resistance, $M_{R,fi,t}$ and concrete cover, c (Erdem, H., 2008)

2.4.4 Model Uncertainty, K

A model uncertainty value K indicates the difference generated by the analytical value to the numerical value of the moment of resistance, M_R . The effects of a theoretical model in representing the actual condition is represented by the model uncertainty. The model uncertainty value is derived from the ratio of analytical value to numerical value. The uncertainty of model uncertainty for K_R , K_E and K_T have a lognormal probability distribution and the mean and variance are given in Table 2.5 for K_E and Table 2.6 for K_R and K_T . In Van Coile, R., (2015) study of reliability-based decision making for concrete element exposed to fire, the parameters of the total model uncertainty, K_T are provided, by Eq. (2.4) and Eq. (2.5) show the formula of the mean value of K_T , μ_{K_T} and coefficient of variation of K_T , $(\sigma_{K_T})^2$ respectively. The model uncertainty for resistance, load and additional model uncertainty, K_M are taken into consideration of the formulation of mean and variance of total model uncertainty.

$$\mu_{K_T} = \mu_{K_R} - \mu_{K_E} - \mu_{K_M} \quad (2.4)$$

$$(\sigma_{K_T})^2 = \sqrt{\sigma_{K_R}^2 + \sigma_{K_E}^2 + \sigma_{K_M}^2} \quad (2.5)$$

The resistance effect, R is represented by relating all the model uncertainty into the total model uncertainty, K_T . (T. Molken, R.V. Coile and T. Gernay, 2017). The formula of resistance effect, R is given in Eq. (2.6).

$$R = \frac{K_R}{K_E K_M} M_R = K_T M_R \quad (2.6)$$

2.4.5 Load Uncertainty

Loads which act on structure varies with respect to the time and space throughout the design life of the structure. The actions on a structure can be divided into two categories which were the thermal action and mechanical action. The actions evaluated in the temperature analysis whereby fire load was the thermal action. On the other hand, permanent load, G imposed load, Q, snow load, S and wind load, W were the examples of mechanical actions during the analysis of structure. Permanent load represents the self-weight of the structure as well as all the fixtures such as ceiling and partition walls whereas the imposed load on a building varies due to its occupancies such as usage by peoples, furniture, vehicles and large concentrate ion of peoples during an event.

Fire load, Q is the sum of energy released in real fire case in a fire compartment and the fire load density, q_f is defined by dividing the fire load with the floor area, A_f of the fire compartment. In EC 1992-1-2, the fire load density is defined by the Eq. (2.7) whereby Ψ_i is the factor of fire load of material i, m_i is the factor of combustion behavior of material i, H_{ui} is the net calorie value of material i, and M_i is the mass of material i. Fire load does not remain constant during the building design life, it varies due to the stochasticity of fire occurrence and the role of active firefighting measures during actual fire case. Fire load is an important measurement in the fire model to evaluate the building structural performance during fire exposure.

$$q_f = \frac{1}{A_f} \sum_i (\Psi_i m_i H_{ui} M_i) \quad (2.7)$$

The ultimate limit state is important to ensure the safeguard of the structure and occupant. Structure failure such as fatigue and excessive deformation on the structure can affect the stability of the structure and even foundation. Hence the ultimate limit state needs to be used to prevent the worst condition from happening. Load combination has to apply to the ultimate limit state design. On the other hand, the serviceability limit state considers the normal function of the structure with consideration of deflection and crack as well as the overall appearance of the structure.

The validation of serviceability limit state is necessary to evaluate the damage on structure appearance, durability and excessive vibration. During the fire scenario, the load's acting on the structure can be derived from the Eq. (2.8). (EN 1990) The design moment induced by design loads, M_{Ed} by R. V. Coile, (2015) in Eq. (2.9) of concrete slabs which subjected to self-weight and imposed load.

$$\sum_{i \geq 1} G_{k,j} + (\Psi_{1,1} \Psi_{1,2}) Q_{k,1} + \sum_{i \geq 1} \Psi_{2,i} Q_{k,i} \quad (2.8)$$

$$M_{Ed} = \max \{ (\gamma_G M_{Gk} + \psi_0 \gamma_Q M_{Qk}) ; (\xi \gamma_G M_{Gk} + \gamma_Q M_{Qk}) \} \quad (2.9)$$

In order to obtain the maximum load combination, the value for the reduction factor for unfavorable permanent load, ξ , the partial factor of permanent load, γ_G and imposed load, γ_Q were all in unfavorable action effect condition. The value set by the National annex of structure members and geotechnical actions in EN 1990 for ξ , γ_G , and γ_Q was 0.85, 1.35 and 1.5 respectively. Besides, the partial factor of imposed load, γ_Q was equal to zero under favorable action effect condition does not give maximum load combination. The characteristic value for uniformly distributed imposed load, q_k and concentrated imposed load, Q_k was set by the National annex given in EN 1991-1-1. The q_k and Q_k values vary according to the function a loaded area either it has a general effect or local effect on the structure. The probabilistic model of resistance parameters was tabulated in Table 2.5.

Table 2.5: Probabilistic Model of Load Parameters

Parameter	Dimension	Probability Distribution	Mean, μ	Co V	Author
K_E	-	LN	1	0.1	[17], [20]
M_G	kNm	N	M_{GK}	$\frac{M_{GK}}{0.1}$	[20]
M_Q	kNm	Gumbel	$\frac{0.2 \chi}{1-\chi} M_{GK}$	$\frac{\frac{0.2 \chi}{1-\chi} M_{GK}}{1.1}$	[20]
g_k	kN/m ²	Normal	g_k	0.1	[19]
q_k	kN/m ²	Gumbel	$0.2q_k$	1.1	[19]
χ	-	-	1.2	8	[22]
l	m	DET	408	-	[19]
			4.44	-	[17]

Note: K_E - Model uncertainty for load ; M_G - Bending moment induced by permanent load ; M_Q - Bending moment induced by imposed load ; g_k - Permanent load ; q_k - Imposed load ; χ - Load ratio ; l - Slab free span.

2.5 Bending Moment Resistance

2.5.1 Eurocode 2

The bending moment can occur when external forces such as permanent load and imposed load are acted on the structural element. The bending moment induced by the permanent load is M_G whereas bending moment induced by the imposed load is M_Q . The combinations of the M_G and M_Q will give the maximum bending moment at the structure. The load ratio, χ of a concrete slab under variable load effect, Q_k has been defined by the ratio of variable load effect to the total combination load effect of variable load plus permanent load, $G_k + Q_k$ as showed in Eq. (2.10).

$$\chi = \frac{Q_k}{Q_k + G_k} = \frac{M_{Qk}}{M_{Qk} + M_{Gk}} \quad (2.10)$$

An assumption was made by combining Eq. (2.8) and Eq. (2.9) whereby M_{Ed} equals to M_{Rd} is to evaluate the baseline safety level of concrete slab without considering any other load effect. Hence, the bending moment induced by the permanent load, M_{Gk} can be calculated by the Eq. (2.11). (Van Coile, R., 2015).

$$M_{Gk} = \frac{M_{Rd}}{\max\{(\gamma_G M_{Gk} + \psi_0 \gamma_Q M_{Qk}); (\xi \gamma_G M_{Gk} + \gamma_Q M_{Qk})\}} \quad (2.11)$$

The safety level of load design requirement of Eurocode 2 need to be ensured by limiting the design bending moment, M_{Ed} value less than the value of design bending moment of resistance, M_{Rd} , the relationship is represented in Eq. (2.12).

$$M_{Ed} < M_{Rd} \quad (2.12)$$

2.5.2 ACI Code

In ACI 216, (1994) approximate method stated that the effect of fire on compression region or the top side of slab was ignored. The bottom part of the slab was exposed to fire lead to deflection to occur and expand more than the top side. When the bottom part of the concrete slab exposed to fire, the reinforcement steel and concrete at this part will gradually lose their tensile strength. Bending moment resistance of a simply supported concrete slab subjected to uniform load throughout the length can be constantly given in Eq. (2.13).

$$M = A_s f_y \left(d - \frac{a}{2} \right) \quad (2.13)$$

The maximum moment occurred at the mid span and the bending moment diagram is appeared to be a parabolic shape. The material strength in this case, f_y was reduced during fire yet the permanent and imposed loads remained constant. The probabilistic model of resistance parameters was tabulated in Table 2.6.

Table 2.6: Probabilistic Model of Resistance Parameters

Parameter	Dimension	Probability Distribution	Mean, μ	Co V	Author
K_R	-	LN	1.1	0.1	[17]
$M_{R,fi,t}$	kNm	DET	57.6	-	[19]
		LN	50.9	-	[20]
			1	10	[17]
$k_{fc}(t)$	-	Beta [$\mu \pm 3\sigma$]	T-dependent conform EN 1992-1-2		[19], [20], [17]

$k_{fy(t)}$	-	Beta [$\mu\pm 3\sigma$]	T-dependent conform EN 1992-1-2		[19], [20]
			1.0	2.0	[17]
$f_{c,20}^0$	MPa	LN	42.9	0.15	[19], [20], [17], [21]
			25.4	9.407	[22]
$f_{y,20}^0$	MPa	LN	581.4	0.07	[19], [20], [17], [21]
			581.395	14.286	[22]
h	mm	DET	200	-	[19]
			150	5000	[17]
			200	-	[20], [21]
			400	80	[22]
Φ	mm	DET	10	-	[21]
b	mm	DET	1000	-	[19], [21]
c	mm	Beta [$\mu\pm 3\sigma$]	15	45.45	[19]
			35	250	[20], [21]
			35	17.5	[22]
s	mm	DET	100	-	[19]
a_b	mm	-	25	125	[17]
a_t	mm	-	25	125	[17]

i_{500}	mm	-	13.8	34.5	[17]
A_{sb}	mm^2	N	785.4	39270	[19]
			223	11150	[17]
			785.4	39270	[20]
			785	39250	[21]
			801	50.063	[22]
A_{st}	mm^2	-	692	34600	[17]
K_T	-	-	1.1	7.86	[20], [17]

Note: K_R - Model uncertainty for resistance ; $M_{R,fi,t}$ - Design value for bending moment resistance ; $k_{fc(t)}$ - Concrete compressive strength reduction factor at t °C ; $k_{fy(t)}$ - Reinforcement yield strength reduction factor at t °C ; $f_{c,20}^0$ - Concrete compressive strength at 20°C ; $f_{y,20}^0$ - Reinforcement yield strength at 20°C ; h - Slab thickness ; Φ - Main reinforcement steel bar diameter ; b - Slab unit width; c - Concrete cover ; s - Reinforcement axis spacing ; a_b - Bottom reinforcement axis distance from slab surface ; a_t - Top reinforcement axis distance from slab surface ; i_{500} - Depth of the 500 °C isotherm ; A_{sb} - Bottom Reinforcement area ; A_{st} - Top Reinforcement area ; K_T - Total model uncertainty.

2.6 Limit State Equation

The limit state equation, G for the determination of system reliability and it can be defined as in Eq. (2.14).

$$G(X) = R(X) - L(X) = 0 \quad (2.14)$$

Limit state equation serves to prevent the load, L effect from exceeding the resistance, R effect in approaching structural failure. The variable parameters, X is taken into account in the system reliability, on the other hand, the random variables R and L were based on X . Limit state equation is important to serve as a baseline to the limit of a system resistance. Failure of a design system is considered valid when the load, L has exceeded the resistance, R . In another word, the system was considered unsafe state when ($G(X) < 0$) and safe state when ($G(X) > 0$). In another word, if load exceeds the resistance the failure of structural members will occur, if resistance exceeds the load structural members is considered safe.

In Van Coile, R. and Bisby, L. (2017), the beam the limit state equation, Z_{STR} in Equation Eq. (2.15) represented the strength limit state for a concrete slab subjected to pure bending.

$$Z_{STR} = M_{R,fi,tE} - M_E = M_{R,fi,tE} - w \frac{l^2}{8} \quad (2.15)$$

The bending moment capacity during the fire, $M_{R,fi,tE}$ and the bending moment induced by load effect, M_E were represented the R and L respectively. Table 2.7 below showed the limit state equations from other publications.

Table 2.7: Limit state equations by other publications.

Author	Limit State Equation
Van Coile, R. and Bisby, L. (2017)	$Z_{STR} = K_R M_{R,fi,tE} - K_E M_E$ $= K_R M_{R,fi,tE} - K_E (M_G + M_Q)$
	$M_{R,fi,tE} = \frac{w_{max,STR} \times l^2}{8}$
Van Coile, R. (2015)	$Z_{STR} = K_R M_{R,fi,tE} - K_E M_E$
	$M_{Ed} = \max \{ (\gamma_G M_{Gk} + \psi_0 \gamma_Q M_{Qk}) ;$ $(\xi \gamma_G M_{Gk} + \gamma_Q M_{Qk}) \}$
	$M_{Gk} = \frac{M_{Rd}}{\max \{ (\gamma_G M_{Gk} + \psi_0 \gamma_Q M_{Qk}) ; (\xi \gamma_G M_{Gk} + \gamma_Q M_{Qk}) \}}$
Molkens, T.,	$Z = K_R R - K_E (G + Q)$
Van Coile, R.,	$R = \frac{K_R}{K_E K_M} M_R = K_T M_R$
Gernay, T. (2017)	$M_R = A_{sb} k_{fy,res} f_{y,20} \left(h - a_b - \frac{A_{sb} k_{fy,res} f_{y,20}}{2 f_{c,20} b} \right)$ $+ \frac{x}{l} A_{st} f_{y,20} \left(h - i_{500} - a_t - \frac{A_{st} k_{y,20}}{2 f_{c,20} b} \right)$
Van Coile, R., Balomenos, G. and Pandey, M. (2018)	$M_{R,fi,t} = A_s k_{fy} f_y \left(h - c - \frac{\Phi}{2} \right) - 0.5 \frac{(A_s k_{fy} f_y)}{b f_c}$

2.7 Methods of Reliability

2.7.1 Monte Carlo Simulation

This simulation was used to solve the integral equation whereby most of the probability risk analysis does not take the algorithm analysis into consideration because of its complexity and time-consuming. Approximations of the sets of a random variable under probability function of the histogram had been carried out with a large size of a random sample, N . It involves a set of random sampling consist of all the basic parameters of resistance and load.

Furthermore, Monte Carlo simulation is an effective tool in checking the failure probability determined from the reliability index. When the R is lesser than L , the limit state value of less than 0 will be obtained. The total number of the limit state condition $R-L < 0$ occurred, it is denoted as the number of failures, $n(R-L < 0)$. The probability of failure, p_f is expressed by the ratio of this number of failure to the total number of trials, N as shown in Eq. (2.16).

$$P_f = \frac{n(R-L < 0)}{N} \quad (2.16)$$

Hasofer, A. M. (2012) had studied the time taken for the fire to spread from the edge of two corresponding rooms by Monte Carlo simulation. All the random variables come with the same set of parameters. Monte Carlo simulation was used in this case to approximate a large size of the independent random sample, N 10,000. The histogram of the probability of time taken for the fire to spread from room 1 to room 4, W against the number of occurrences was shown in Figure 2.14.

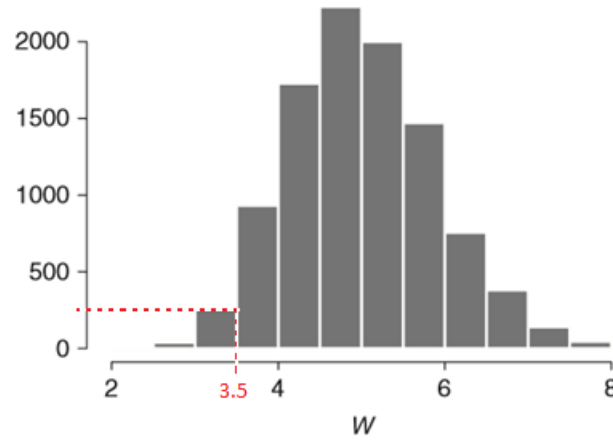


Figure 2.14: Histogram of fire spread against the number of occurrences.
(Hasofer, A. M., 2012)

The probability of fire spread from room 1 to room 4 within the time 3.5 minutes was obtained by sum up the numbers of values for W less than 3.5 min and later it was compatible to the probability of failure by using the Eq. (2.17).

$$p_f \left(\frac{n(W < 3.5)}{N} \right) = \frac{298}{10,000} = 0.03 \quad (2.17)$$

2.7.2 First-Order Reliability Method (FORM)

FORM was a frequently used method to analyze the reliability of structure under fire by evaluating the reliability index, β . The approximation of the probability of failure was obtained by the Eq. (2.18) in Sudret, B., Der Kiureghian, A., (2000) study on stochastic finite element methods and reliability of reliability index, β and standard normal cumulative distribution function, Φ .

$$P_f = \Phi(-\beta) \quad (2.18)$$

The integrals were calculated by Eq. (2.19) when parameters were transformed into a non-dependent and normally distributed parameters. (Breitung, K., 1984).

$$P_{f_SORM} = 1 - \Phi(\beta) \quad (2.19)$$

An iterative solution algorithm was performed in order to determine the design point fall on the limit state curve. All the parameter in limit state function was converted to standard normal space and any point with extreme value fell outside the limit state function can be determined as showed in Figure 2.15. (Haldar, A., Mahadevan, S., 2000)
The failure point on the design point was identified using mathematical programming methods.

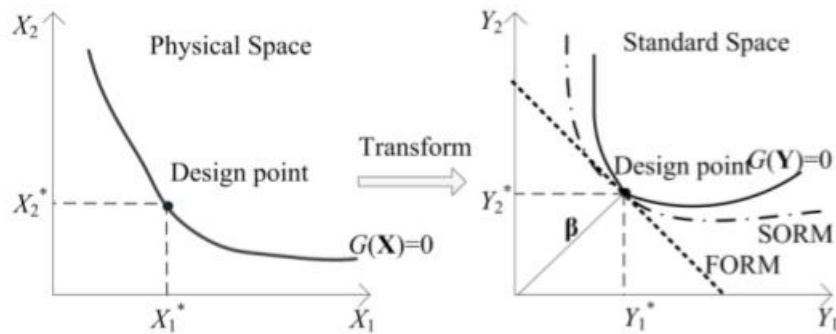


Figure 2.15: Failure probability using FORM. (Haldar, A., Mahadevan, S., 2000)

2.7.3 Second-Order Reliability Method (SORM)

The accuracy of the equation of failure probability approximation in equation 2.19 was increased by attempting SORM. The difficulty in the computation of second order derivatives in matrix form was performed in SORM. In Breitung, K., 1984 study on the approximations for multi-normal integral, the approximation of second-order probability of failure was evaluated using the theory of asymptotic approximations represented by Eq. (2.20).

$$P_{f_SORM} = \Phi(-\beta) \prod_{i=1}^{n-1} \frac{1}{\sqrt{1+\Psi(\beta)k_i}} \quad (2.20)$$

SORM was applicable when its second order reliability index, β_s falls within the acceptable range of a parabolic approximation using the Eq. (2.21).

$$|P_{fpara} - \Phi(-\beta_s)| \leq 0.05 P_{fpara} \quad (2.21)$$

2.8 Reliability Index or Probability Failure

The limit state function of failure is expressed in the relation $G(X) < 0$ from the possible solution of limit state function $G(X)=0$. The ratio of both the possible solutions $G(X) < 0$ and $G(X) > 0$ represent the structure reliability.

The probability failure, p_f in continuous distribution function is stated in Eq. (2.22) whereas the p_f in a normally distributed joint density function was evaluated in Eq. (2.23). (T. Balogh, L. G. Vigh, 2016).

$$p_f = P | G(X) < 0 | = \int_{G(X) < 0} f(X) dX \quad (2.22)$$

$$p_f = \Phi\left(-\frac{\mu}{\sigma}\right) = \Phi(-\beta) \quad (2.23)$$

The reliability index of $\beta > 3.8$ for the ultimate limit state in non-fire conditions need to be fulfilled in fire resistance of structure was mentioned in EN 1990. In Guo, Q. R., (2015) paper of structural reliability assessment under fire, the failure probability, P_f of system performance in continuous distribution function was illustrated by the shaded area in Figure 2.16.

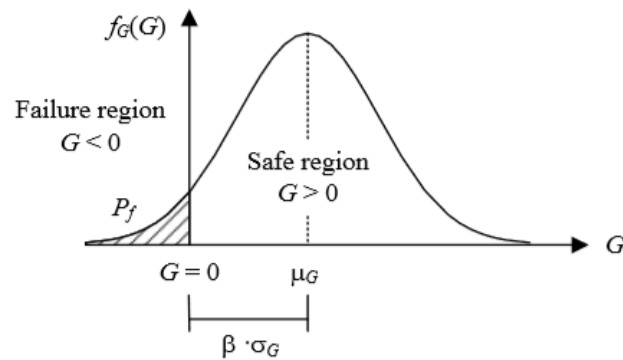


Figure 2.16: Characteristic of a system performance function, G . (Guo, Q. R., 2015)

CHAPTER 3

METHODOLOGY

3.1 Structural Model

3.1.1 Buildings Layouts

A structural plan of Block E at FEGT UTAR, Perak is used to provide layout and dimensions of the building. A software application, AutoCAD is used in visualizing the building's 2-dimensional structure of reinforced concrete samples. AutoCAD consists of Block E ground floor first floor and second floor dimension as shown in Figure 3.1, 3.2 and 3.3 respectively. In this study, the section which is under evaluation is highlighted in Figure 3.4.

The layout of fire compartments in a building is significant to evaluate the fire scenarios which occurred inside the compartment. The ground floor layout is different from the other's floor whereas the layout of the first floor and second floor are identical. All the levels in the building are accessible to each other through the lift and staircases whereby 2 staircases and a lift are available to service the occupants at each floor level.

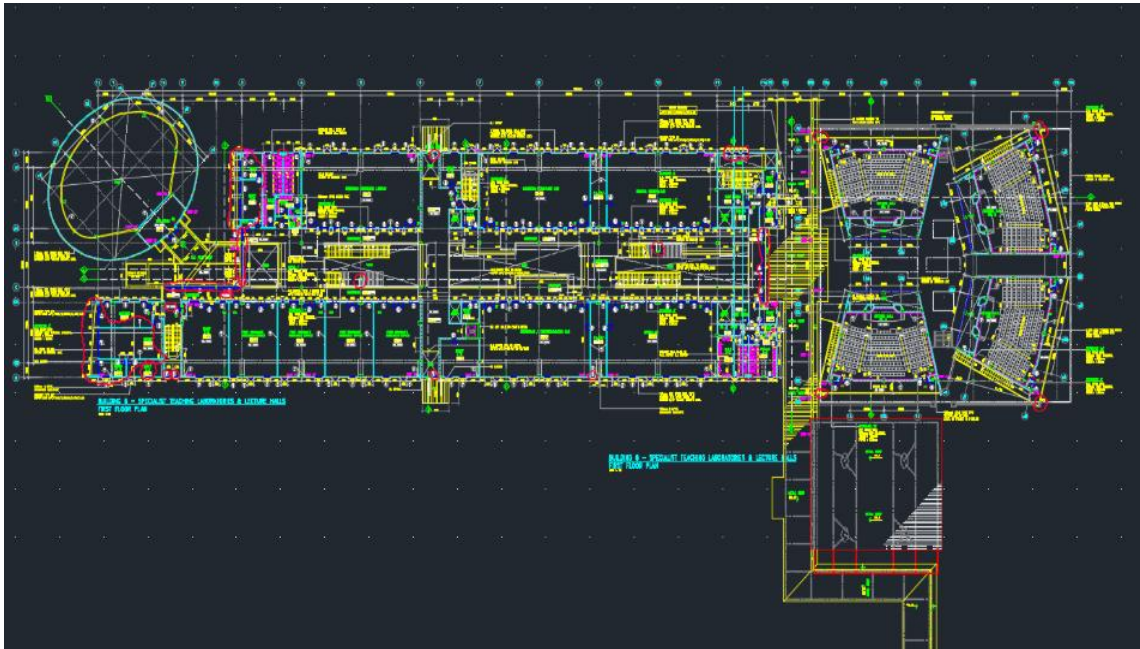


Figure 3.1: AutoCAD drawing of Block E ground floor.

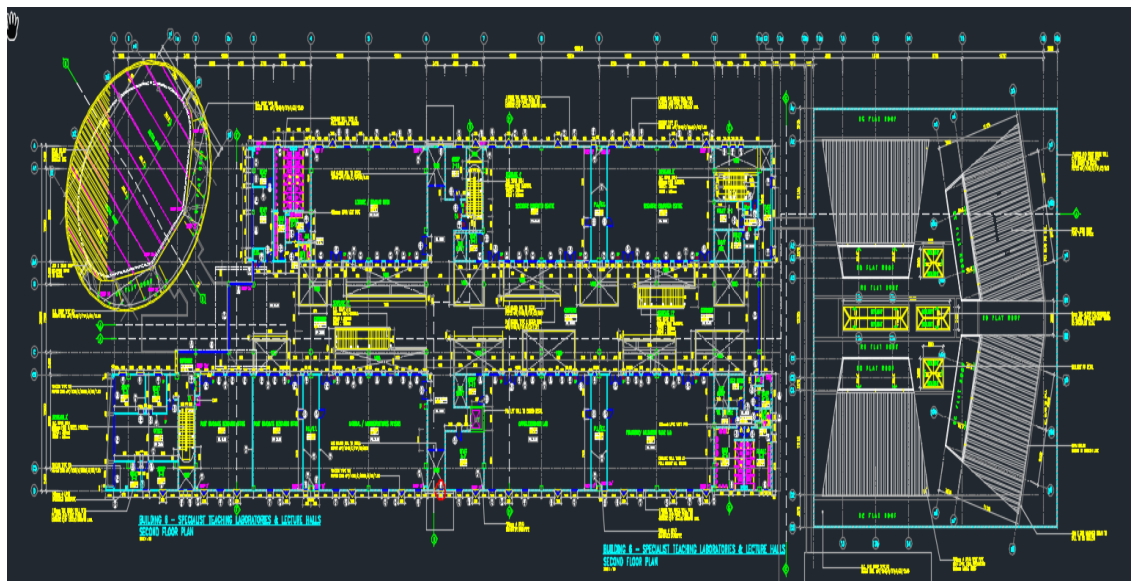


Figure 3.2: AutoCAD drawing of Block E first floor.

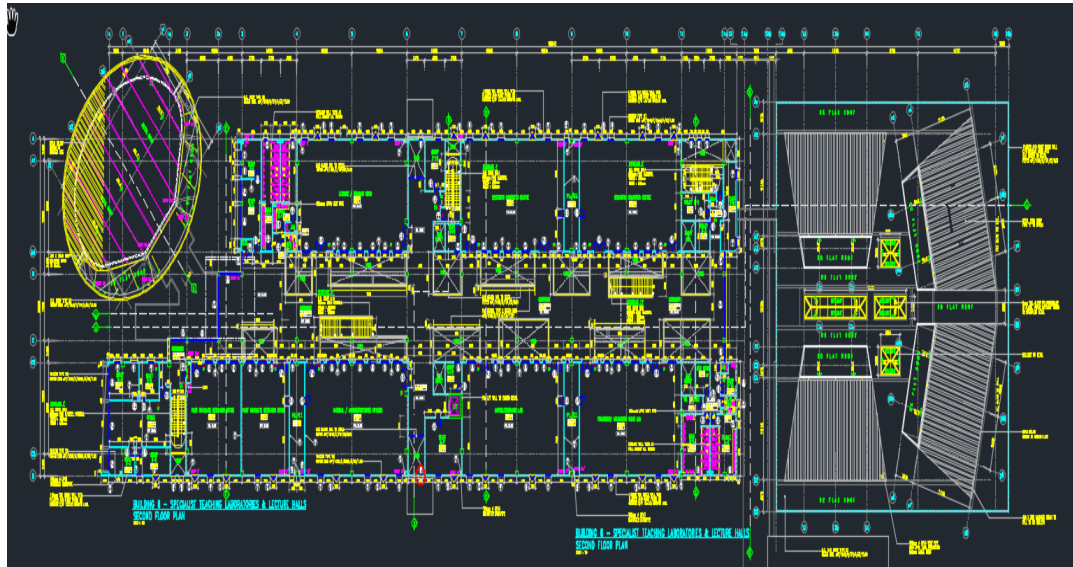


Figure 3.3: AutoCAD drawing of Block E second floor.

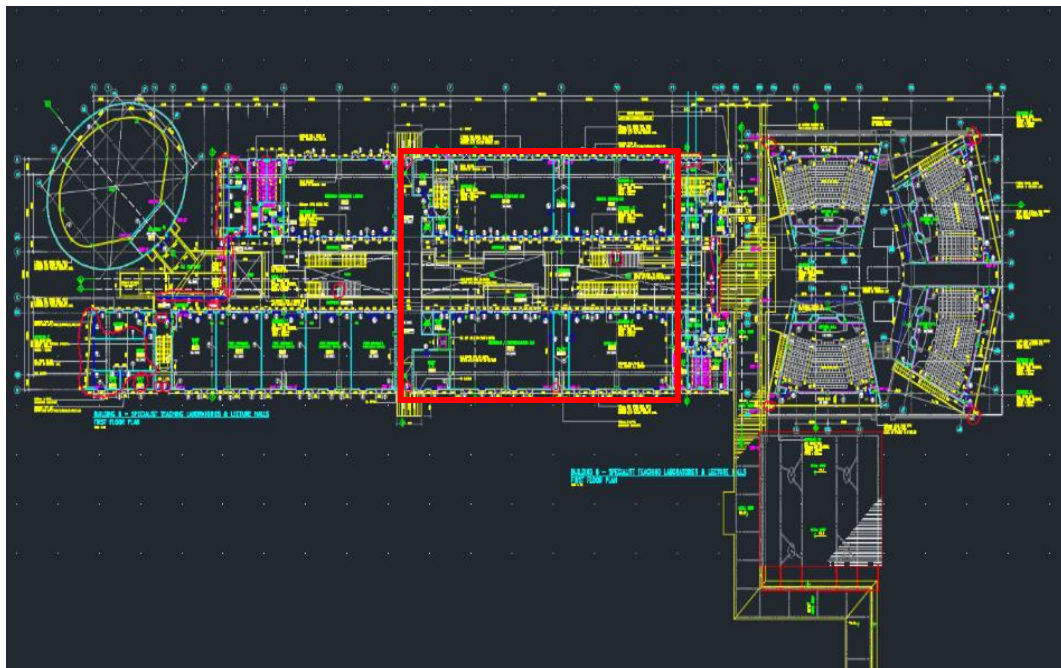


Figure 3.4: The area of study in Block E.

3.1.2 On-site Measurements

The detailed dimensions of structures are a procedure of documentation in the methodology phase. The AutoCAD provides a high precision of structure's dimensions to numbers of decimal places. The existing structure has dimensions which are not compatible with the actual dimensions given in the structural plan where the deviation of dimensions occurred on the existing structure. The dimensions of the beam are important as a reference value for the calculation in structural design. Hence, measurements are carried out on the Block E structure dimension by using the laser range meter shown in Figure 3.5. A total of 15 beam types and 3 column types with different dimensions are measured and the width and depth for each element are tabulated in Table 3.1.



Figure 3.5: A laser range meter is used to measure the dimension of the structure.

Table 3.1: Dimension of beams and columns.

Beams	Dimension (mm) (width x depth)
Beam 1	650 x 800
Beam 2	850 x 1500
Beam 3	375 x 800
Beam 4	300 x 1100
Beam 5	650 x 1050
Beam 6	675 x 875
Beam 7	150 x 875
Beam 8	250 x 875
Beam 9	200 x 600
Beam 10	450 x 750
Beam 11	550 x 800
Columns	Dimension (mm) (width x depth)
Column 1	650 x 650
Column 2	800 x 800
Column 3	500 x 500
Round Column	Dimension (mm)
Column 1	650

3.2 ETABS 2016 Modelling

The building undergoes structural modeling and analysis using a structural analysis software which is ETABS 2016. ETABS 2016 is preferred methods of modeling in this study because of the high accuracy and fast running features. The model is created by starting with the development of the schematic drawing of the block e building. Information such as the beam, column and wall location as well as the room dimensions are referred from the AutoCAD drawings into the ETABS schematic drawing. On the other hand, the dimension of structural elements such as width and depth which unavailable in AutoCAD are obtained from the on-site measurement methodology explained in section 3.1.2. This building materials properties of concrete and reinforcement are defined in ETABS using the values in Table 3.2. Frame section is later defined to specify the frame section properties such as the shapes, materials and dimensions of the section. The frame section shape definition in shown in Figure 3.6 whereas the materials and dimensions definition is given in Figure 3.7.

Table 3.2: Block e building materials properties.

Building Properties	Value
(i) Concrete	
Specific weight	25 kN/m ³
Modulus of elasticity	31000 N/mm ²
(ii) Concrete grade 25/30	
Cylinder crushing strength	25 N/mm ²
Cube strength	30 N/mm ²
(iii) Concrete grade 30/37	
Cylinder crushing strength	30 N/mm ²
Cube strength	37 N/mm ²
Concrete compressive strength	25 MPa
(iv) Reinforcement grade 500	
Modulus of elasticity	200000 N/mm ²
yield strength	500 MPa

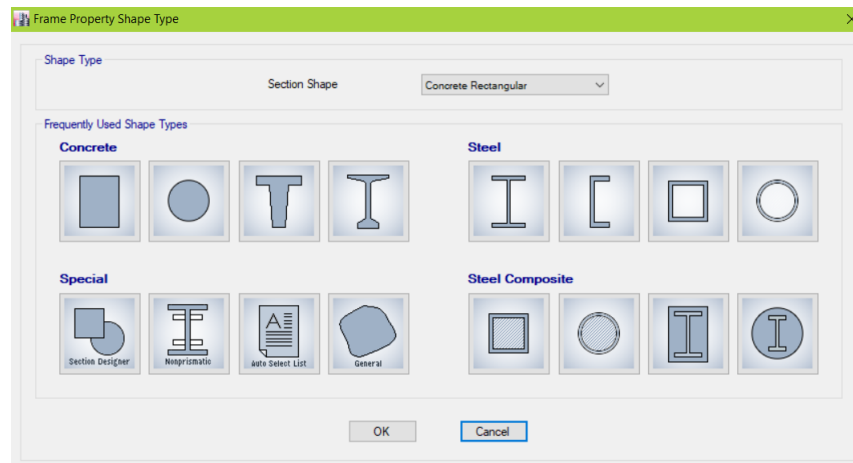


Figure 3.6: Shape definition of frame section.

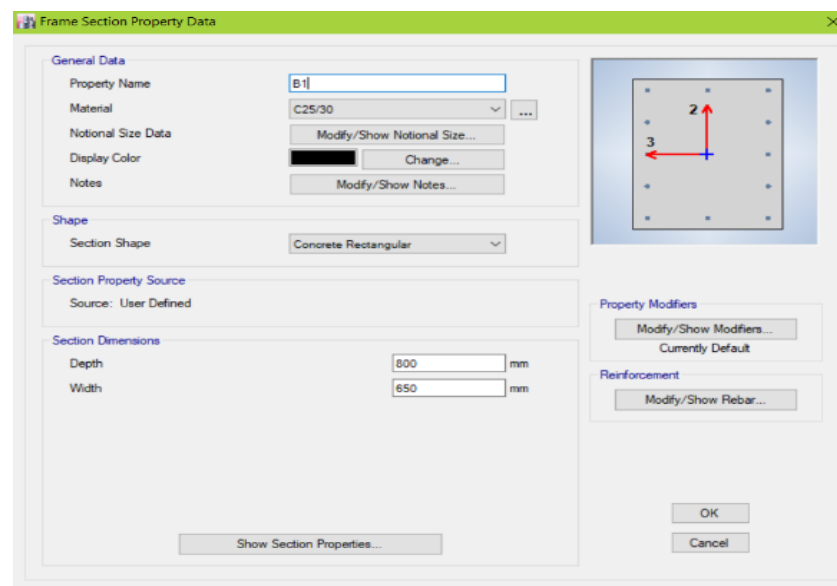


Figure 3.7: Material and dimension definition of frame section.

After defining the frame section properties, different types of load are assigned onto the frame section of building. The type of variable load, G_k present in the building are categorized according to the function of the loaded area and is distributed uniformly along the section. Mosley, Hulse and Bungey had suggested the values for variable load according to the function of that area as shown in Table 3.3.

Table 3.3: Variable loads Defined in ETABS 2016. (Mosley, Hulse and Bungey, 2012)

Loaded Area	Variable Loads, q_k (kN/m ²)
Office	3.0
Laboratory	3.2
Classroom	4.0
Corridor	3.0
Rooftop	0.4

The grid lines created in the ETABS model have navigation purpose which allowed the building to be viewed from different directions of the plan view and elevation view. The side section view, elevation section view and three-dimensional view of the buildings are shown in Figure 3.8, Figure 3.9 and Figure 3.10 respectively.

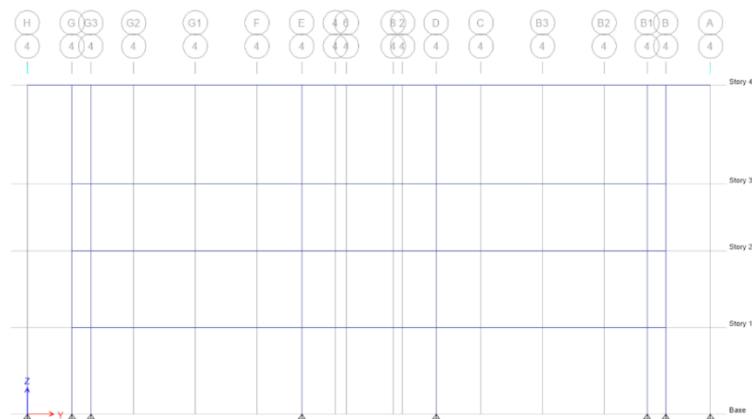


Figure 3.8: Side section view of building in ETABS 2016.

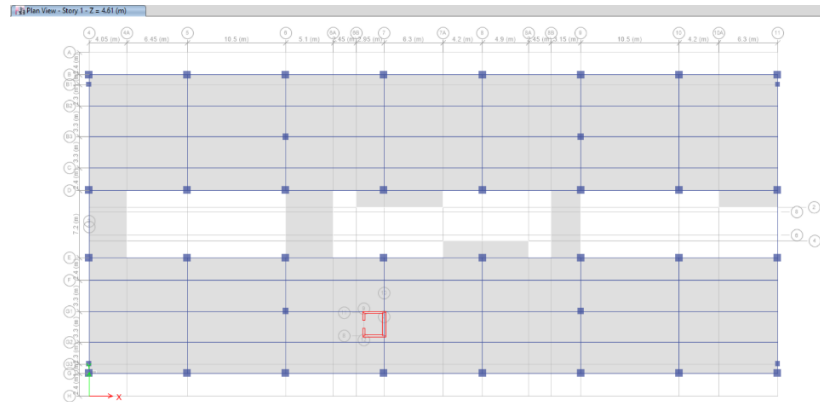


Figure 3.9: Elevation section view of building first floor in ETABS 2016.

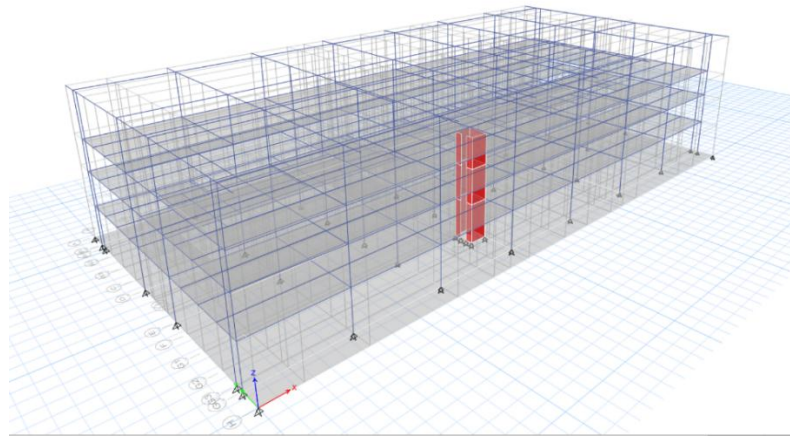


Figure 3.10: 3-dimensional schematic drawing of building in ETABS 2016.

Fire can occur in all the compartment of the building whereby each of the compartments has different occupancy and load. In the institutional building, places where students, computers, hazardous material are present are considered as sensitive compartments during the fire. Therefore, analysis of the fire scenario is required to be conducted on the compartment to evaluate the fire hazard risk on the occupants. The factors such as fire plume escape from the openings of the compartment and heat transfer through the radiation and convection process are not considered in the compartment fire analysis. Hence, external members of the building such as the corridor

and balcony are not evaluated in this study. In this study, four compartments from different levels of the building are selected as a sample compartment to represent the actual scenario of fire occurrence. The represented types of fire compartment are the classroom, office, laboratory and computer lab. The characteristics of these four fire compartments are tabulated in Table 3.4. Furthermore, the locations of classroom, office, laboratory and computer room that will undergo structural analysis in AutoCad are highlighted in Appendix A (i) to (iv) respectively.

After running the ETABS 2016 model on the structure, the beam with the highest moment is selected as the beam will undergo structural analysis in chapter 4. In fire room classroom, there are two types of beams present inside the room which are the beam number 3 and 5 whereas the rest of the fire room office, laboratory and classroom have 3 beam types which are beam number 1, 2 and 3. The location of beams in computer room, office, laboratory and classroom are highlighted and labeled in Figure 3.11 to Figure 3.14.

Table 3.4: Characteristics of 4 fire compartments subjected to fire.

Fire Room	Floor Level	Total Floor Area (m²)	Length, L (m)	Width, w (m)	Height, H (m)	Figure
Classroom	First floor	236.4	18.5	12.78	3.6	Appendix A (i)
Office	Ground floor	34.4	3.02	11.4	4.61	Appendix A (ii)
Laboratory	Second floor	236.4	16.6	14.24	3.6	Appendix A (iii)
Computer Room	Ground floor	233.6	19.5	11.98	4.61	Appendix A (iv)

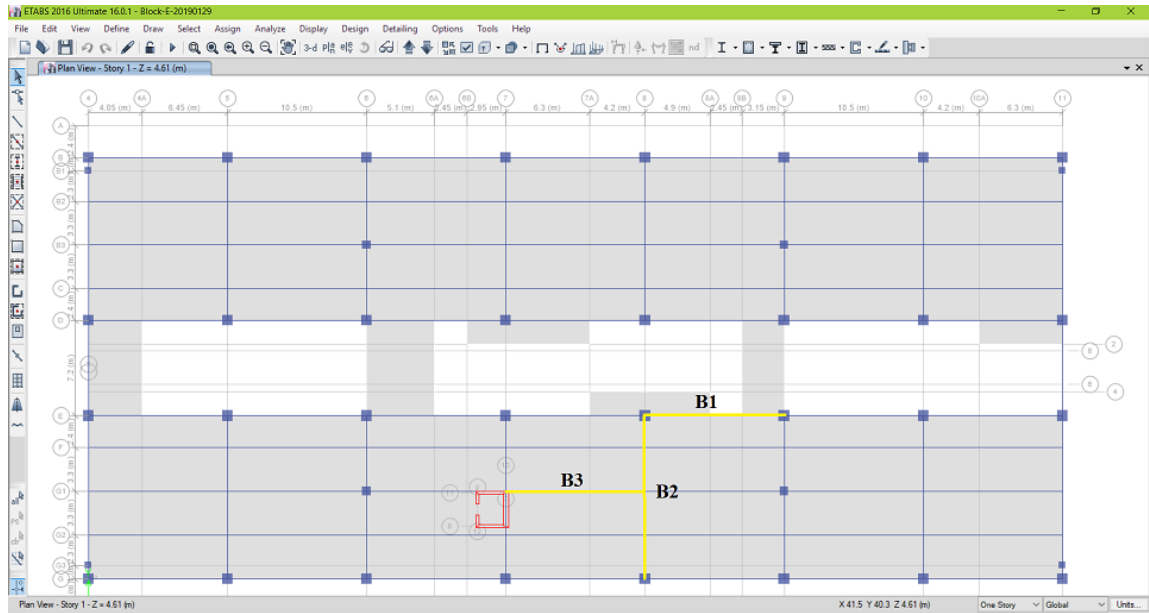


Figure 3.11: Beams location in computer room.

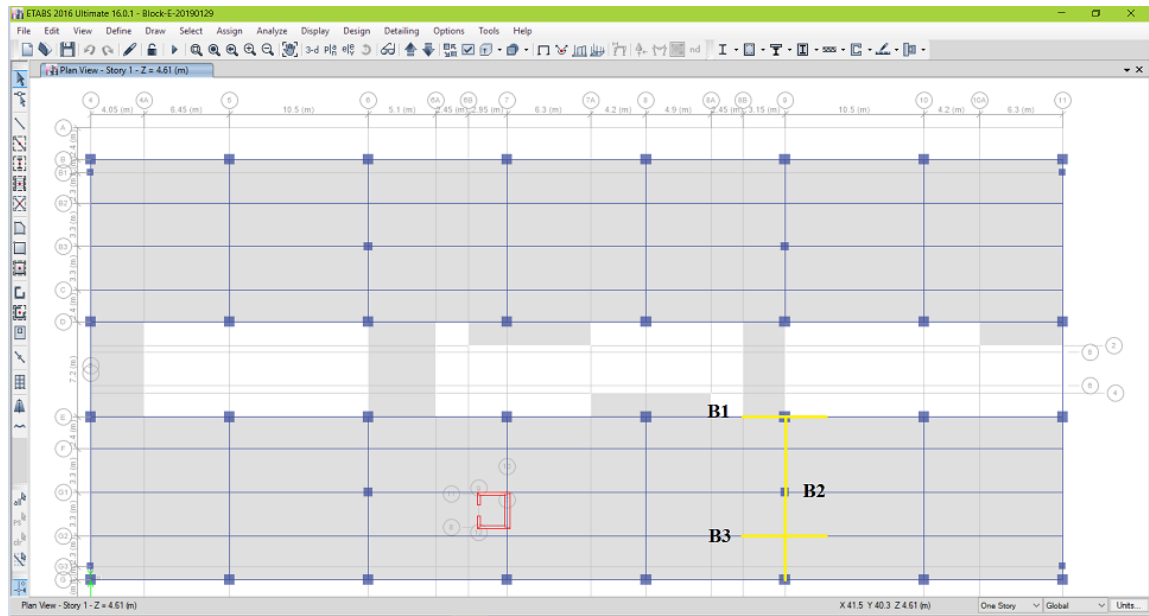


Figure 3.12: Beams location in office.

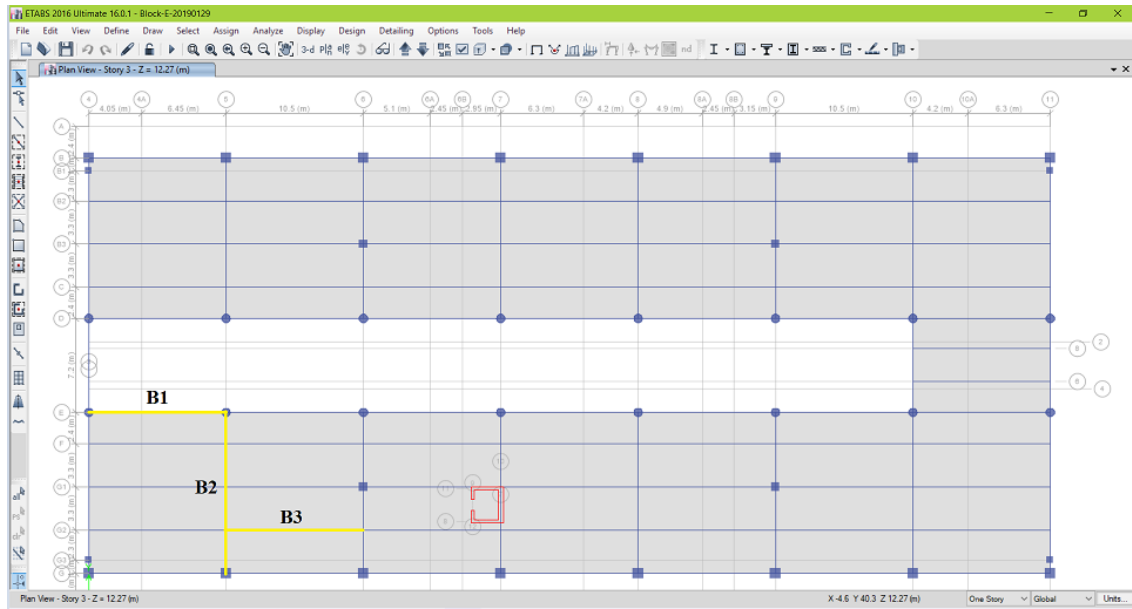


Figure 3.13: Beams location in laboratory.

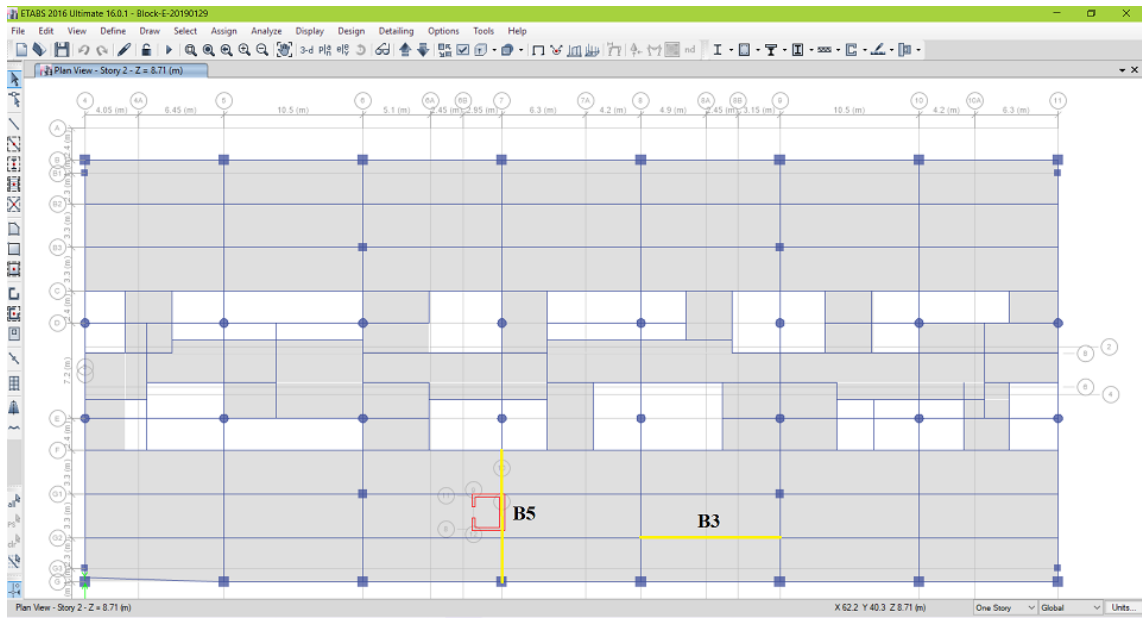


Figure 3.14: Beams location in classroom.

3.3 Fire Resistance Analysis Process

The evaluation of the structural response of a building during an accidental event of fire subjected to many uncertainties. The requirement of a lot of information on the elements such as the increased temperature development effect on the fire severity and the property changes of building materials during the fire is needed to propose a methodology of assessment. In this study, the proposed method to assess the load bearing capacity of the structural elements is represented in the flowchart in Figure 3.15. The assessment first started with the on-site evaluation of the building's structure to collect basic information such as the measurement of the beam, column and slab. During the actual fire event, the characteristics of fire-exposed structural elements are assumed to undergo structural degradation such as deflection. The above situation can be the assumed fire damage that occurred at fire event. An investigation on the fire severity is carried by determining the load bearing capacity using the FORM method. The result from the intended load bearing capacity is further evaluated to compare the reliability index with the target reliability index, $\beta_{t,50}$ defined in EN 1990 which is 3.8 for fifty years of the reference period. From the safety perspective, a conclusion is made on the safety of structural elements during fire.

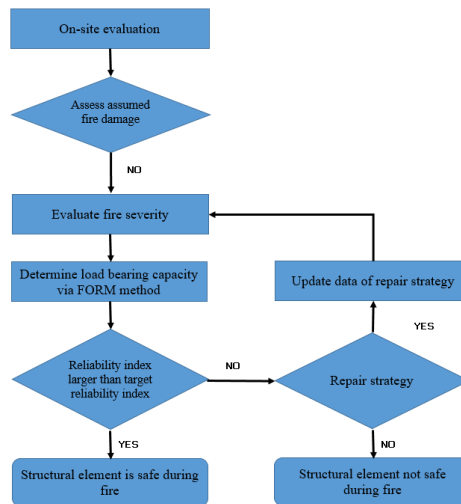


Figure 3.15: Flowchart of methodology for fire assessment of structural element's load bearing capacity.

During the actual fire situation, the loads are lower than the load at the maximum design condition of normal temperature. The assessment of load exists in the building during the accidental fire event can provide information on the stability of structural elements. Hence, the limit state of fire demand with consideration of the load combination is needed which is different from the load combination at a normal design situation. In this fire design situation, the permanent loads and variable loads are combined according to EN 1990. The frequent value of variable loads is derived from the multiplication of the characteristic variable loads, Q_k and the combination factor for the frequent value of variable loads, Ψ_1 . As an example, the variable loads is greatly depend on the function served by the building, the institutional building falls on the category with combination factor for the frequent value of a variable load, Ψ_1 of 0.7 as provided in Figure 3.16. The design load combination in EN 1990 for the accidental fire design situation, $E_{d,f}$ is the combined effect of permanent load, G_k and the frequent value of variable load as stated in Figure 3.17. The equation for fire design load combination is represented in Eq. (3.15).

$$E_{d,f} = G_k + \Psi_1 Q_k \quad (3.15)$$

On the other hand, different codes such as the United State Standards (ASCE) and Australia Standard (SA) had recommended the permanent load and variable load with their respective value of combination factor. The limit state load combination equation at fire situation of the above codes is tabulated in Table 3.5.

Action	ψ_0	ψ_1	ψ_2
Imposed loads in buildings, category (see EN 1991-1-1)			
Category A : domestic, residential areas	0,7	0,5	0,3
Category B : office areas	0,7	0,5	0,3
Category C : congregation areas	0,7	0,7	0,6
Category D : shopping areas	0,7	0,7	0,6
Category E : storage areas	1,0	0,9	0,8
Category F : traffic area, vehicle weight $\leq 30\text{kN}$	0,7	0,7	0,6
Category G : traffic area, $30\text{kN} < \text{vehicle weight} \leq 160\text{kN}$	0,7	0,5	0,3
Category H : roofs	0	0	0
Snow loads on buildings (see EN 1991-1-3)*			
Finland, Iceland, Norway, Sweden	0,70	0,50	0,20
Remainder of CEN Member States, for sites located at altitude $H > 1000\text{ m a.s.l.}$	0,70	0,50	0,20
Remainder of CEN Member States, for sites located at altitude $H \leq 1000\text{ m a.s.l.}$	0,50	0,20	0
Wind loads on buildings (see EN 1991-1-4)	0,6	0,2	0
Temperature (non-fire) in buildings (see EN 1991-1-5)	0,6	0,5	0
NOTE The ψ values may be set by the National annex.			
* For countries not mentioned below, see relevant local conditions.			

Figure 3.16: The value for the combination factor for variable loads, Ψ_1 . (EN 1990)

Design situation	Permanent actions		Leading accidental or seismic action	Accompanying variable actions (**)	
	Unfavourable	Favourable		Main (if any)	Others
Accidental (*) (Eq. 6.11a/b)	$G_{k,j,\text{sup}}$	$G_{k,j,\text{inf}}$	A_d	$\psi_{1,i}$ or $\psi_{2,i} Q_{k,i}$	$\psi_{2,i} Q_{k,i}$
Seismic (Eq. 6.12a/b)	$G_{k,j,\text{sup}}$	$G_{k,j,\text{inf}}$	$A_{Ed} = \eta A_{Ek}$	$\psi_{2,i} Q_{k,i}$	

(*) In the case of accidental design situations, the main variable action may be taken with its frequent or, as in seismic combinations of actions, its quasi-permanent values. The choice will be in the National annex, depending on the accidental action under consideration. See also EN 1991-1-2.

(**) Variable actions are those considered in Table A1.1.

Figure 3.17: Permanent action and variable action in design accidental situation. (EN 1990)

Table 3.5: Limit state load combination equation at fire situation by different codes.

Codes	Permanent Load	Variable Load	Load Combination
Eurocode 0 (2002)	G_k	$0.7Q_k$	$G_k + 0.7 Q_k$
US Standard, ASCE (2010)	$1.2 G_k$	$0.5 Q_k$	$1.2 G_k + 0.5 Q_k$
Australia/ New Zealand Standard (2002)	G_k	$0.4 Q_k$	$G_k + 0.4 Q_k$

The material thermal properties are important in determining the temperature of the compartment during fire. The materials that made up the wall and ceiling had thermal properties which are used in the Etabs model. The heat loss of materials is different and they are characterizing according to factors such as the heat capacity, c_p , density, ρ and thermal conductivity, λ . The different building materials are available and their respective thermal properties are suggested by EN 1990-1-2 and represented in Figure 3.18.

Material	Temperature [°C]	λ [W/m/K]	ρ [kg/m ³]	c_p [J/kg°C]
Normal weight concrete	20	2	2300	900
	200	1,63	2300	1022
	500	1,21	2300	1164
	1000	0,83	2300	1289
Light weight concrete	20	1	1500	840
	200	0,875	1500	840
	500	0,6875	1500	840
	1000	0,5	1500	840
Steel	20	54	7850	425
	200	47	7850	530
	500	37	7850	667
	1000	27	7850	650
Gypsum insulating material	20	0,035	128	800
	200	0,06	128	900
	500	0,12	128	1050
	1000	0,27	128	1100
Sealing cement	20	0,0483	200	751
	250	0,0681	200	954
	500	0,1128	200	1052
	800	0,2016	200	1059
CaSi board	20	0,0685	450	748
	250	0,0786	450	956
	450	0,0951	450	1060
	1050	0,157	450	1440
Wood	20	0,1	450	1113
	250	0,1	450	1125
	450	0,1	450	1135

Figure 3.18: Thermal properties of building materials. (EN 1990-1-2)

3.3.1 Limit State Equation

Limit state equation evaluated the structure reliability and modeling of structure based on the limit state equation in defining the resistance of the structure to load applied. The pure bending characteristics of the structure are represented in the limit state function which served as a safety margin. According to EN 1990, the limit state equation is valid when the design moment induced by design load, M_{Ed} is less than the design moment of

resistance, M_{Rd} . The relationship of M_{Ed} less than M_{Rd} needed to be verified and represented in Eq. (3.24).

$$M_{Ed} \leq M_{Rd} \quad (3.24)$$

The limit state function is represented by $G(X)$ as a function of the random vector in reliability analysis, and the function is equal to zero, $G(X) = 0$. Failure of reliability analysis is solved by numerically integrating the joint probability density function, $f_x(X)$ in failure probability, P_f via several reliability methods such as MCS, FORM and SORM over the region of failure as showed in Eq. (3.24). (Guo, Q. R., 2015)

$$G(X) < 0 \quad (3.25)$$

In Van Coile, R. and Bisby, L. (2017), the beam the limit state equation, Z_{STR} in Eq. (3.26) represented the strength limit state for a concrete slab subjected to pure bending. The bending moment capacity during the fire, M_{Rd} and the bending moment induced by load effect, M_{Ed} were represented the R and L respectively. Equation 3.4 below showed the limit state equations used in structural design.

$$\begin{aligned} Z_{STR} &= K_R M_{Rd} - K_E M_{Ed} \\ &= K_R M_{Rd} - K_E (M_G + M_Q) \end{aligned} \quad (3.26)$$

3.3.2 Uncertainties in Limit State Equation

The uncertainties present in the limit state equation such as the beam width, b beam depth, d , concrete compressive strength, f_{ck} , reinforcement yield strength, f_{yk} , model uncertainty for resistance, K_r and model uncertainty for load, K_e will be analyzed in the

FOSM (sec. 3.3.3) and FORM (sec. 3.3.4). These uncertainties served as basic variables in the evaluation of structural analysis, all of the variables are independent of each other. These uncertainties are not model via a deterministic approach but through the probability distribution functions of the uncertainties.

An EasyFit software is used to obtain the mean, μ and standard deviation, σ of uncertainties which had a large number of data distributions. A minimum of 5 sets of input data needs in order to run the statistical distribution. EasyFit is able to select the most suitable probability distribution that fits into the input data with the respective mean, μ and standard deviation, σ value. Random variables such as concrete compressive strength, f_{ck} and reinforcement yield strength, f_{yk} both have a lognormal distribution. However, the probabilistic values of concrete compressive strength, f_{ck} and reinforcement yield strength, f_{yk} changes during elevated temperature are undetermined due to the lack of statistical information available. Hence, the probabilistic values for mean and coefficient of variance of f_{ck} and f_{yk} are taken the same values at the ambient temperature of 20°C which are 42.9, 0.15 and 581.4, 0.07 respectively. (Van Coile, R., 2015)

In this study, sets of beam width, b and beam depth, d data from the on-site measurements are imported into EasyFit to obtain the mean, μ and standard deviation, σ value. Ten sets of beam 1 on-site cross section measurements are analyzed in EasyFit as given in Table 3.6. The EasyFit fitting analysis results for beam width has a mean, μ of 659.7 and standard deviation, σ of 28.852 whereas beam depth has a mean, μ of 802 and standard deviation, σ of 15.895. The input data of beam width, b a best normal distribution fitting, their EasyFit results of mean, μ and standard deviation, σ and the graph of probability density function are given in Figure 3.18 and Figure 3.19. Besides, the input data of beam depth, d a best normal distribution fitting, their EasyFit results of mean, μ and standard deviation, σ and the graph of probability density function are given in Figure 3.20 and Figure 3.21.

Table 3.6: Input data of beam width, b and depth, d in EasyFit.

Beam width, b	Beam depth, d
658	821
697	823
703	813
643	800
665	806
622	815
689	788
623	791
645	780
652	783

Fitting Results		
#	Distribution	Parameters
1	Lognormal	$\sigma=0.00813$ $\mu=6.3099$
2	Lognormal (3P)	$\sigma=0.20279$ $\mu=3.0886$ $\gamma=527.61$
3	Normal	$\sigma=5$ $\mu=550$

Figure 3.19: Fitting analysis result Beam 1 width, b.

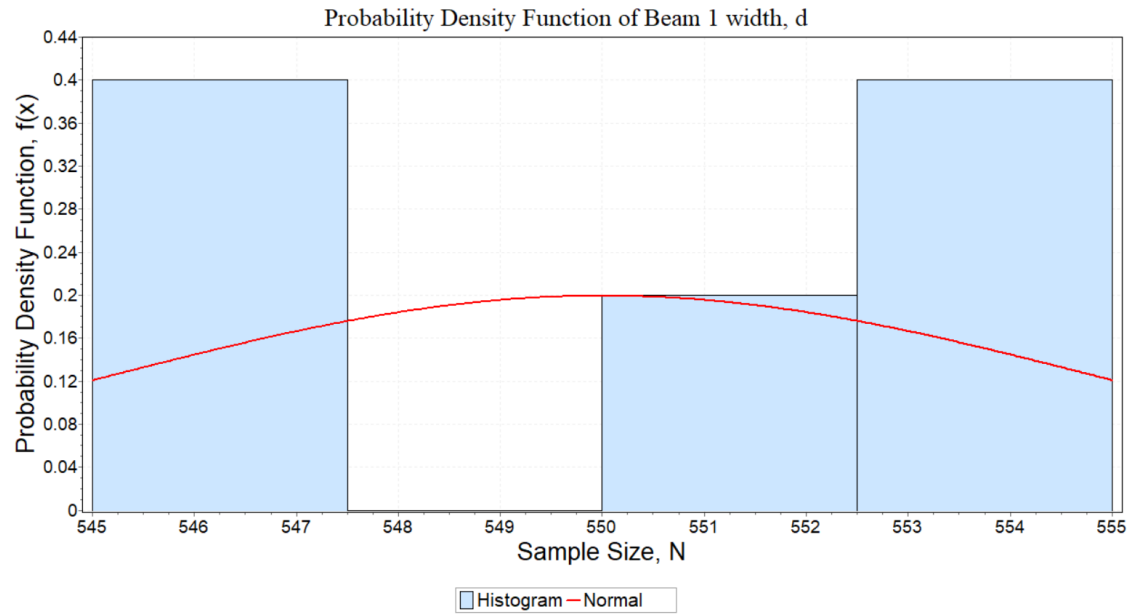


Figure 3.20: Graph of the probability density function of Beam 1 width, b.

Fitting Results		
#	Distribution	Parameters
1	Lognormal	$\sigma=0.00688$ $\mu=6.4769$
2	Lognormal (3P)	$\sigma=0.1468$ $\mu=3.4108$ $\gamma=619.35$
3	Normal	$\sigma=5$ $\mu=650$

Figure 3.21: Fitting analysis result Beam 1 depth, d.

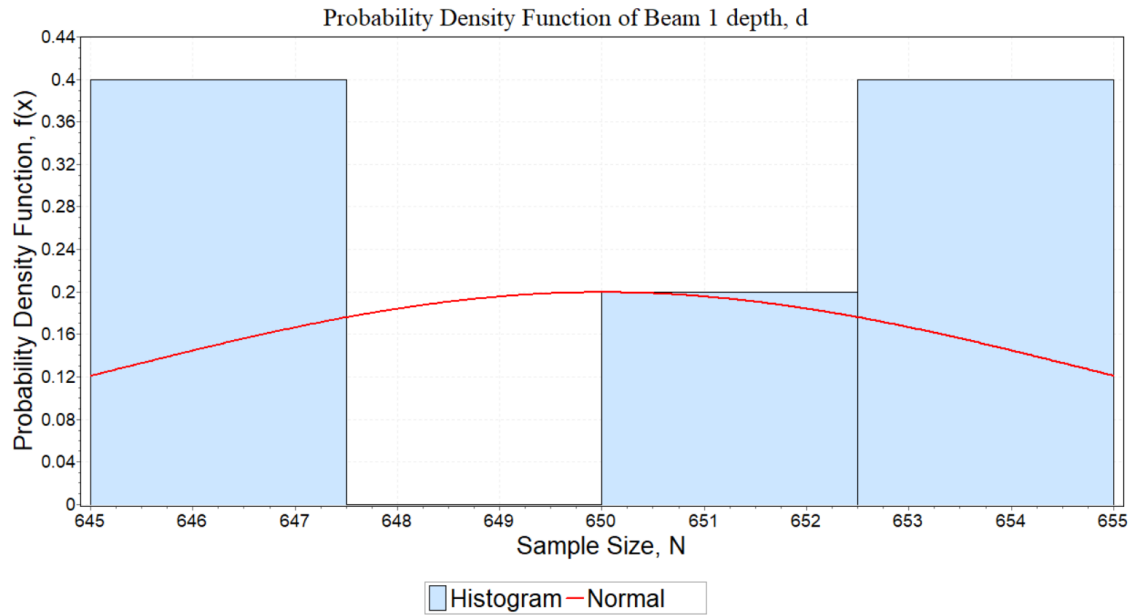


Figure 3.22: Graph of the probability density function of Beam 1 depth, d.

The result from EasyFit for beam width and depth of beam 1 are tabulated in Table 3.7 together with other load and resistance uncertain parameters in the limit state Eq. (3.26). On the other hand, probabilistic model for the rest of the uncertainties such as concrete compressive strength, f_{ck} , reinforcement yield strength, f_{yk} , model uncertainty for resistance, K_r and model uncertainty for load, K_e is obtained from literature studies which are constantly updated. The probabilistic model consisted of the probabilistic distribution type, mean, and variance.

Table 3.7: Results of beam width, b and beam depth, d of four beams type from EasyFit.

Beam No	Beam Width, b (mm)		Beam Depth, d (mm)	
	Mean, μ	Standard Deviation, σ	Mean, μ	Standard Deviation, σ
1	550	5	650	5
2	800	5	1200	5
3	300	5	650	5
5	950	5	500	5

Table 3.8: Probabilistic model of load and resistance uncertain parameters.

Parameter	Dimension	Probability Distribution	Mean, μ	Standard Deviation, σ	Author
b	mm	Normal	Refer to Table 3.7		EasyFit
d	mm	Normal	Refer to Table 3.7		EasyFit
$f_{ck,20}^{\circ C}$	MPa	Lognormal	42.9	0.15	[18], [20], [22]
			28.08	12.5	[22]
$f_{yk,20}^{\circ C}$	MPa	Lognormal	581.4	0.07	[18], [20], [22]
			293.03	11.5	[22]

K_R	-	Lognormal	1.1	0.11	[18]
K_E	-	Lognormal	1	0.1	[18], [22]

3.3.3 Reliability index manual calculation

The First-Order Second-Moment method (FOSM) is used in the manual calculation of the reliability index, β . In FOSM, the limit state equation must be a linear equation and only the mean and standard deviation of the random variables are considered in the equation of reliability index, β . The second moment statistic of mean, μ and standard deviation, σ the random variables are useful in the reliability index, β formulation. The reliability index, β is expressed in equation 3.12 which derived by Nowak, A. S., and Collins, K. R., 2013.

$$\beta = \frac{\sum_{i=1}^n a_i \mu x_i}{\sqrt{\sum_{i=1}^n (a_i \sigma x_i)^2}} \quad (3.12)$$

Total six random variables are used in FOSM analysis which includes in the limit state equation are the concrete compressive strength, f_{ck} , reinforcement yield strength, f_{yk} , beam width, b , beam height, d , model uncertainty for resistance, K_R and model uncertainty for load, K_E . The mean, μ and standard deviation, σ of the above four random variables, X_i are given in Table 3.7. The limit state equation is known as the G performance function $G(X)$ of X number of random variables. The Moment resistance is denoted as R whereas load effect is donated as L . Hence, the limit state equation now became Eq. (3.13)

$$G(f_{ck}, f_{yk}, b, d, K_R, K_E) = R(K_R) - L(K_E) \quad (3.13)$$

3.3.4 Reliability index Matlab calculation

Matlab have various functions such as mathematical computational, algorithm development, structural modeling and structural data analysis. Matlab has a Ferum 4.1 compiler and it consists of 2 major files on this structural analysis which are the gfun file and inputfile. The First-Order Reliability method (FORM) is used in the Matlab calculation of the reliability index, β . FORM solved the linear polynomial equation of the limit state equation with the power of one.

In gfun file, the limit state equations with the random variables are defined as well as the equation for both resistance effects and load effects. On the other hand, the distribution type, mean and variance of random variables used in the limit state equation redefined in inputfile. FORM analysis in Matlab is run to obtain the output of reliability index, β .

CHAPTER 4

RESULTS AND DISCUSSION

4.0 Fire Resistance Analysis

This study presents the beam structural behavior analysis under parametric fire exposure and the safety of structure. The steps for the analysis of building's fire resistance are listed in the flow chart as shown in Figure 4.1. Further explanation on the 5 steps of building's fire resistance analysis is found from subsection 4.1 to 4.5.

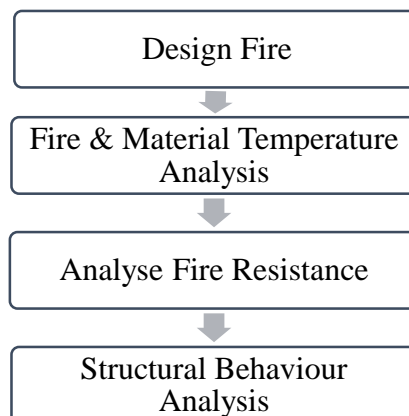


Figure 4.1: Steps for the analysis of building's fire resistance.

4.1 Design Fire

Fire rooms are subjected to the Eurocode parametric fire exposure in this study. The response of fire temperature in different fire room under the parametric fire exposure is compared to the ISO 834 fire exposure and evaluated.

4.1.1 Eurocode Parametric Fire

The Eurocode parametric fire is a fully developed design fire which the need to be resisted building structure need to resist. This fire model represented the natural fire exposure which has taken into consideration of physical -characteristics of the compartment such as the compartment's ventilation factor, opening factor and thermal properties of the material. The parametric fire model is only applicable to fire room with floor area that less than 500 m², room height less than 4 m and the absence of roof opening.

The parametric fire is more realistic than the standard fire model which does not consider the fire compartment characteristics. The equation of Eurocode parametric fire temperature, T_g (°C) is calculated using the heat and mass balance equation and can be determined according to Eq. (4.1).

$$T_g = 20 + 1325 (1 - 0.0324 e^{-0.2 t^*} - 0.204 e^{-1.7 t^*} - 0.472 e^{-19 t^*}) \quad (4.1)$$

The fictitious time, t^* is given in equation Eq. (4.2).

$$t^* = \Gamma t \quad (4.2)$$

The t is the time in hour and Γ equation is shown in equation Eq. (4.3).

$$\Gamma = \frac{(O / b)^2}{(0.04 / 1160)^2} \quad (4.3)$$

Opening factor, O must range from 0.02 to 0.2 m^{1/2} as shown in Eq. (4.4) and b is the thermal inertia.

$$O = \frac{A_v \sqrt{H_v}}{A_t} \quad (4.4)$$

Here, the dimensions of room's vertical opening are necessary to calculate the opening factor, the values for the total area of vertical opening, A_v, average height of vertical opening, H_v, total enclosure area, A_t are provided in Table 4.2. The thermal inertia, b explained the amount of heat energy that the room's boundary material, wall, roof and floor can absorb. Thermal inertia Eq. (4.5) consisted of the thermal conductivity, λ density, ρ and heat capacity, c_p of the fire room's boundary materials, these values are derived from EN 1992-1-2 in Table 4.1 which is the normal weight concrete at ambient temperature. The acceptable value for thermal inertia should range from 100 to 2200 J/m²s^{1/2}K.

$$b = \sqrt{\lambda \rho c_p} \quad (4.5)$$

Table 4.1: Thermal properties of room boundary material.

Thermal Properties of Normal Weight Concrete	Values	Reference
Thermal conductivity, λ (W/mK)	2	EN 1992-1-2
Density, ρ (kg/m ³)	2300	EN 1992-1-2
Heat Capacity, c _p (J/kg ⁰ K)	900	EN 1992-1-2
Thermal Inertia, b (J/m ² s ^{1/2} K)	2035	EN 1992-1-2

4.1.2 Opening Factor

Opening factor is also called as the ventilation factor which indicates the amount of oxygen present in a fire room. Opening factor takes into account the area of the vertical openings, A_v area of total area of the enclosure, A_t and the height of the compartment, H which is mentioned in Eq. (4.4). In all the fire rooms studied, there are more than one window opening on the wall and hence the calculation of opening factor is based on the multiple opening presences in the room. The types of opening existed in the fire rooms are windows and door only, the average height of the window and door are taken as the height of vertical opening, H_v . During the actual fire outbreak, all the window and door are assumed to be opened for occupant evacuation. Besides, it is also expected that the air flow throughout the vertical openings are the same and implied that no wind flow effect occurs through the openings which may increase the rate of fire burning. (Buchanan & Abu, 2017) In order to visualize the location of vertical openings in a fire room for opening factor calculation, an AutoCad drawing of classroom is drawn and is shown in Figure 4.2.

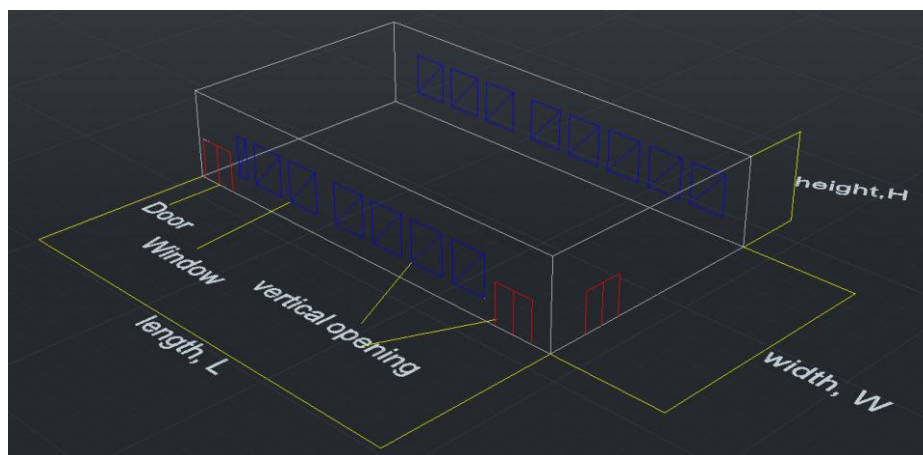


Figure 4.2: AutoCad drawing of multiple vertical openings presence in fire room for opening factor calculation.

Opening factor has affected the fuel burning rate and fire temperature reached in fire rooms. The fire room with the largest total area of vertical openings will give rise to the highest opening factor. Laboratory has the largest vertical openings and hence this room has the highest opening factor among the fire rooms. The opening factor in descending order is $0.0963 \text{ m}^{1/2}$, $0.0848 \text{ m}^{1/2}$, $0.0816 \text{ m}^{1/2}$ and $0.0192 \text{ m}^{1/2}$ which represents laboratory, computer room, classroom and office respectively. Table 4.2 presented the values of opening factor with dimensions of vertical opening in four fire rooms.

Table 4.2: Opening factor of four fire rooms.

Fire Room	Total area of the vertical openings, A_v (m^2)	Average height of vertical opening, H_v (m)	Total area of enclosure, A_t (m^2)	Opening Factor, O ($\text{m}^{1/2}$)
Classroom	40.1	2	694.7	0.0816
Office	2.35	2	173.5	0.0192
Laboratory	47.3	2	694.7	0.0963
Computer Room	41.3	2	689.1	0.0848

4.2 Fire & Material Temperature Analysis

4.2.1 Fire Load in Compartments

Fire load can greatly affect the temperature that the fire can reach in a building compartment. In different compartment of the building, the fire growth largely depends on the presence of the amount of fuel. The fuel load inside fire room is divided into permanent and variable load. Permanent load such as table and shelf are fixed inside the room whereas variable load such as chair and book those are movable. Each individual type of flammable materials in the compartment serves as a fuel for burning and they are classified into 3 main types which are wood, paper and consumables. The state of fuel that burned can be in many states such as solid, liquid and gas and may have different burning characteristics. For example, solid fuel type such as wooden tables and chairs are present in classrooms and offices whereas liquid fuel type such as chemicals and flammable solutions are found in laboratories. A calculation of the total mass of fuels available in 4 types of compartments in Block E building is tabulated in Table 4.3.

The burning materials released heat energy in the atmosphere and the amount of release can be expressed in term of the calorific value, ΔH_c and energy contained value, E . The properties of the burning material are taken into account during the calculation of fire load, Q_{fi} , the product of the sum of combustible material, M , the net calorific value, ΔH_c divide by the total compartment floor area, A_f defined the fire load equation. The recommended value for the net calorific value of burning material, ΔH_c , is suggested by EC1 used in column three in Table 4.4. In this parametric fire model, all the fuel presence inside the fire room is assumed to be totally burnt out. The equation of fire load, Q_{fi} which provided in EC1 is given in Eq. (4.6). The calorific value, ΔH_c , energy contained value, E , fire load density, e_f and total fire load, Q_{fi} are calculated and presented in column eight in Table 4.4.

$$Q_{fi} = \frac{\sum M \times \Delta H_c}{A_f} \quad (4.6)$$

Table 4.3: Total mass of fuel presence in different fire compartment.

Types of Fire Compartment	Materials	List if Items	Quantity	Mass, M (kg)	Total Mass, M (kg)
Classroom	Wood	Chair	130	5	3250
		Small Table	130	20	
Office	Wood	Chair	4	5	140
		Small Table	4	20	
		Shelf	2	20	
	Paper	Book	20	0.5	50
	Plastic	Computer	3	5	15
Laboratory	Wood	Chair	30	7	1350
		Large Table	8	80	
		Shelf	10	50	
	Chemical	Alcohol	-	15	15
Computer Room	Wood	Chair	30	5	870
		Large Table	8	80	
	Plastic	Computer	30	5	150

Table 4.4: Total fire load in different fire compartment.

Types of Fire Room	Material	Calorific Value	Weight	Energy Contained Value	Total Floor Area	Fire Load Energy Density	Total Fire Load
		ΔH_c	M	$E = M \Delta H_c$	A_f	e_f	Q_{fi}
		(MJ/kg)	(kg)	(MJ)	(m ²)	(MJ/m ²)	(MJ/m ²)
Classroom	Wood	17.5	3250	56875	236.4	240.59	240.6
Office	Wood	17.5	140	2540	34.4	71.22	111.2
	Paper	20	50	1000		29.07	
	Plastic	25	15	375		10.9	
Laboratory	Wood	17.5	1350	23625	236.4	99.94	103.11
	Chemical	50	15	750		3.17	
Computer Room	Wood	17.5	870	15225	233.6	65.18	81.2
	Plastic	25	150	3750		16.05	

4.2.2 Maximum Compartment Temperature

In a room fire, the fire development is dependent on the total fire load, opening factor of the fire room and thermal properties of internal boundary materials. The realistic parametric fire undergoes two phases which are the fire development/heating phase and

the decay/cooling phase. During the heating phase of fire in room, the fuel inside the fire room continues to burn while emitting heat energy that raises the material temperature inside the apartment to maximum temperature, T_{\max} . Once the fuel load is exhausted, the room temperature starts to drop after a certain time and this is called the decay phase. Hence, the fire duration from the start of fire to the maximum fire temperature, t_{\max} and cooling time need to be determined. The temperature time relation of fire rooms is categorized into heating phase and decay phase of fire and tabulated in Table 4.7.

The equation of time to reach the maximum fire temperature, t_{\max} and the maximum fictitious time, t^* is given by Eq. (4.7) and Eq. (4.8) respectively.

$$t_{\max} = \frac{0.2 \times 10^{-3} \times Q_{fi,t}}{0} \quad (4.7)$$

$$t^* = t_{\max} \times \Gamma \quad (4.8)$$

The increase in compartment temperature is important to be examined since it can gradually damage the structural elements. The rate of fuel burning is affected by the opening factor, O . The expected maximum temperature, T_{\max} followed the temperature-time curves which incorporate the total fire load, $Q_{fi,t}$ into the calculation of t^* . The expected maximum temperature, T_{\max} is calculated using the Eq. (4.1).

When the fire temperature reaches maximum temperature, T_{\max} , fire starts to enter the cooling phase. The fire temperature drops gradually at the decay temperature, T_{decay} until the fire is suppressed or diminishes after consuming all the fuel. The fire temperature at decay phase, T_{decay} is given by Eq. (4.9).

$$T_{\text{decay}} = T_{\max} - 250 (3 - t^*_{\max}) (t^* - t^*_{\max}) \quad (4.9)$$

Table 4.5 presents the fire load, Q_{fi} , time to reach maximum fire temperature, t_{max} , and maximum fire temperature, T_{max} . The time of fire burn either slow or fast is greatly affected by variables such as the fire load, Q_{fi} and opening factor. According to Eq. (4.7), the time to reach the maximum fire temperature, t_{max} is directly proportional to the fire load, Q_{fi} and inversely proportional to the opening factor. Fire rooms that achieved the maximum fire temperature at the shortest time are computer room, laboratory, classroom and office and the time to reach the maximum fire temperature, t_{max} is 0.19 s, 0.21 s, 0.58 s and 1.16 s respectively.

In office, the time to reach the maximum fire temperature, t_{max} is the longest duration, which is 1.16 hours or 69.6 minutes. The office is provided with 111.2 MJ/m² fire load and opening factor of 0.0192 m^{1/2}. When the opening factor in office provide low ventilation, the speed of fire release heat will decrease and led to a slow fire development. Hence, the fire in office took the longest time to complete the fire growth and release heat the slowest with the limited oxygen available when compared to other fire room with a higher opening factor.

Table 4.5: Fire load, Q_{fi} and time to reach maximum fire temperature, t_{max} in fire rooms.

Fire Room	Fire load, Q_{fi} (MJ/m ²)	Opening Factor, O (m ^{1/2})	Time to reach maximum fire temperature, t_{max} (hr)	Maximum fire temperature, T_{max} (°C)
Classroom	240.6	0.0816	0.58	909.4
Office	111.2	0.0192	1.16	569
Laboratory	103.1	0.0963	0.21	812.5
Computer room	81.2	0.0848	0.19	768

The fire room took times to achieve the full fire development of heating phase from initial fire. From the results, time to reach the maximum fire temperature, t_{\max} in classroom, office, laboratory and computer room are 0.58 hr, 1.16 hr, 0.21 hr and 0.19 hr respectively. Moreover, all the fire room except the office had reached their maximum fire temperature, t_{\max} before 1 hour fire duration.

Right after 1 hour duration of fire, the room temperature starts to drop which indicate that the fire started to enter the decay phase. The decay phase starts due to the depletion of the fire material in the room. When fire load is insufficient to continue to support the burning fire and thus fire temperature drops and this situation is said as a fuel controlled fire development. The fire temperature will gradually decrease until the fire is suppressed and this will bring the temperature back to the ambient temperature of 27°C. Hence, the fire load is said to have a greater impact on the fire development and level of fire severity. Table 4.6 is constructed using Eq. (4.1) for fire heating phase and Eq. (4.9) for decay phase. This table presented the details of fire development in four fire rooms from zero to 4 hours fire duration. The time to reach the maximum fire temperature, t_{\max} and the maximum temperature is to indicate the end of fire heating phase and the start of the decay phase. A full step of Table 4.6 (a) results are given in Appendix C, the calculation is based on classroom as a template for different conditions in other fire room.

Table 4.6: Temperature time relation at different fire room:**(a) Classroom**

Phase	Heating Phase			Decay phase						
Time (hr)	0.19	0.21	<u>0.58</u>	1	1.16	1.5	2	2.5	3	4
T (°C)	759	772.2	<u>909.4</u>	603.5	483.7	230.9	27	27	27	27

(b) Office

Phase	Heating Phase					Decay phase				
Time (hr)	0.19	0.21	0.59	1	<u>1.16</u>	1.5	2	2.5	3	4
T (°C)	176.4	192.3	397.4	532.3	<u>569.0</u>	550.6	523.4	496.3	469.1	414.8

(c) Laboratoty

Phase	Heating Phase		Decay phase							
Time (hr)	0.19	<u>0.21</u>	0.59	1	1.16	1.5	2	2.5	3	4
T (°C)	789.6	<u>812.5</u>	353.7	27	27	27	27	27	27	27

(d) Compute room

Phase	Heating Phase	Decay phase								
Time (hr)	<u>0.19</u>	0.21	0.59	1	1.16	1.5	2	2.5	3	4
T (°C)	<u>767.9</u>	746	373	27	27	27	27	27	27	27

4.2.3 Realistic Temperature-Time Curve

The ISO 834 standard fire is used as a nominal fire model to the design fire. The ISO 834 fire curve is the most frequently used standard temperature-time curve in Eurocode and it can provide a different perspective on the safety of fire design. The ISO 834 standard fire model expressed the temperature with respect to the only parameter of time and do not restrict to the area of the compartment. Detailed explanation on ISO 834 can be found in Chapter 3.4.

Using the temperature-time relation at different fire room in Table 4.7, four fire rooms realistic temperature-time curves together with the ISO 834 standard fire curve are plotted in Figure 4.3. The realistic temperature-time curves are labeled with the maximum temperature, T_{\max} achieved to indicate the effect of the fire room type on the fire temperature over fire duration. As the parametric fire temperature-time curve considered the full fire development from fire growth until fire suppression, the curve pattern showed a surge to peak fire temperature, T_{\max} before dropping to ambient temperature. On the other hand, the ISO 834 standard fire curve is unlike the parametric fire temperature-time curve, it exhibited a steady continuous growth of temperature over time. The fire temperature obtained from different fire rooms using Eurocode parametric fire is combined with the ISO 834 standard fire in the same temperature-time curve for further comparison and classification purpose.

When comparing the temperature-time curve of ISO 834 fire and in real fire case, the ISO 834 fire curve displayed only a full fire development without considering the fire growth and decay phase. The four types of parametric fire curves highlighted the same trend of increase then decrease in fire temperature but with a different time, maximum fire temperature, and curve gradient at different fire duration due to the variation of opening factor and fire load inside the room. The overall fire heating phase

climbs to the maximum value within the time range between 0 to 1.16 hours before starting to fall to ambient temperature. As fire duration went by, the fire temperature tended to decline except the curve with opening factor $0.0091 \text{ m}^{1/2}$. The computer room temperature-time curve illustrated a sharp linear upward trajectory, it took 0.19 hour or 11.4 minutes to reach maximum fire temperature. Moreover, a fast decay rate is observed in the curve in computer room and the room temperature decline significantly to ambient temperature within 1 hour fire duration. Similarly, the laboratory temperature-time curve showed a same trend with the temperature-time curve in computer room. Computer room and laboratory both have a larger value in opening factor, which allowed a higher burning rate. Larger openings in computer room and laboratory enable more oxygen fed into the room for combustion and rapid heat dissipation, hence the temperature-time curve displayed a steep gradient during heating and decay phase.

The office with the smallest opening factor is observed to has the smallest gradient of during all phases of fire development in 4 hours fire duration. The temperature-time curve in office has a remarkably slow fire heating and fire decay process compared to the other curves. Due to the reason of small opening factor, O in office, the ventilation provided to the room was low and the fire undergoes the heating process and not reach the maximum fire temperature, T_{\max} . Besides, office took the longest time of 1.16 hours to reach maximum fire temperature of 569°C . The fire temperature reached by office during the 4 hour fire duration is observed to have a fire temperature 300°C to 500°C lower than the other curves. The fire temperature of Eurocode parametric fire and ISO 834 fire correspond to different fire duration is given in Table 4.7. The fire duration varies from fire initiation to 4 hours.

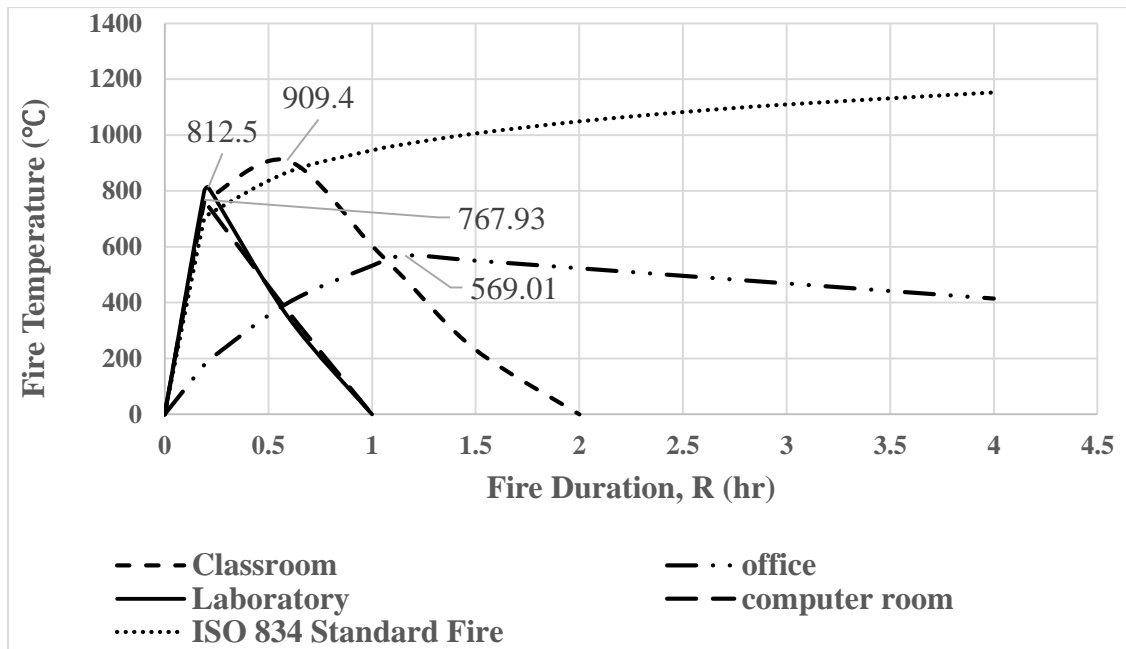


Figure 4.3: Temperature-time curve of the different opening factor of fire room.

Table 4.7: Temperature of Eurocode parametric fire and ISO 834 fire at different fire duration.

Fire Duration, R (hr)	Eurocode Parametric Fire Temperature (°C)				ISO 834 Fire Temperature (°C)
	Classroom	Office	Laboratory	Computer Room	
1	603.5	532.2	27	27	945.3
1.5	230.8	550.6	27	27	1006
2	27	523.4	27	2	1049
2.5	27	496.3	27	27	1082.4
3	27	469.1	27	27	1107.7
4	27	414.8	27	27	1152.8

4.2.4 Concrete and Steel Temperature Increases

The determination of the increase in concrete and steel temperature at different time of fire exposure is an important step. Various methods are proposed in paper of Annelies. D.W on the concrete and steel temperature calculation such as the test method, calculation method and a more accurate 2d finite element computer program.

In this study, the concrete and steel temperature is determined through thermal calculation as proposed by the Eurocode. It is assumed that total heat generated is transferred to the concrete. The Wickström method provides a method for the manual calculation of determining the temperature of the fire exposed to the normal weight concrete. The temperature of steel reinforcement, T_s and concrete temperature, T_c is given by Eq. (4.9) and Eq. (4.10) respectively.

$$T_s = (1 - 0.0616 t^{-0.88}) T_{\max} \quad (4.10)$$

$$T_c = (0.18 \ln \frac{t}{d'^2} - 0.81) T_s \quad (4.11)$$

Here, t is time at fire temperature and d' is the effective depth from concrete surface to the center of steel reinforcement. When concrete and steel temperature increase during time of fire exposure, the concrete compressive strength, f_{ck} and reinforcement yield strength, f_{yk} decrease gradually. The strength reduction of normal weighted concrete and steel reinforcement at elevated temperature is explained in chapter 3. The values of concrete temperature, T_c and steel reinforcement temperature, T_s are tabulated in Table 4.9. A full steps of concrete temperature, T_c and steel reinforcement temperature, T_s formulations are given in Appendix D, the calculation is based on classroom as a template for different conditions in other fire room.

After identifying the concrete and steel temperature during fire exposure, the reduction in strength of concrete and steel is needed to be determined. During fire, the material of structural elements changed their properties when temperature increased. Concrete and embedded steel reinforcement are affected and reduced in their strength. The changes in the properties of concrete and steel are according to the Eurocode. The steel temperature, T_s and concrete temperature, T_c is lower than the room temperature due to minor heat loss during the heat transfer. The difference in steel temperature, T_s and concrete temperature, T_c from the fire room temperature is not the same, the percentage of reduction is 23.8 %, 8.6 %, 50.1 % and 53% for classroom, office, laboratory and computer room respectively. A table of concrete compressive strength, f_{ck} and reinforcement yield strength, f_{yk} of different fire room at different fire duration, R is tabulated in Appendix F.

The mechanical properties of steel reinforcement are reversible because the steel reinforcement tends to regain the strength to its initial strength as the steel temperature closer to the ambient temperature. The reinforcement attained the maximum strength when the steel temperature is at ambient or any temperature below 100°C . The reduced concrete compressive strength, f_{ck} , and the reduced reinforcement yield strength, f_{yk} are calculated based on the value of siliceous aggregates and concrete temperature Θ given in EN 1992-1-2 in Figure 3.7 and tabulated in Table 4.8.

Table 4.8: Concrete and steel reinforcement temperature and strength during 4 hours of fire.

Fire Room	Classroom	Office	Laboratory	Computer room
Time to reach maximum fire temperature, t_{\max} (hr)	0.59	1.16	0.21	0.19
Maximum fire temperature, T_{\max} (°C)	909.4	569	812.5	767.9
Concrete temperature, T_c (°C)	31.53	484.34	31.53	31.53
Steel reinforcement temperature, T_s (°C)	26.51	407.24	26.51	26.51
Concrete compressive strength reduction factor at T_{\max}, $k_{fc,T_{\max}}$	0.3105	0.5697	0.7923	0.7556
Concrete compressive strength, f_{ck}	7.452	13.67	19.01	18.93
Reinforcement yield strength reduction factor at T_{\max}, $k_{fy,T_{\max}}$	0.1164	0.5225	0.6933	0.7386
Reinforcement yield strength, f_{yk}	48.2	216.3	287	305.8

4.2.6 Cross Section Reduction/ Spalling

Spalling is defined as the fall off of concrete layer from the concrete surface when under fire exposure. Eurocode 1992-1-2 recommends the 500°C isotherm theory when the concrete structure experiences a very high temperature increase during fire. The 500°C isotherm method explains that at temperature below 500°C, the concrete remains at full strength. Once the temperature has reached 500 °C and above, the concrete is assumed to have damaged so that its cover has spalled off as shown in Figure 4.5. The 500°C isotherm method is applicable only when the opening factor, O of a parametric fire exposure value is higher than $0.14 \text{ m}^{1/2}$.

Spalling can be developed by forming of a minor hole in concrete cover in the depth of beam to the total damage of cover from all three exposed sides of the beam. The removal of cover can damage the beam and expose the embedded steel reinforcement to the atmosphere. This spalling phenomenon is the major reason for the reduction in concrete cross section, with a smaller area of concrete available to withstand the member forces and member may be subjected to deteriorate in load bearing capacity. The cross section of a structural member is reduced during the fire exposure and the cover of the member cross section spalls or not is assumed to have no strength and stiffness.

In this study, the concrete beam has a cover depth of 60 mm and exposed to fire on the three sides of the beam as shown in Figure 4.5. The beam width, b losses the cover on both side which is total of 120 mm cover to new width size, b_{fi} whereas the beam depth, d losses the bottom cover to new depth, d_{fi} . When the fire rooms of classroom, office, laboratory and computer room had respectively reached their maximum fire temperature, T_{max} of 909.4 °C, 569 °C, 812.5 °C and 768 °C. All the beams in the fire rooms experienced spalled off of beam cover after exceeding 500 °C according to the 500°C isotherm theory. The new depth, d_{fi} is noticed to have the same

value with the original beam depth, d , which is the distance from the top of the beam surface to the center of tension reinforcement. The reduced cross section of the affected beams with new width, b_{fi} and same beam depth, d_{fi} are represented in Table 4.9.

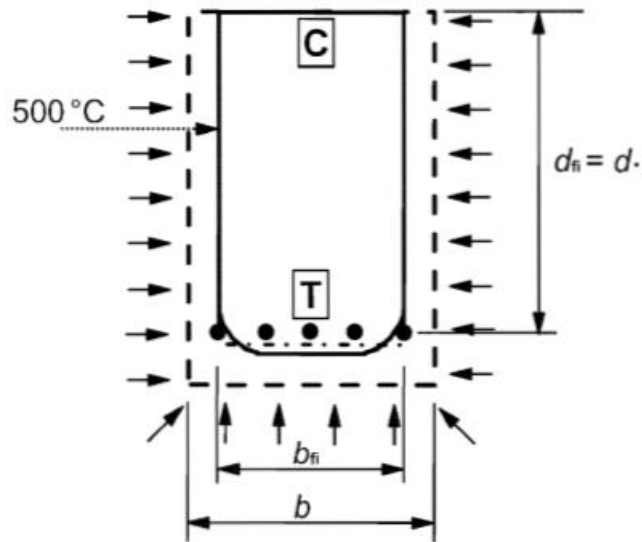


Figure 4.4: The reduced cross section of beam after spalling. (EC 1992)

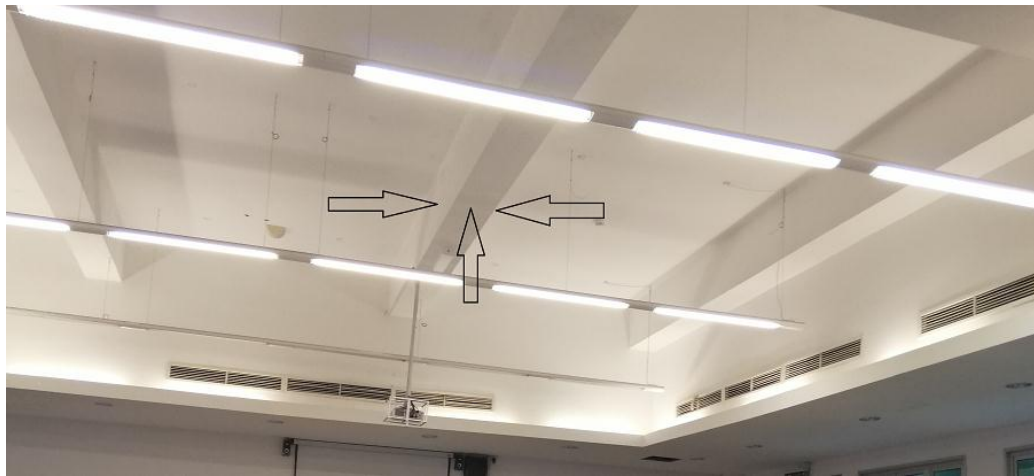


Figure 4.5: Fire exposure on three sides of the beam.

Table 4.9: The reduced cross section of beams after spalling.

Beam No.	Cross section (mm) (b x d)	Reduce cross section (mm) (b_{fi} x d_{fi})
B1	650 x 800	530 x 740
B2	850 x 1500	730 x 1440
B3	375 x 800	255 x 740
B5	1050 x 650	930 x 590

4.3 Structural Behavior Analysis

The Eurocode has proposed three methods of assessing the fire resistance of a building structure which are the time domain, temperature domain and strength domain. In this study, the fire resistance is examined in term structural strength in which required the resistance of structure during the fire to be greater than or equal to the fire severity for which the struture exposed to during fire. A structure that has enough moment capacity, $M_{R,fi}$ to the design moment, $M_{d,fi}$ during fire will attain sufficient fire resistance and similar structure with design moment higher than the moment capacity will suffering from structural failure and collapse. The relationship is given in Eq. (4.11)

$$M_{R,fi} > M_{D,fi} \quad (4.11)$$

4.3.1 Fire Severity

The fire severity is expressed as the design moment, $M_{D,fi}$ of structure during fire which results from the design loads. The design moment, $M_{D,ambient}$ of beam follows the limit state load combination of 1.35 permanent load, G_k plus 1.5 variable load, Q_k at ambient condition whereas limit state load combination used at fire, $M_{D,fi}$ is 1.0 permanent load, G_k plus 0.7 variable load, Q_k . The design moment, M_d at ambient and at fire can be obtained from the modelling results derived from the ETABS 2016 modelling. The modelling enable load combination equation at ambient and at fire to be defined into the system before the design moment is analyzed.

The results of the design moment at ambient condition and at fire together with the percentage of reduction are represented in Table 4.10. Reduction in design moment, M_R is observed in all types of beams present in fire room when compared with the design moment at ambient. The percentage of design moment reduction from ambient to fire condition varies from 36.9 % to 75.3 %. Figure 4.6 and Figure 4.7 shown example of the classroom beam 3 ETABS 2016 modeling results at ambient and at the fire.

Table 4.10: Design moment, M_D at ambient condition and at fire.

Fire Room	Beam No.	Cross section (mm)	Design Moment at ambient, M_d (kNm) ($1.35G_k + 1.5Q_k$)	Design Moment at fire, $M_{d,fi}$ (kNm) ($G_k + 0.7Q_k$)	Percentage of reduction (%)
Classroom	B3	375 x 800	937.62	32.19	96.5
	B5	1050 x 650	938.97	286.69	69.4
Office	B1	650 x 800	763.61	218.53	71.3
	B2	850 x 1500	1601.22	571.93	64.2
	B3	375 x 800	983.53	33.61	96.5
Laboratory	B1	650 x 800	513.15	179.67	64.9
	B2	850 x 1500	3829.26	1673.64	56.2
	B3	375 x 800	615.82	27.6	95.5
Computer Room	B1	650 x 800	763.61	218.53	71.3
	B2	850 x 1500	4653.35	1685.44	63.7
	B3	375 x 800	1071.34	33.53	96.8

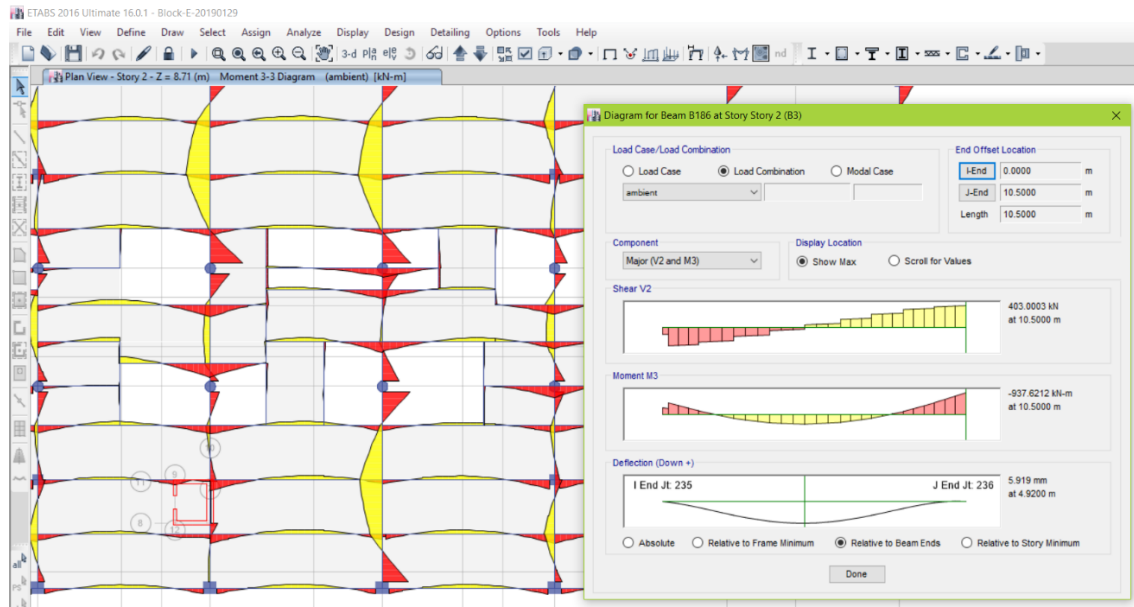


Figure 4.6: Design moment, M_D of classroom beam 3 at ambient.

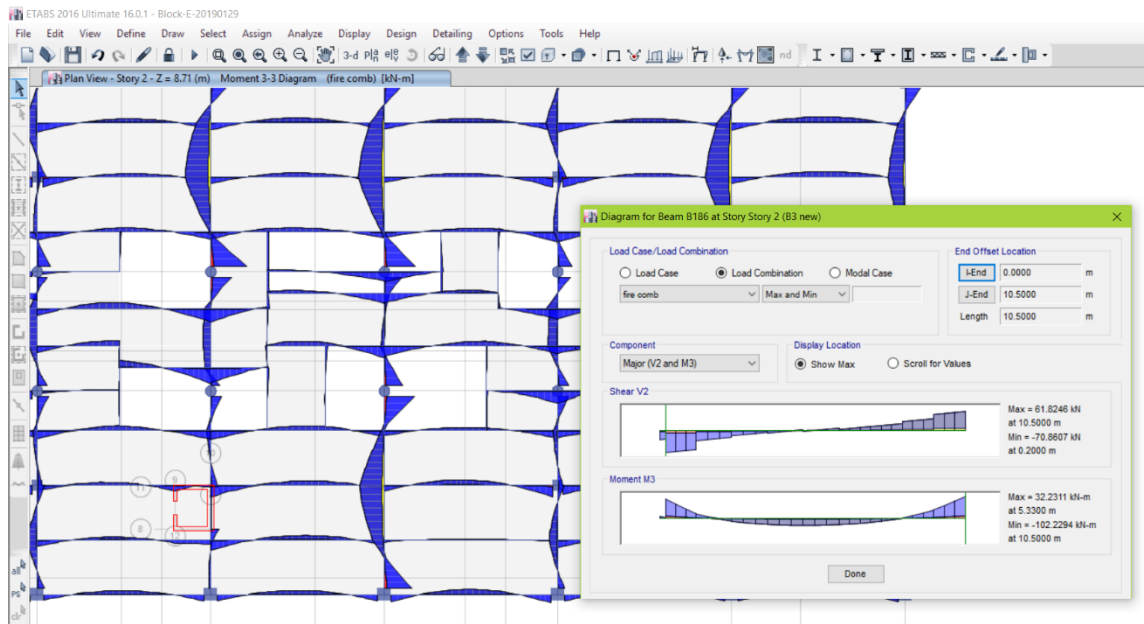


Figure 4.7: Design moment, M_D of classroom beam 3 at fire.

4.3.2 Fire resistance

The fire resistance is denoted as the moment resistance, M_R of beam during fire. The resisting moment of reinforced concrete structure follows the design condition at the ultimate limit state. A rectangular stress block diagram of a doubly reinforced beam is shown in Figure 4.8 and used in the ultimate limit state design. A concrete compressive force, F_{cc} and reinforcement tensile force, F_{sc} are developed during the compression of concrete beam section. During equilibrium, both the compressive and tensile forces must balance each other. The resisting moment, M_R of the doubly reinforced rectangular beam section is the sum of concrete compressive force, F_{cc} and reinforcement tensile force, F_{sc} given in Eq. (4.12).

$$M_R = F_{cc} + F_{sc} \quad (4.12)$$

The horizontal forces of concrete compressive force, F_{cc} and reinforcement tensile force, F_{sc} taking moment of resistance about the tension reinforcement and the formulas are represented by Eq. (4.13) and Eq. (4.14) respectively.

$$F_{cc} = 0.45 f_{ck} (b \times) Z \quad (4.13)$$

Z is the distance from the centroid of compression force, F_{cc} to the tension force of reinforcement, F_{st} .

$$F_{sc} = 0.87 f_{yk} A_s' Z_1 \quad (4.14)$$

Z_1 is the distance from the centroid of compression reinforcement, F_{sc} to the tension force of reinforcement, F_{st} . A_s' is the area of compression reinforcement.

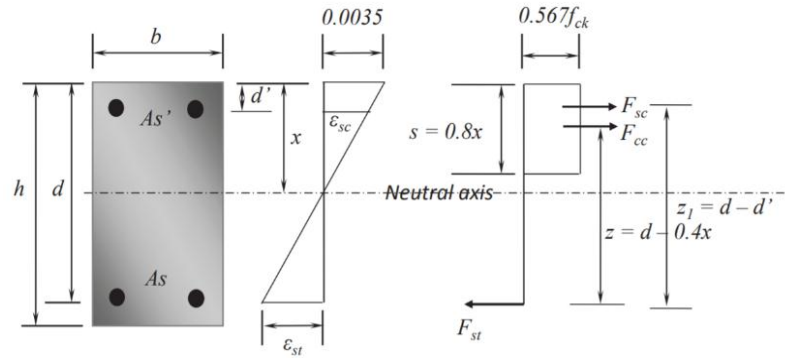


Figure 4.8: Section, stress and strain block diagram of a doubly reinforced beam.

(W. H. Mosley, 1990)

ETABS 2016 modeling had provided the minimum tension and compression reinforcement area needed in the structural design. By referring to the minimum area of reinforcement, the required area of reinforcement can be estimated using the table of reinforcement areas and perimeters given in EN 1990 given in Figure 4.9. The required area of reinforcement will be slightly higher than the minimum area of reinforcement suggested by ETABS. A concrete beam is good in compression but poor in the tensile strength, hence the compression reinforcement is important in the moment capacity of the compression section. Hence, the moment resistance will increase when the area of compression reinforcement, A_s' increase. A table of area of compression reinforcement, A_s' and area of tension reinforcement, A_s in different beam type is constructed and presented in Table 4.11.

Sectional areas of groups of bars (mm ²)										
Bar size (mm)	Number of bars									
	1	2	3	4	5	6	7	8	9	10
6	28.3	56.6	84.9	113	142	170	198	226	255	283
8	50.3	101	151	201	252	302	352	402	453	503
10	78.5	157	236	314	393	471	550	628	707	785
12	113	226	339	452	566	679	792	905	1020	1130
16	201	402	603	804	1010	1210	1410	1610	1810	2010
20	314	628	943	1260	1570	1890	2200	2510	2830	3140
25	491	982	1470	1960	2450	2950	3440	3930	4420	4910
32	804	1610	2410	3220	4020	4830	5630	6430	7240	8040
40	1260	2510	3770	5030	6280	7540	8800	10100	11300	12600

Figure 4.9: Table of reinforcement areas and perimeters. (EN 1990)

Table 4.11: Area of compression and tension steel reinforcement in different beam type.

Fire Room	Beam No.	Minimum As (mm²)	Minimum As' (mm²)	Number and size of tension bar	As (mm²)	Number and size of compression bar	As' (mm²)
Classroom	B3	8815	8813	8H16	12880	6H20	11340
	B5	23849	23841	9H20	25470	7H25	24080
Office	B1	7499	7680	6H20	11340	4H25	7840
	B2	12750	12750	7H20	15400	8H16	12880
	B3	9351	9331	8H16	12880	6H20	11340
Laboratory	B1	5200	5200	6H16	7260	7H12	5544
	B2	12750	12750	7H20	15400	8H16	12880
	B3	5340	5355	4H25	7840	7H12	5544
Computer Room	B1	7499	7680	6H20	11340	4H25	7840
	B2	12750	12750	7H20	15400	8H16	12880
	B3	10612	10611	5H20	12880	6H20	11340

By using the equation of resisting moment, M_R in Eq. (4.12), the moment resistance at ambient, $M_{R,ambient}$ and moment resistance at maximum fire temperature, $M_{R,fi}$ can be calculated by developed a deterministic model. The moment resistance at maximum fire temperature, $M_{R,fi}$ indicates the most critical moment resistance in beam. Full calculation steps are provided in Appendix E. The results of moment resistance, $M_{R,fi}$ at different fire duration are tabulated in Table 4.12.

Moment resistance at ambient, $M_{R,ambient}$ is the highest value that a beam can be attained because under ambient condition, both the concrete and reinforcement do not suffer from strength degradation due to fire. The value of concrete compressive strength, f_{ck} and reinforcement yield strength, f_{yk} during ambient temperature are kept at 24 MPa and 414 MPa. On the other hand, the moment resistance during fire is the most critical moment at which the beam experienced the highest temperature at fire room. From the results shown in Table 4.12, the beams in fire room suffered the lowest moment resistance, M_R during fire duration at 0.59 hours, 2 hours, 0.21 hours and 0.21 hours for classroom, office, laboratory and computer room respectively.

A degradation of moment resistance during fire is observed in all types of beams present in fire room when comparing with the moment resistance at ambient. The percentage of reduction in moment resistance from ambient, $M_{R, ambient}$ compared to moment resistance at fire condition, $M_{R,fi}$ varies from 27.1 % to 88.4 %. The results of the moment resistance at ambient condition and at fire together with the percentage of reduction are represented in Table 4.12. Eq. (4.15) represented the equation for percentage of reduction (%) in moment resistance, M_R .

$$\text{Percentage of reduction (\%)} = \frac{M_{R,ambient} - M_{R,fi}}{M_{R,ambient}} \times 100\% \quad (4.15)$$

Table 4.12: Moment of resistance, M_R at ambient condition and at fire

Fire Room	Beam No.	Cross Section (mm)	Moment Resistance at ambient, $M_{R,ambient}$ (kNm)	Moment Resistance at fire, $M_{R,fi}$ (kNm)	Percentage of Reduction (%)
Classroom	B3	375 x 800	3016	351.8	88.3
	B5	1050 x 650	4774.8	698.5	85.3
Office	B1	650 x 800	2460	1177.2	52.2
	B2	850 x 1500	7190.8	3446.6	52.0
	B3	375 x 800	3018.3	1445	52.1
Laboratory	B1	650 x 800	1630.6	1131.2	30.6
	B2	850 x 1500	7190.8	2465	65.7
	B3	375 x 800	1709	1187	30.5
Computer Room	B1	650 x 800	2451	1786.9	27.1
	B2	850 x 1500	7188.1	5235.5	27.2
	B3	375 x 800	3012.5	2194.7	27.1

Different types of beam cross section and area of reinforcement give different response during fire and initiate moment resistance, M_R . It can be seen that the beams in fire room display a similar curve with the increase of fire duration. The trend of the moment resistance, M_R is observed to be decreased when fire duration increasing until the point where the maximum fire temperature reached. During fire, the loads acted on beam are expected to reduce and the resisting moment of beam will decrease at the same time. The point where the moment resistance, M_R marked the lowest value is the critical moment resistance during fire, $M_{R,fi}$ of the beam experienced during the entire fire duration.

The moment resistance, M_R tends to remain constant after the beam temperature drops to ambient temperature and later the curve stayed the same. Moment resistance of beams in classroom levels off from 2.5 hours to 4 hours of fire duration, R . On the other hand, laboratory and computer room started to stabilize faster than classroom when the moment resistance of beams stayed constant from 0.21 hours to 4 hours of fire duration, R . Four graphs of moment resistance at fire, $M_{R,fi}$ at different fire duration, R are plotted from Figure 4.10 to Figure 4.13 which consisted of fire room of classroom, office, laboratory and computer room respectively. The lowest value of moment resistance during fire, $M_{R,fi}$ for each beam is label in the graph.

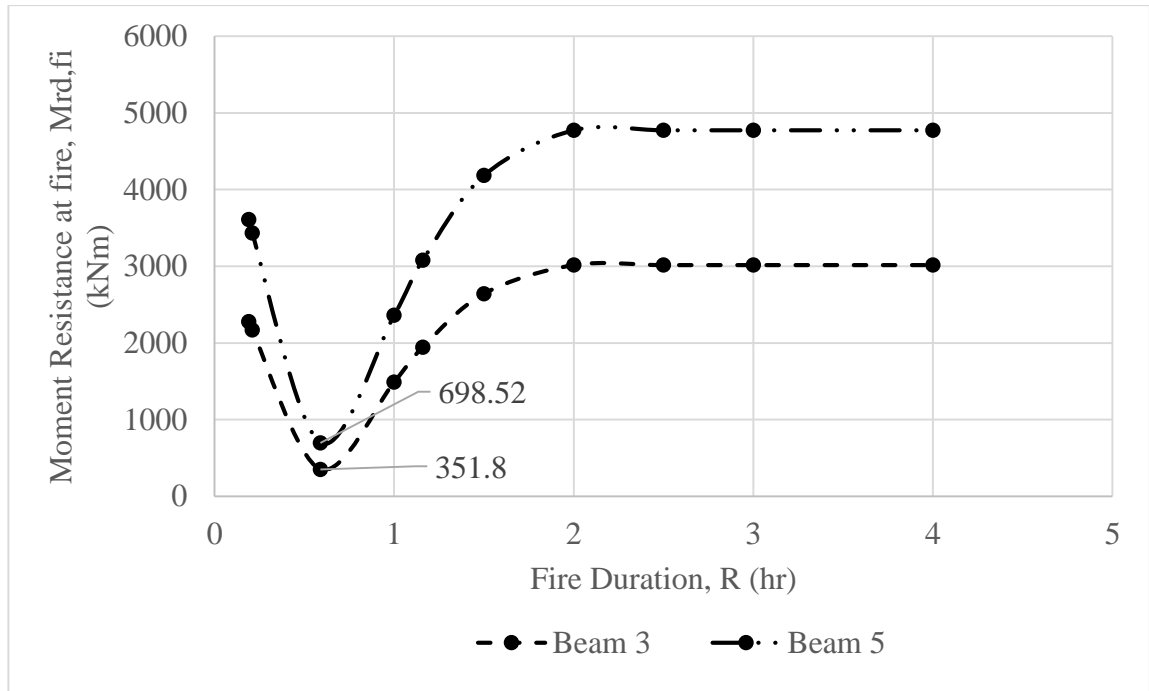


Figure 4.10 : Moment resistance at fire, $M_{R,fi}$ of beams during different fire duration, R in classroom.

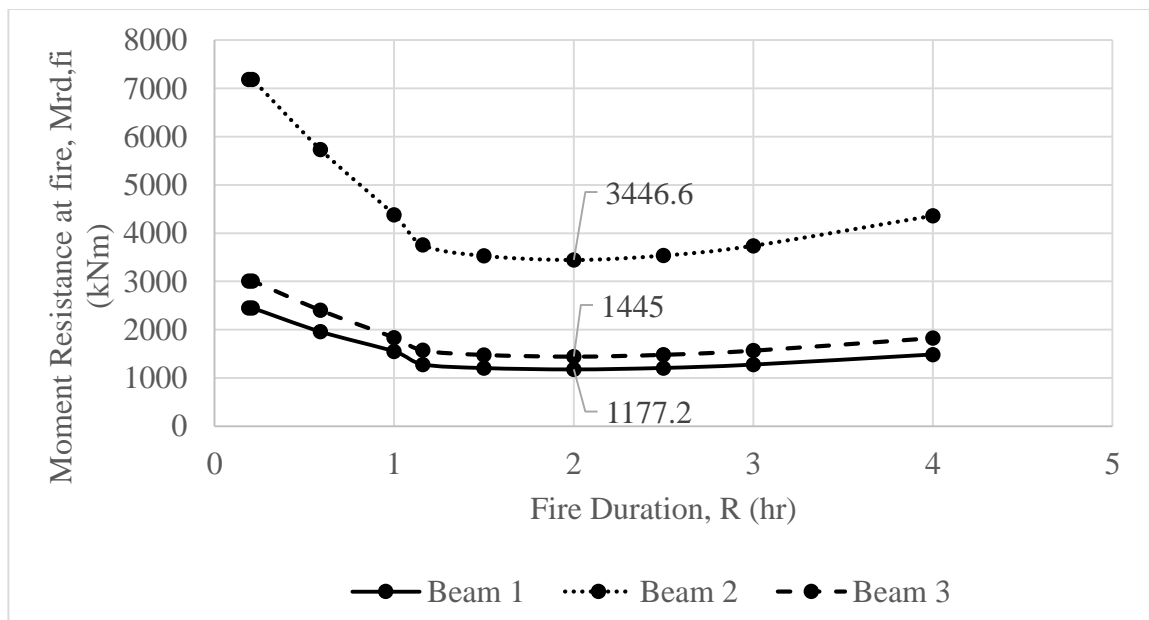


Figure 4.11: Moment resistance at fire, $M_{R,fi}$ of beams during different fire duration, R in office.

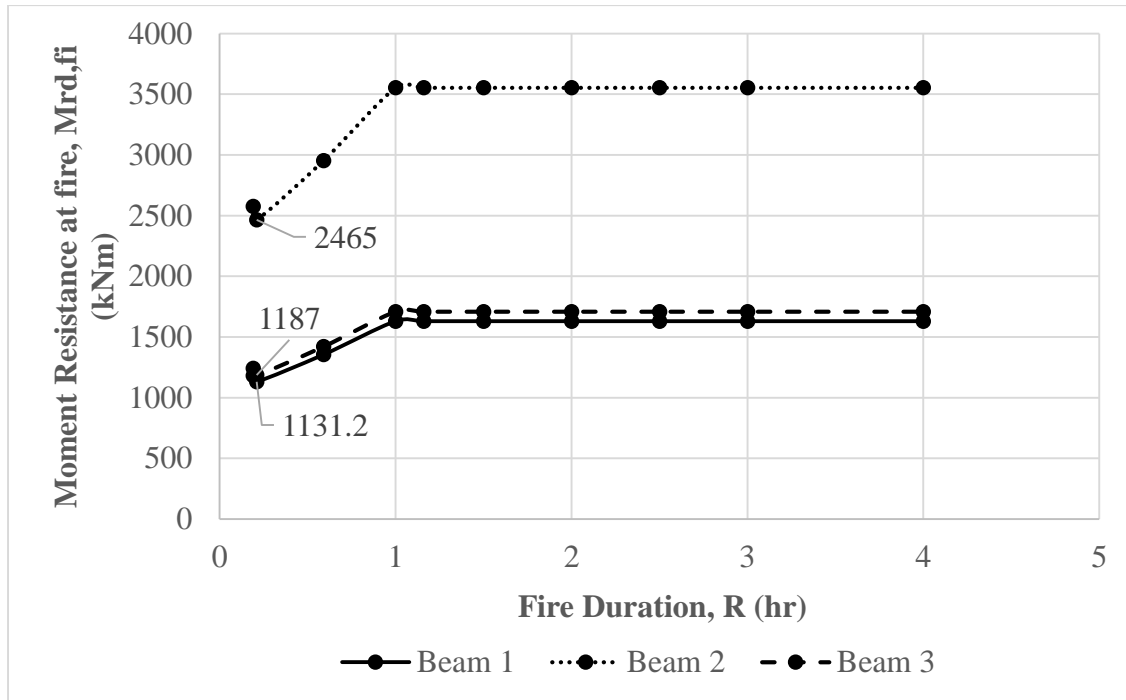


Figure 4.12: Moment resistance at fire, $M_{R,fi}$ of beams during different fire duration, R in laboratory.

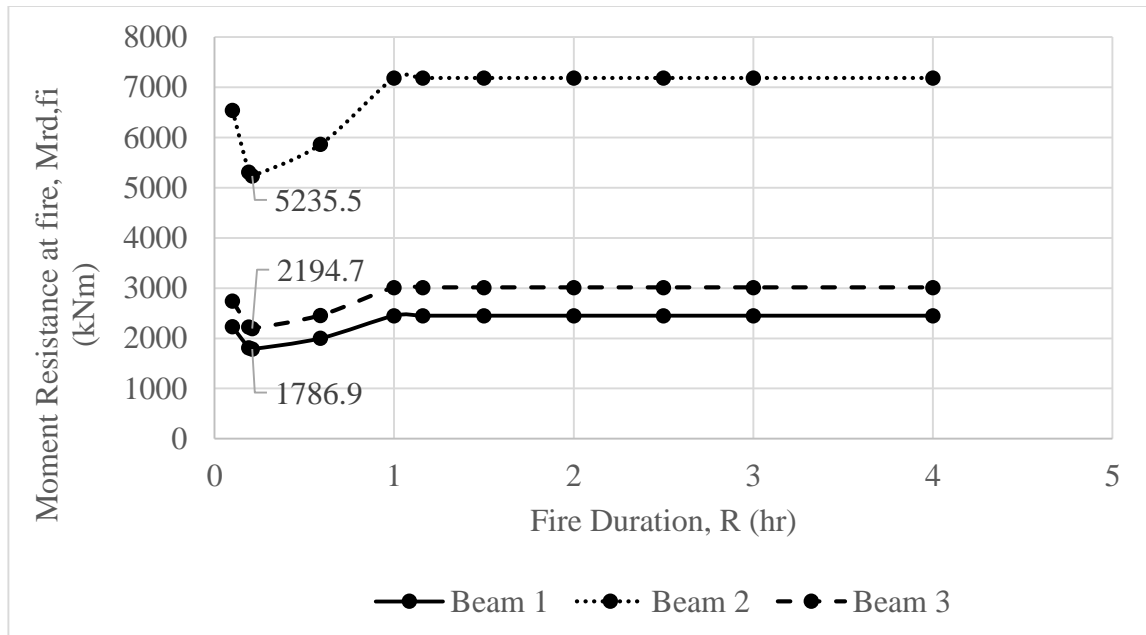


Figure 4.13: Moment resistance at fire, $M_{R,fi}$ of beams during different fire duration, R in computer room.

A comparison of moment resistance at fire, $M_{R,fi}$ with the design moment at fire, $M_{D,fi}$ is shown in Table 4.13. The comparison is performed to verify the safety of beams during fire exposure by fulfilling the relation mentioned in Eq. (4.11) Moment resistance, $M_{R,fi}$ during fire of all beam are observed to be greater than the design moment at fire, $M_{D,fi}$. The results from the comparison have shown all of the total twelve beams are found stable during fire.

The design moment at fire, M_D in column 4 in Table 4.14 acts as a threshold moment value for the beams to resist during fire. During fire, any resisting moment, M_R which fall below the design moment, M_D will be considered as fail. In other word, all the beam under analysis have resistance sufficient during the four hours period of fire duration. Safety condition is met when the moment resistance at fire, M_R in all beam is greater than the design moment at fire, M_D . Hence, conclusion can be made on the fire rating of all beam is more than four hours during fire according to the results in Table 4.13.

Fire rating of beam is determined to indicate the time at which the beams are able to resist under different fire duration. Moment resistance, M_R of beams at fire duration from 0.19 hours to 4 hours to conclude the fire rating of beams, and results is tabulated in Table 4.13. The lowest moment resistance, M_R of beam is underlined in Table 4.13 to represent the most critical moment resistance, M_R of the beam experience during the entire fire duration. The most critical moment resistance, M_R that occurred in classroom, office, laboratory and computer room occurred at 0.59 hour, 2 hour, 0.21 hour and 0.21 hour respectively.

Table 4.14: Comparison of moment resistance at fire, $M_{R,fi}$ with the design moment at fire, $M_{D,fi}$.

Fire Room	Beam No.	Cross Section (mm)	Design Moment at fire, $M_{D,fi}$ (kNm) ($G_k + 0.7Q_k$)	Moment Resistance at fire, $M_{R,fi}$ (kNm)
Classroom	B3	375 x 800	32.19	351.8
	B5	1050 x 650	286.69	698.5
Office	B1	650 x 800	218.53	1282.3
	B2	850 x 1500	571.93	3756.1
	B3	375 x 800	33.61	1574.6
Laboratory	B1	650 x 800	179.67	1131.2
	B2	850 x 1500	1673.64	2465
	B3	375 x 800	27.6	1187
Computer Room	B1	650 x 800	218.53	1812.2
	B2	850 x 1500	1685.44	5309.1
	B3	375 x 800	33.53	2225.8

4.4 Reliability Analysis

Reliability analysis is important in indicating the level of safety in structural beams changes at fire exposure. For this purpose, structural safety of beam can be achieved when the reliability index during fire, β_{fi} is greater than the target reliability index, β_{target} of 3.8 for 50 years standard period suggested by EN 1990. From the evaluation, the fire severity and fire resistance, parameters such as the beam width, beam depth, concrete compressive strength, f_{ck} and reinforcement yield strength, f_{yk} are recognized as significant parameters which impose changes in moment capacity, as well as the reliability of the beam under fire exposure. The reliability of beams in different fire rooms are evaluated from zero fire duration, R to 4 hours, by changing the parameters mentioned above. In this study, two methods are adapted to carry out the reliability analysis, which is the First Order Reliability Method (FORM) and First Order Second Moment (FOSM). The reliability analysis of First Order Second Moment (FOSM) and First Order Reliability Method (FORM) will be further discussed in section 4.4.1 and section 4.4.2 respectively.

The results of fire rating obtained from section 4.3.2 had concluded that all the beams in fire room do not suffer from structural failure during the four hours fire duration. Hence, the FOSM and FORM analysis are performed on the beams given that the fire is assumed to burn continuously and predict the most critical fire temperature that can be reached in the fire room without considering the depletion of fuel over time. In other word, the fire is no longer fuel controlled fire in section 4.2.3.

Parameters such as the opening factor, O and thermal properties of boundary materials, b of fire room are the dependent variables affecting the development of fire and strength changes on the concrete and reinforcement. All fire room is observed to undergo have a constant rise in fire temperature due to heating phase, with no transition in phase occurred. In other word, the fire only undergoes the heating phase but no decay phase during the entire four hours of fire duration.

The fire temperature, T in classroom, office and computer room have exceeded $1000\text{ }^{\circ}\text{C}$ after 1 hour fire duration whereas laboratory has achieved the lowest fire temperature and achieved maximum fire temperature of $775.62\text{ }^{\circ}\text{C}$ at 4 hours fire duration. At 1 hour fire duration, all the fire room has exceeded $500\text{ }^{\circ}\text{C}$ and spalling occurred. During the fourth hours of fire duration, the fire room classroom, office, laboratory and computer room marked the highest temperature of $1199.6\text{ }^{\circ}\text{C}$, $1211.4\text{ }^{\circ}\text{C}$, $775.6\text{ }^{\circ}\text{C}$, $1249.8\text{ }^{\circ}\text{C}$. By using the Eq. (4.1) to calculate the fire temperature, $T\text{ (}^{\circ}\text{C)}$ reached by fire rooms in 4 hours fire duration, the results are plotted in Figure 4.14.

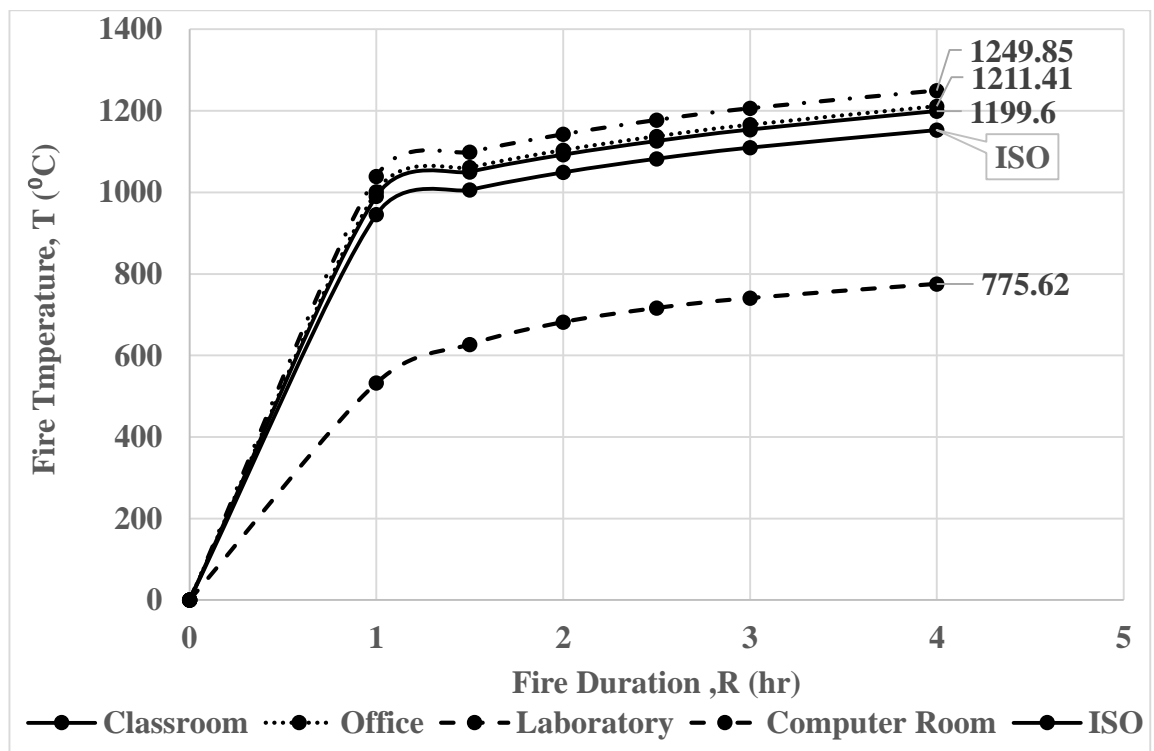


Figure 4.14: Fire temperature, $T\text{ (}^{\circ}\text{C)}$ reached by fire rooms in 4 hours fire duration.

By identifying the fire temperature reached, the moment resistance of beam at fire, $M_{R,fi}$ can be identified. The calculation of moment resistance at fire, $M_{Rd,fi}$ is same as the steps given in Appendix E. The moment resistance of beam under increasing fire temperature, $M_{Rd,fi}$ predicted a gradual decrease in the beam reliability index, β until it reached the fourth hours fire duration for which the highest fire temperature occurred. Furthermore, the concrete compressive strength, f_{ck} and reinforcement yield strength, f_{yk} drop accordingly to the increase in fire temperature. Results of the concrete compressive strength, f_{ck} and reinforcement yield strength, f_{yk} of four fire rooms at decreasing fire temperature is provided in Appendix G.

Beam 2 in office, laboratory and computer room has the highest moment resistance in fire when compare to beam 1 and beam 3 in the same room. Beam of large steel reinforcement provided the beam with higher moment of resistance. Beam 2 has a large area in compression, A_s and tension, $A_{s'}$ steel reinforcement, compare to beam 1 and beam 3, A_s and $A_{s'}$ in office and computer room is 20080 m², 17700 m² and 15400 m², 12880 m² in laboratory. The same observation is also found in classroom whereby beam 3 is found to have a higher moment resistance in fire when compared to beam 5. Beam 3 has A_s and $A_{s'}$ in order of 12880 m² and 11340 m² compare to values of A_s and $A_{s'}$ in beam 5 with greater value 31440 m² and 31400 m² respectively. The graph of moment resistance, $M_{Rd,fi}$ in different fire duration of increasing fire temperature is given in Figure 4.15, Figure 4.16, Figure 4.17 and Figure 4.18 in the order of classroom, office, laboratory and computer room.

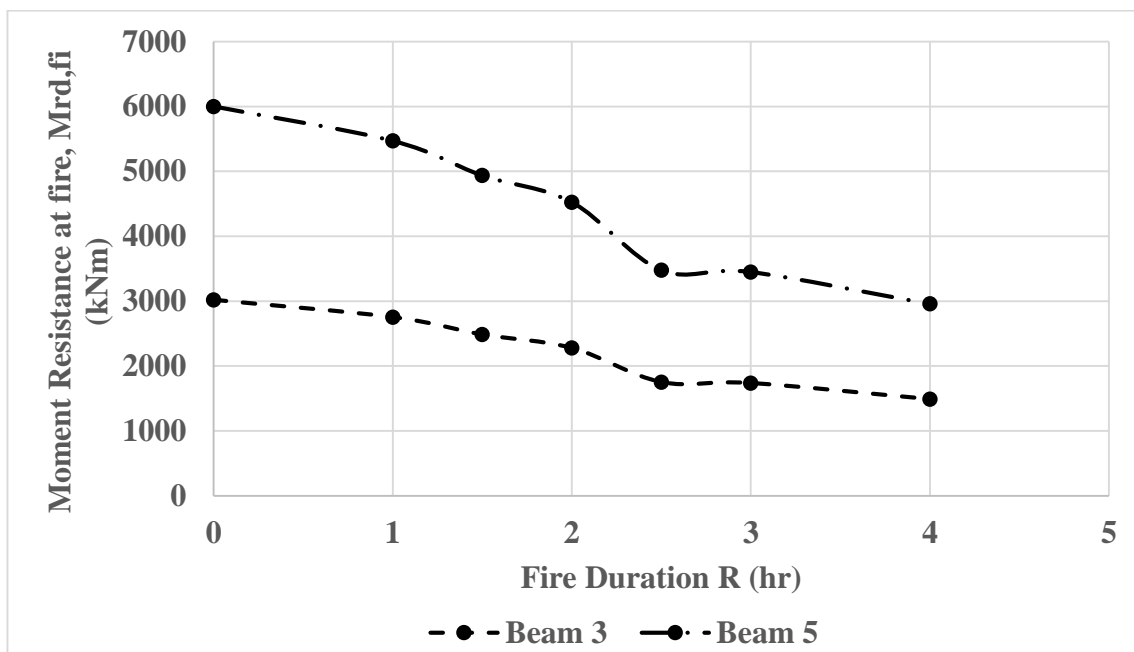


Figure 4.15: Moment Resistance at fire, $M_{rd,fi}$ in classroom.

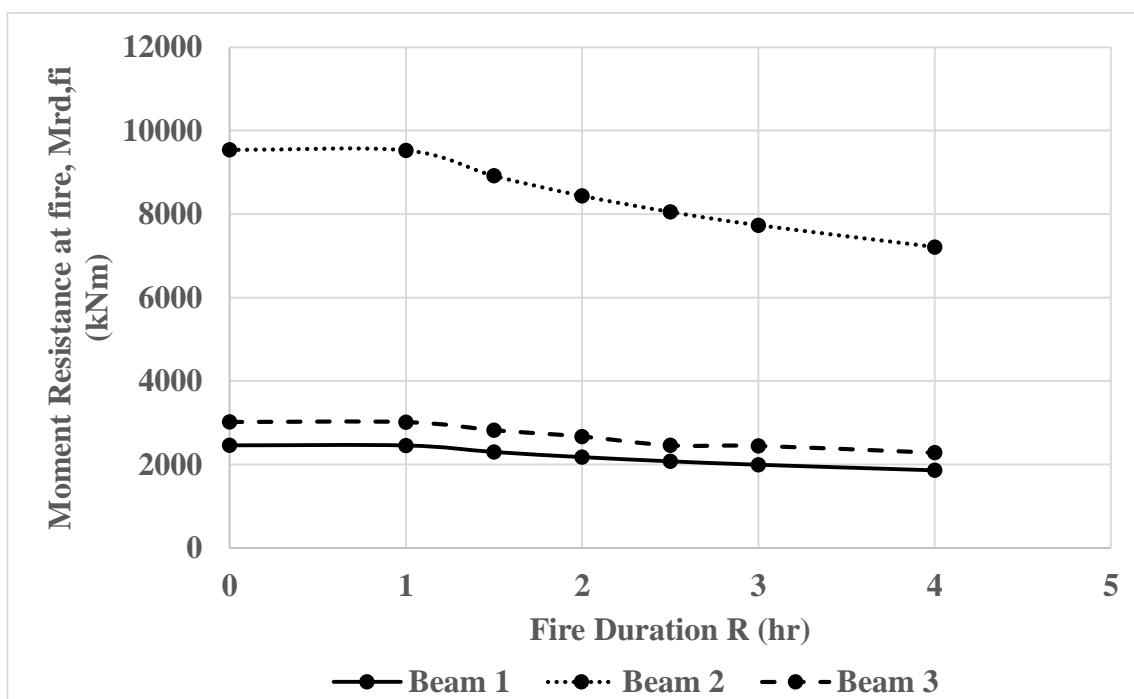


Figure 4.16: Moment Resistance at fire, $M_{rd,fi}$ in office.

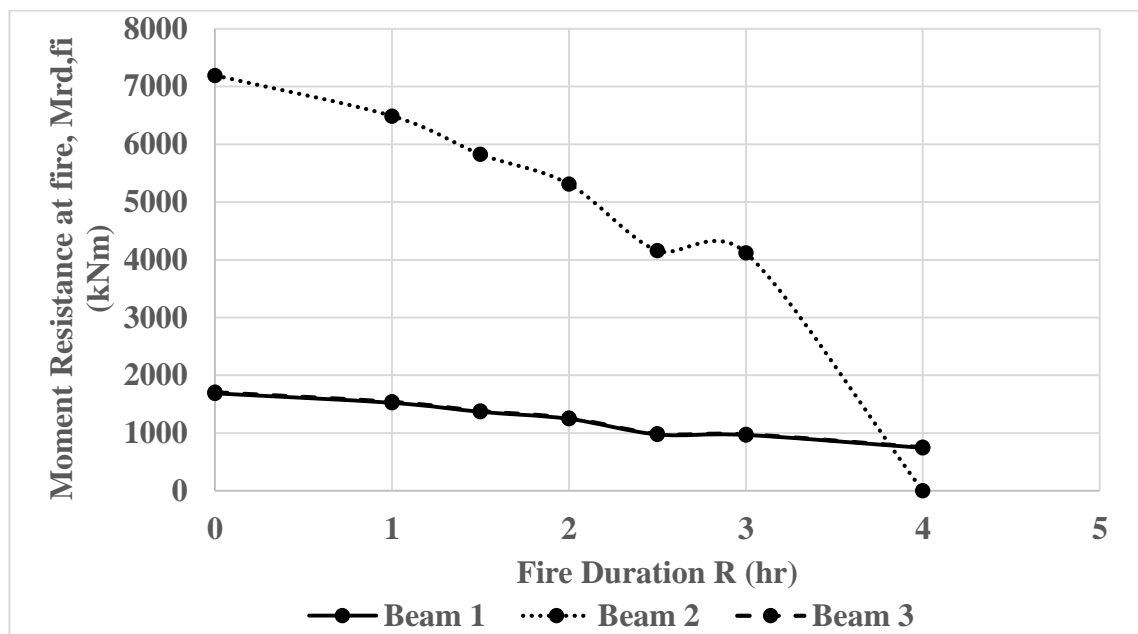


Figure 4.17: Moment Resistance at fire, $M_{Rd,fi}$ in laboratory.

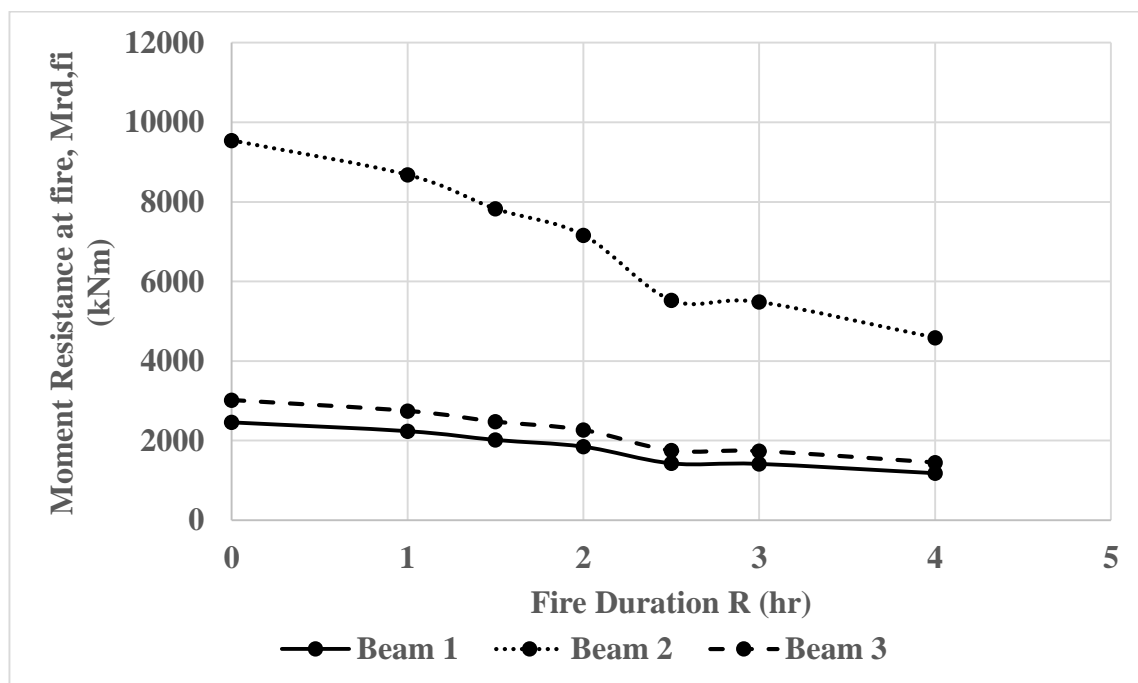


Figure 4.18: Moment Resistance at fire, $M_{Rd,fi}$ in computer room.

4.4.1 FORM

The MATLAB is used to perform the First Order Reliability Method (FORM) analysis of reliability index formulation of beam under fire exposure. In FORM analysis of beam, the limit state equation, $G(X)$ for beam are divided into resistance effect, $R(X)$ and load effect, $L(X)$. The resistance equation is calculated deterministically without considering the probabilistic data of random variables. The random variables in load effect are the same as the resistance effect except for the model uncertainty for load, K_E is used instead of the model uncertainty for resistance, K_R .

On the other hand, load input in MATLAB made use of the probabilistic data of the five random variables of concrete compressive strength, f_{ck} and reinforcement yield strength, f_{yk} , beam width, b , beam depth, d and model uncertainty for resistance, K_R . The probabilistic data of random variables used in load effect are given in Table 3.8. Both the resistance and load equation varies according to uncertain parameters such as the area of compression reinforcement, A_s and area of tension reinforcement, $A_{s'}$, concrete compressive strength, f_{ck} and reinforcement yield strength, f_{yk} , beam width, b and beam depth, d of the beam. In other word, in different fire room, the uncertain parameters change accordingly to the temperature change and in turn give different resistance and load equation as input in MATLAB analysis. Appendix H showed the full steps of FORM reliability analysis in classroom beam no 1 as a template for the other fire rooms and beams type.

The results of reliability index, β using FORM method are tabulated in Table 4.15. From the results of reliability index, β , all the beam in classroom, laboratory and computer room started to fail from 1 hour fire duration until 4 hours fire duration. On the contrary, beams in office fail at fire duration thirty minutes later than the other rooms, the reliability index, β for beam 1, beam 2 and beam 3 are 3.42, 3.78 and 3.44 respectively. The reliability index, β of beam which is lower than the target

reliability index, β_{target} of 3.8 is underlined in Table 4.15. The underlined reliability index, β represents the failure of beam which is less than the target reliability index, β_{target} of 3.8 for 50 years standard period suggested by EN 1990.

Besides, the results of reliability index, β from Table 4.15 together with the target reliability index, β_{target} of 3.8 are plotted into graph and given in Figure 4.19, Figure 4.20, Figure 4.21, and Figure 4.22 in the order of classroom, office, laboratory and computer room. The trend of reliability index, β in all fire rooms are noticed to drop steeply over the fire duration, R . As the fire temperature continues to rise in fire rooms, the strength of concrete and reinforcement decrease, and led to decrease in the moment resistance of beam in fire, $M_{Rd,fi}$ as well as the reliability index, β of beam.

Table 4.15: Reliability index, β of beams using FORM method.

Fire Room	Beam No.	Reliability Index during fire, β_R							
		Target	Fire Duration, R (hr)						
			0	1	1.5	2	2.5	3	4
Classroom	B3	3.8	3.9	<u>3.27</u>	2.54	1.95	0.16	0.13	-0.91
	B5	3.8	4.21	<u>3.58</u>	2.88	2.28	0.49	0.44	-0.61
Office	B1	3.8	3.88	3.87	<u>3.42</u>	3.04	2.72	2.45	1.97
	B2	3.8	4.25	4.24	<u>3.78</u>	3.40	3.08	2.81	2.33
	B3	3.8	3.90	3.89	<u>3.44</u>	3.06	2.74	2.46	1.99
Laboratory	B1	3.8	3.89	<u>3.19</u>	2.45	1.82	1.15	0.09	-1.69
	B2	3.8	4.24	<u>3.54</u>	2.80	2.17	0.50	0.44	-1.35
	B3	3.8	3.88	<u>3.18</u>	2.45	1.81	0.16	0.09	-1.69
Computer Room	B1	3.8	3.87	<u>3.23</u>	2.53	1.92	0.17	0.10	-1.11
	B2	3.8	4.24	<u>2.59</u>	2.89	2.28	0.52	0.46	-0.77
	B3	3.8	3.90	<u>3.25</u>	2.55	1.94	0.18	0.12	-1.09

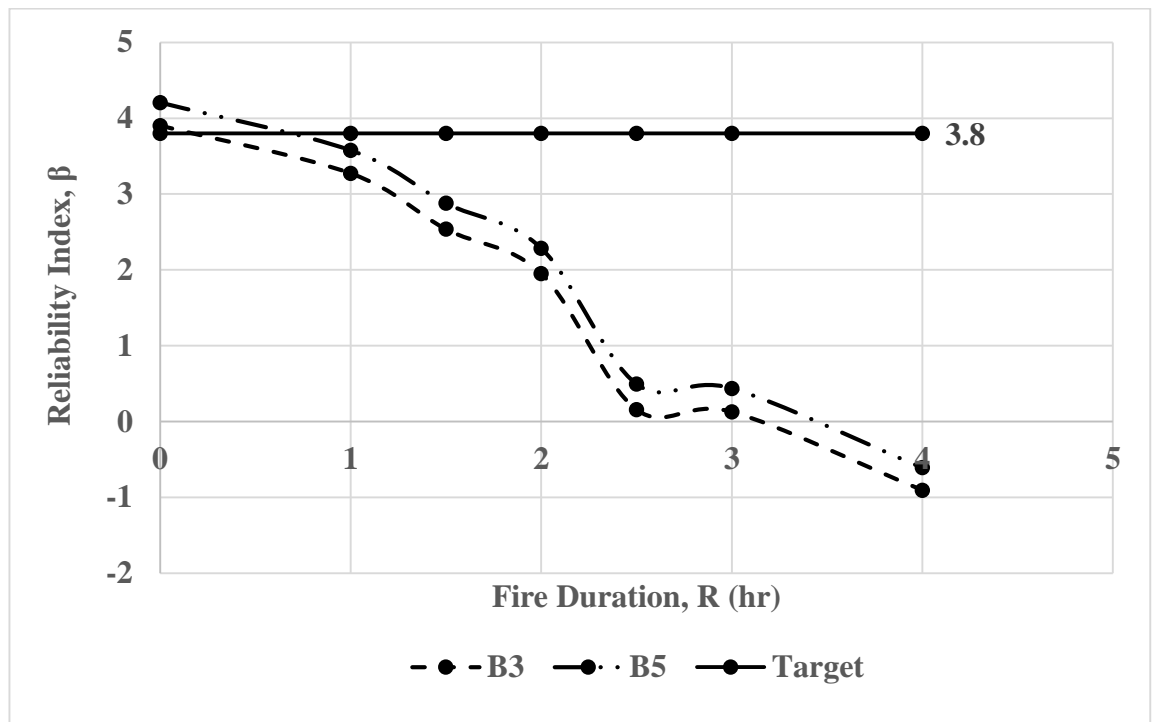


Figure 4.19: Reliability index, β of beams in classroom using FORM methods.

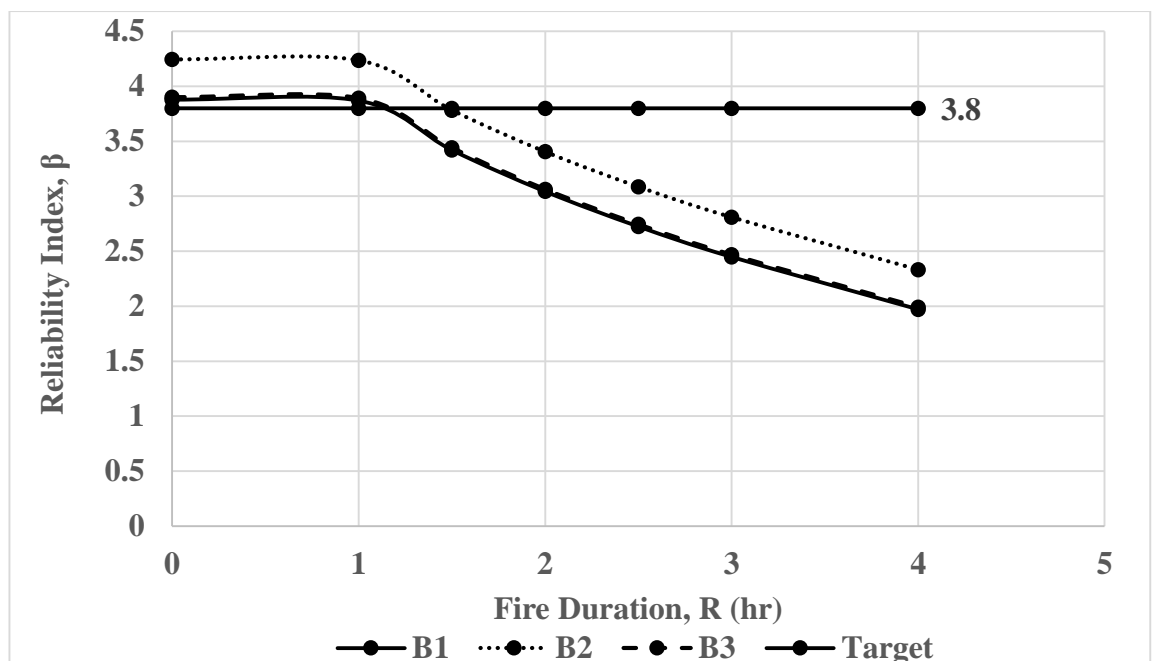


Figure 4.20: Reliability index, β of beams in office using FORM methods.

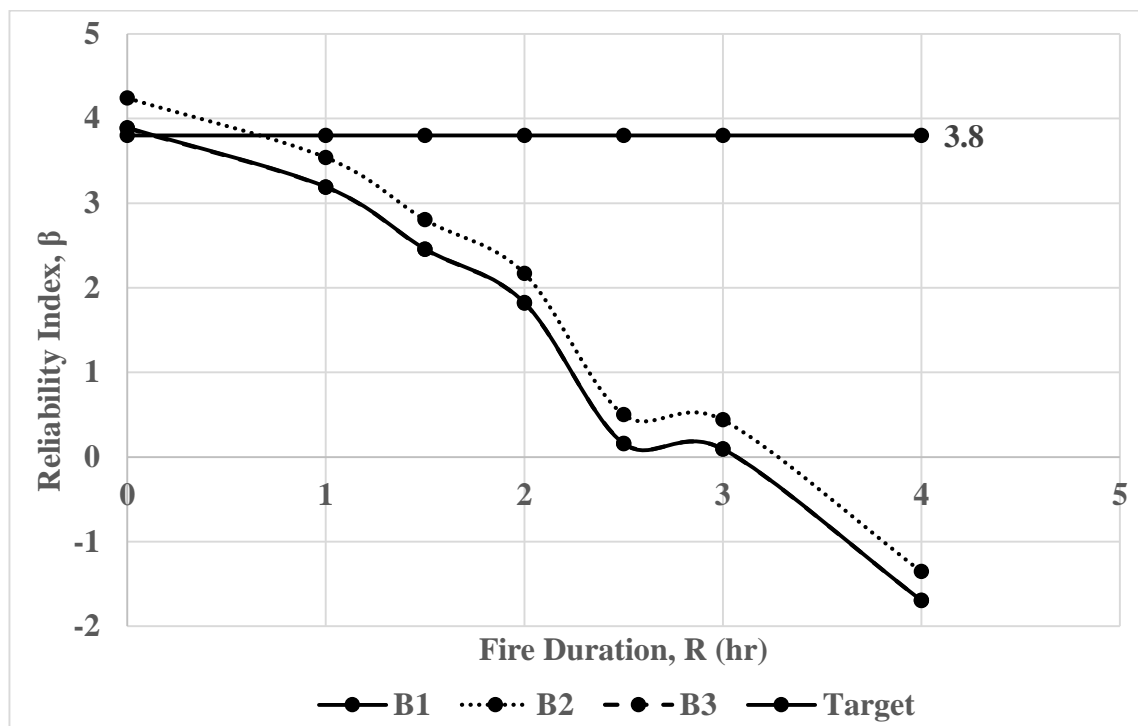


Figure 4.21: Reliability index, β of beams in laboratory using FORM methods.

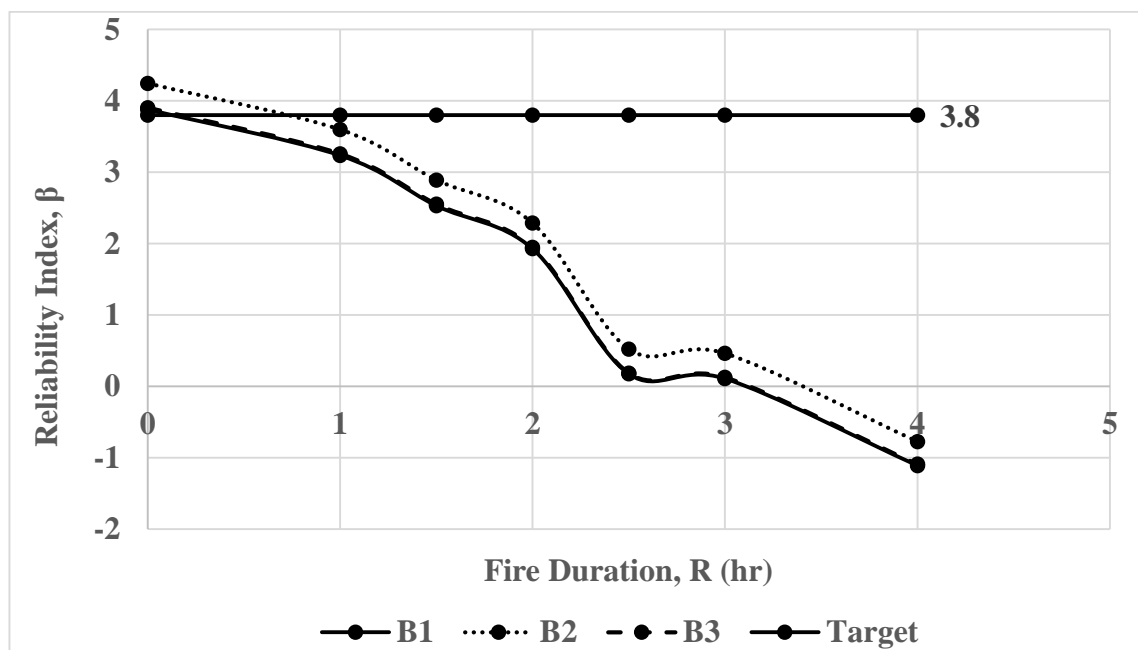


Figure 4.22: Reliability index, β of beams in computer room using FORM methods.

4.4.2 FOSM

The FOSM reliability analysis used the equation of reliability index provide in Eq. (3.12). In FOSM analysis of beam, the limit state equation, $G(X)$ for beam are divided into resistance effect, $R(X)$ and load effect, $L(X)$. Both the resistance equation and load equation are calculated in nominal value and considering the probabilistic data of random variables. The random variables in resistance equation and load equation are concrete compressive strength, f_{ck} and reinforcement yield strength, f_{yk} , beam width, b , beam depth, d and model uncertainty for resistance, K_R and model uncertainty for resistance, K_E . The probabilistic data of random variables are given in Table 3.8.

Similarly to the FORM analysis, both the resistance and load equation varies according to uncertain parameters such as the area of compression reinforcement, A_s and area of tension reinforcement, A_s' , concrete compressive strength, f_{ck} and reinforcement yield strength, f_{yk} , beam width, b and beam depth, d of the beam. Hence, in different fire room, the uncertain parameters change accordingly to the temperature change and in turn give different resistance and load equation. Appendix I showed the full steps of FOSM reliability analysis in classroom beam no 1 as a template for the other fire rooms and beams type.

The results of reliability index, β using FOSM method are tabulated in Table 4.16. The overall trend of beam reliability index, β in fire rooms are discovered to remain similar to the trend in FORM analysis. When observing the trend of the lower part of curves in classroom, laboratory and computer room, the reliability index, β during 2.5 hours to 3 hours showed minor decrease which only varies slightly from 0.07 to 0.27. From the results of FOSM analysis, it can be clearly seen that the overall reliability index, β during fire is higher than the reliability index generated from FORM analysis. In classroom, beam 3 failed at 1.5 hours with reliability index, β 3.19 whereas the result of the same beam at 1.5 hours in FORM analysis has a

measurable lower reliability index, β of 2.53. The comparison showed that FORM provides a more conservative analysis of beam reliability by giving a lower reliability index, β . Besides, graph of reliability index, β in different fire rooms are plotted and given in Figure 4.23, Figure 4.24, Figure 4.25, and Figure 4.26 in the order of classroom, office, laboratory and computer room.

Table 4.16: Reliability index, β of beams using FOSM method.

Fire Room	Beam No.	Reliability Index, β							
		Target	Fire Duration, R (hr)						
			0	1	1.5	2	2.5	3	4
Classroom	B3	3.8	4.4	3.85	<u>3.19</u>	2.58	0.36	0.28	-1.32
	B5	3.8	4.65	4.13	<u>3.49</u>	2.91	0.78	0.7	-0.83
Office	B1	3.8	4.36	4.38	3.98	<u>3.65</u>	3.34	3.1	2.57
	B2	3.8	4.67	4.66	4.3	3.97	<u>3.69</u>	3.42	2.95
	B3	3.8	4.5	4.4	4.01	<u>3.67</u>	3.3	3.09	2.6
Laboratory	B1	3.8	4.4	<u>3.7</u>	3	2.3	0.3	0.2	-2.7
	B2	3.8	4.67	4.09	<u>3.42</u>	2.78	0.78	0.71	-2.07
	B3	3.8	4.38	<u>3.78</u>	3.08	2.41	0.33	0.23	-2.67
Computer Room	B1	3.8	4.37	3.8	<u>3.1</u>	2.5	0.3	0.2	-1.63
	B2	3.8	4.67	4.41	<u>3.51</u>	2.91	0.82	0.74	-1.06
	B3	3.8	4.4	3.9	<u>3.2</u>	2.54	0.4	0.3	-1.62

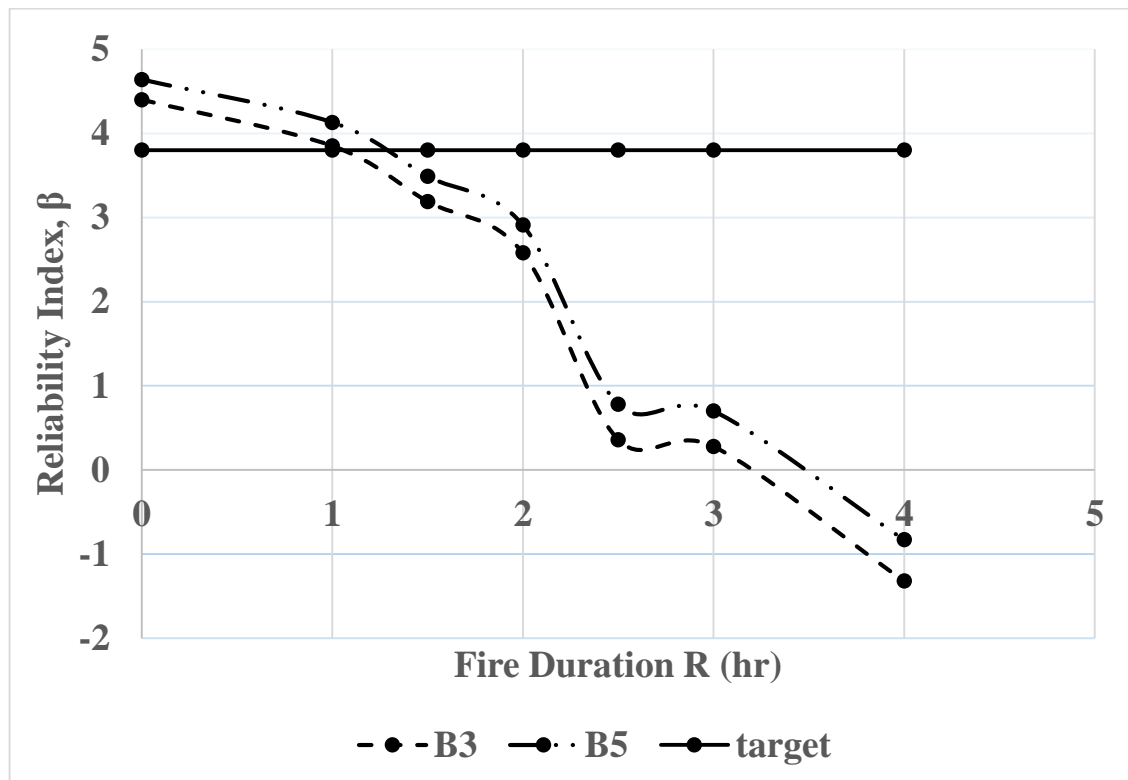


Figure 4.23: Reliability index, β of beams in classroom using FOSM methods.

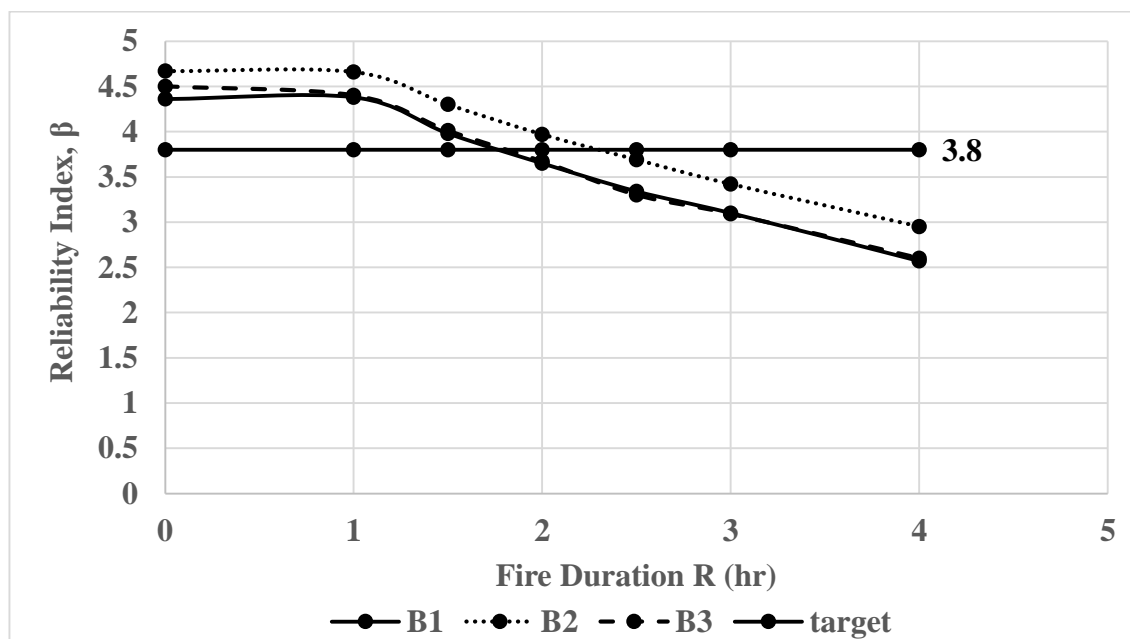


Figure 4.24: Reliability index, β of beams in office using FOSM methods.

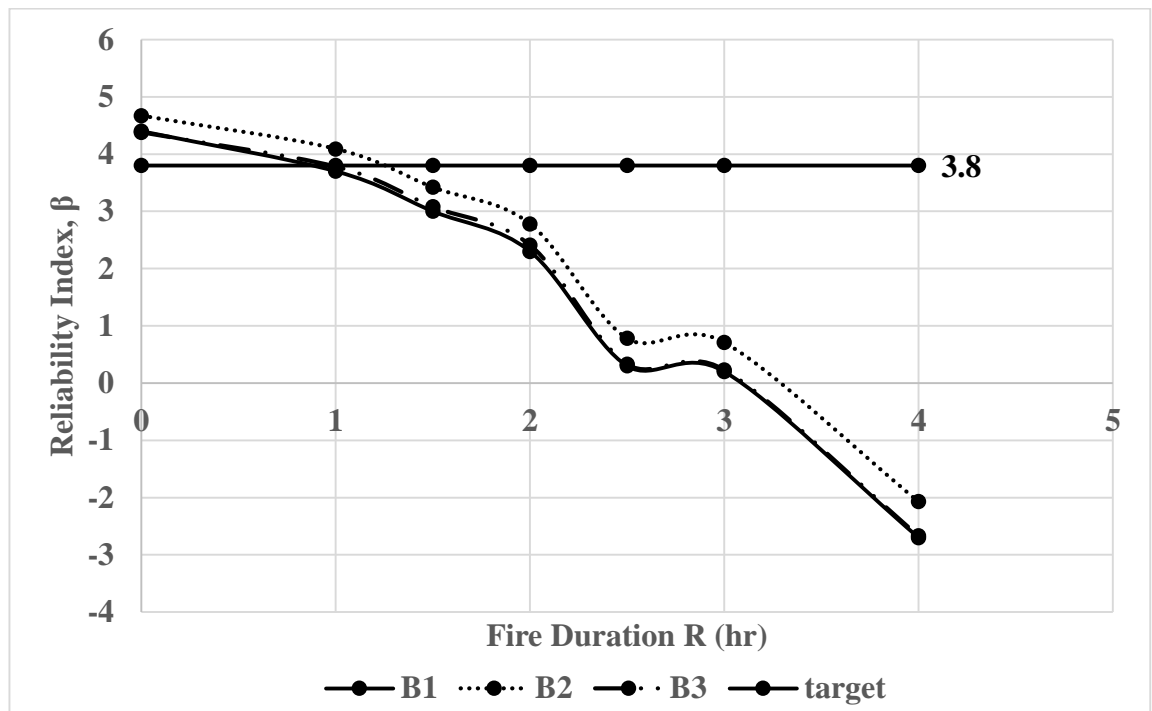


Figure 4.25: Reliability index, β of beams in laboratory using FOSM methods.

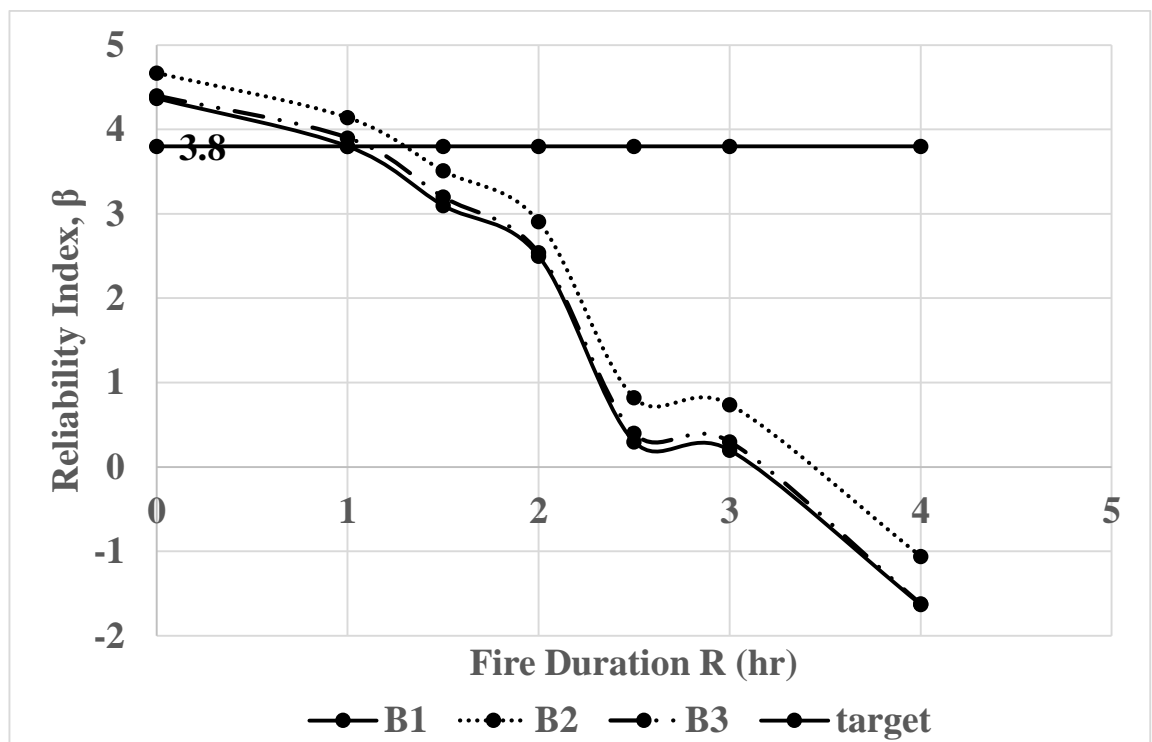


Figure 4.26: Reliability index, β of beams in computer room using FOSM methods.

CHAPTER 5

CONCLUSION

5.1 Conclusion

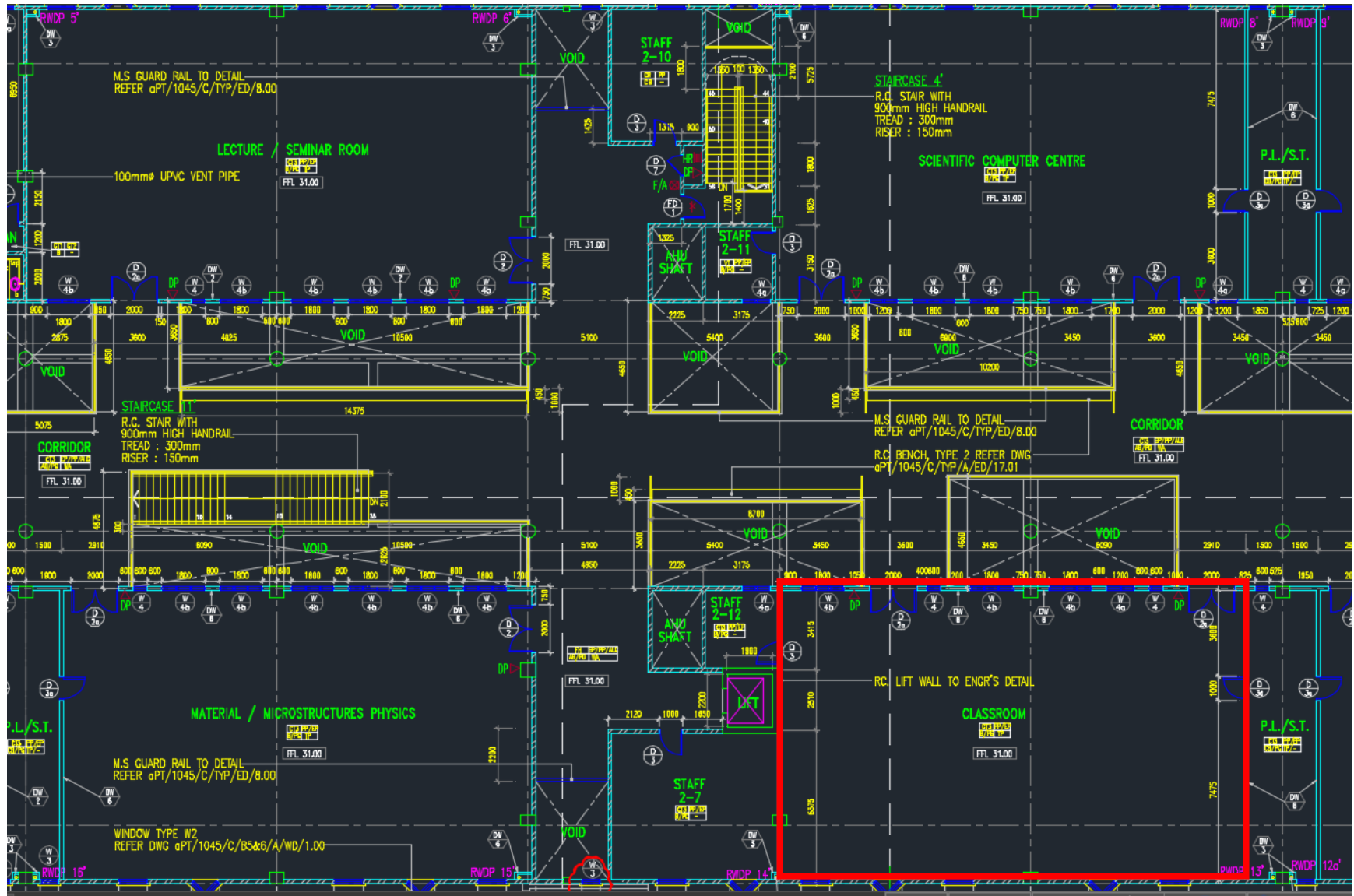
Fire accidents have shown that the building damage can be significant. The range of fire temperature, T_g in fire rooms is 27°C to 909.4°C (Cond. 1), 27°C to 1200°C (Cond.2). The range of fire load, Q_{fi} in different fire rooms is from 8.12 MJ/m^2 to 240.6 MJ/m^2 . When used the fire load combination ($1.0 G_k + 0.7 Q_k$) of EC2, It is seen that in fire conditions at limit fire load, the structural resistance is still higher, plastic hinges have not formed and thus collapse is avoided. The ultimate strength limit state equation was used to find the reliability index and the reliability index of the beams was found 4.0 and above. The significant variables found from the Matlab analysis was yield strength followed by the model uncertainty parameters, which affect the moment of resistance the most.

The method used in the calculation of reliability index by First-Order Second-Moment method (FOSM) whereas the calculation of reliability index by Matlab is First-Order Reliability method (FORM). The values of overall target reliability, β_t and the reliability index, β are compared in order to evaluate the structural performance under condition 2 where the fire is not restricted by the depletion of fuel. In EC 1990, target reliability, β_t is 3.8 for the ultimate limit state in non-fire condition for 50 years reference period. The beam is not able to sustain the load safely if the reliability index drops below 3.8. The results show that the target reliability reached

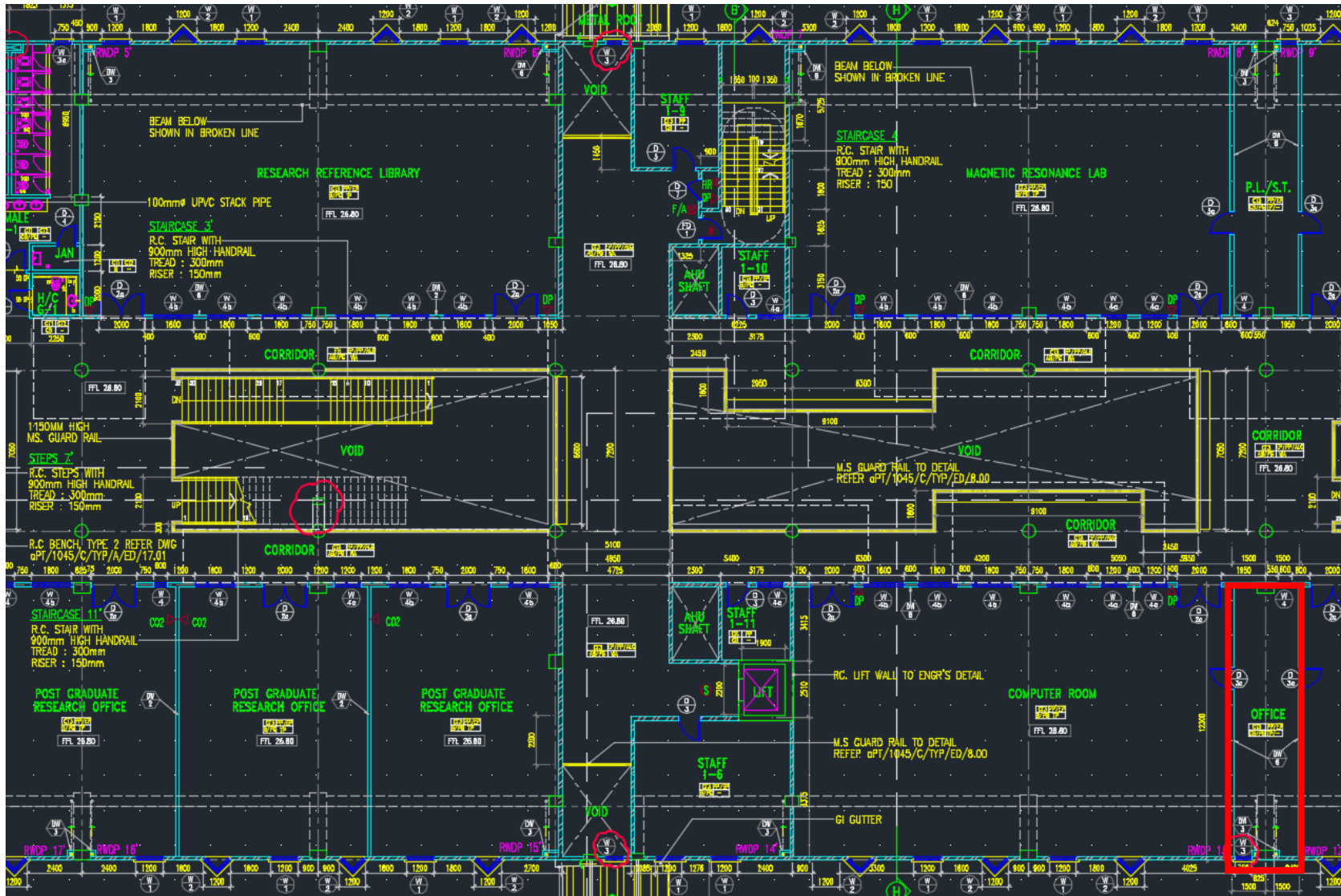
after 1 hour of fire using FOSM. The results of reliability index, β determined from FORM analysis drop below 3.8 started from 1 hour and 1.5 hours whereas FOSM analysis drop below 3.8 started from 1 hour, 1.5 hours, 2 hours and 2.5 hours. Hence, the overall results of reliability index concludes from FORM more conservative than FOSM. The results achieved are close to which has been published by EC2, Nowak & Eamon. In conclusion, the selected methodology is performing well in achieving the evaluation of structure reliability and this process can be used for the assessment of buildings affected by fire with duration of 1 to 4 hours.

Beams which fall under the target reliability, β_t are considered unsafety but the effects of the beam of failure on the performance of overall structure are remain unknown. Global analysis of the effects of fire on all the structural elements such as beams, columns, and slabs can be carried out using FORM and FOSM analysis methods proposed. The results from global analysis of structure provide a more holistic approach on the safety of structure under fire exposure. Further remediation actions can be proposed based on the findings from global analysis of structure.

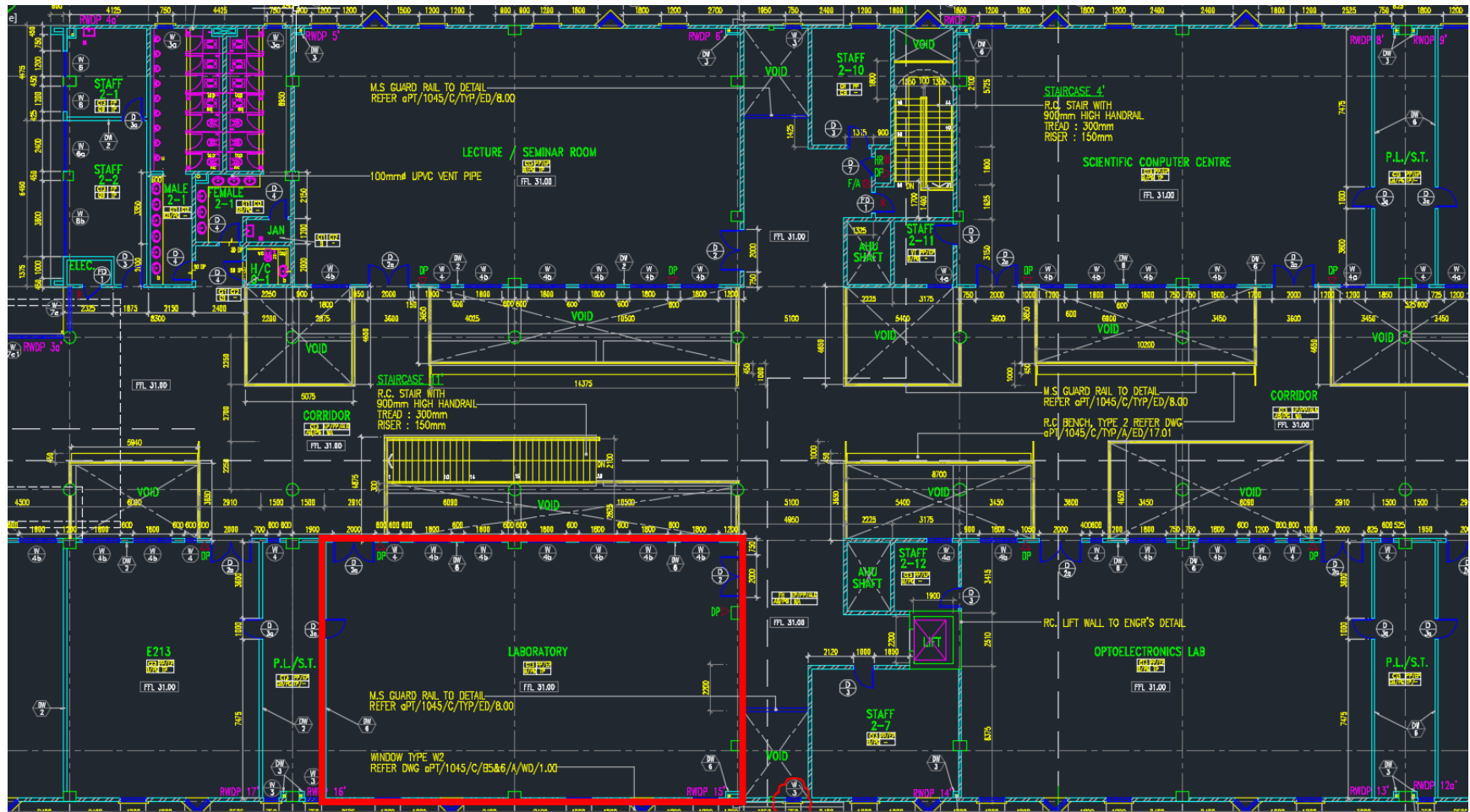
APPENDIX A (i) Location of classroom in AutoCad drawing.



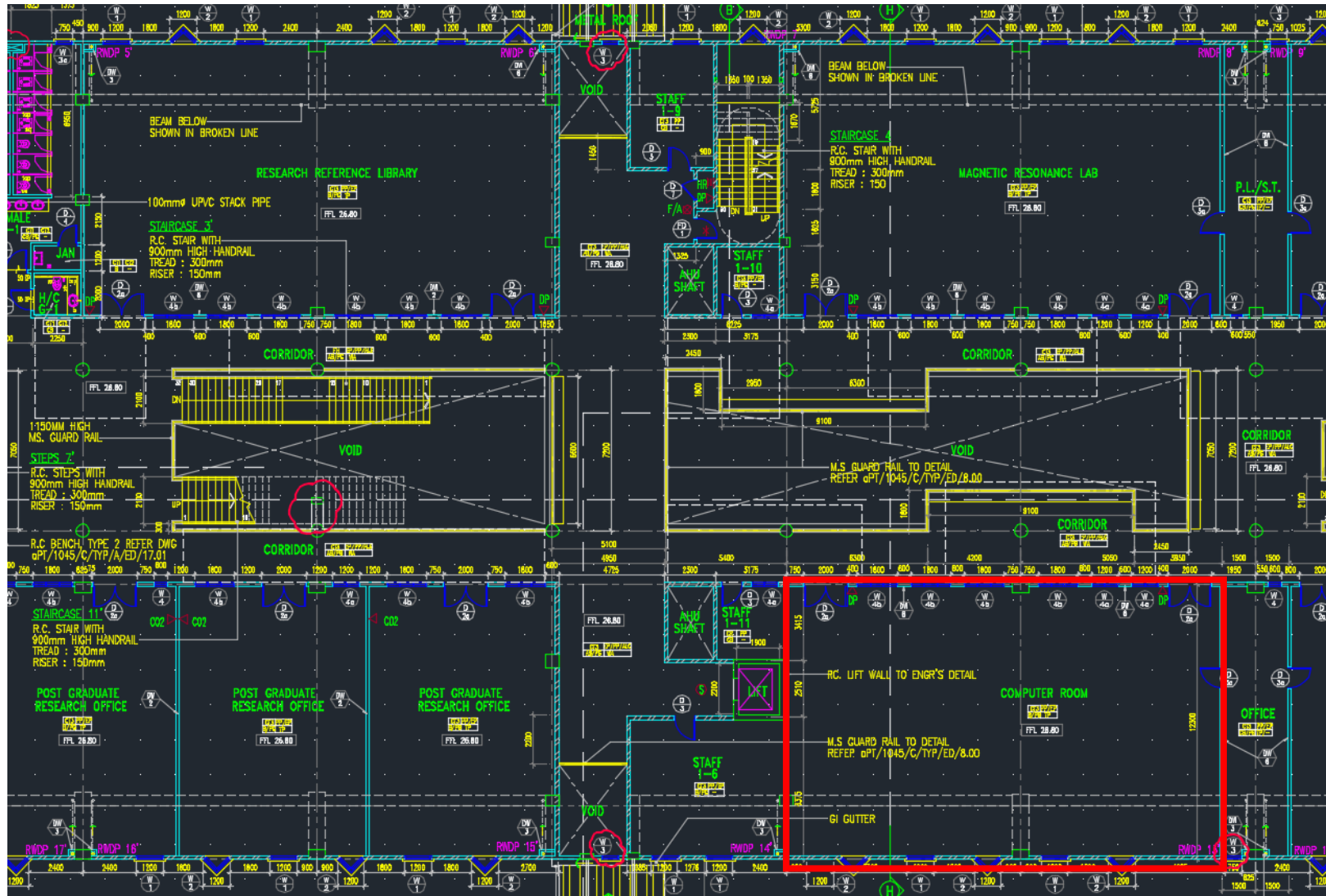
(ii) Location of office in AutoCad drawing.



(iii) Location of laboratory in AutoCad drawing.



(iv) Location of computer room in AutoCad drawing.



APPENDIX B: On-site pictures of fire rooms with types of fuel load available.



(a) classroom



(b) office



(c) laboratory



(d) computer room

APPENDIX C: Calculation of time and fire temperature in classroom at heating phase and decay phase.

(i) Given Information:

• Total weight or burning material in classroom, M (kg)	=3250 kg (wood material)
• Calorific Value, ΔH_c (MJ/kg)	= 17.5 MJ/kg (wood)
• Total floor area, A_f (m ²)	= 236.4 m ²
• Total room area, A_t (m ²)	= 694.7 m ²
• Total vertical opening area, A_v (m ²)	= 40.1 m ²
• Height if vertical opening area, H_v (m)	= 2 m
• Thermal conductivity, λ (W/mK)	= 2 W/mK
• Density, ρ (kg/m ³)	= 2300 kg/m ³
• Heat Capacity, c_p (J/kg ⁰ K)	= 900 J/kg ⁰ K

(ii) Heating Phase

1. Fire load, Q_{fi} (MJ/m ²)	$Q_{fi} = \frac{M \Delta H_c}{A_f} \quad (\text{From Eq. (4.6)})$ $= \frac{3250 \text{ kg} \times 17.5 \text{ MJ/kg}}{236.4 \text{ m}^2}$ $= 240.6 \text{ MJ/m}^2$
---	--

2. Opening Factor, O (m ²)	$O = \frac{A_v \sqrt{H}}{A_t} \quad (\text{From Eq. (4.4)})$ $= \frac{40.1 \text{ m}^2 \times \sqrt{2 \text{ m}}}{694.7 \text{ m}^2}$
--	---

$$= 0.0816 \text{ m}^{1/2}$$

3. Time to reach maximum fire temperature,

t_{\max} , (hr)

$$t_{\max} = \frac{0.2 \times 10^{-3} \times Q_{fi,t}}{0} \quad (\text{From Eq. (4.7)})$$

$$= \frac{0.2 \times 10^{-3} \times 240.6 \text{ MJ/m}^2}{0.0816 \text{ m}^{1/2}}$$

$$= 0.589 \text{ hr}$$

4. thermal inertia, b ($\text{J/m}^2\text{s}^{1/2}\text{K}$)

$$b = \sqrt{\lambda \rho c p} \quad (\text{From Eq. (4.5)})$$

$$= \sqrt{2 \frac{\text{W}}{\text{mK}} \times 2300 \text{ kg/m}^3 \times 900 \text{ J/kg}^0\text{K}}$$

$$= 2035 \text{ J/m}^2\text{s}^{1/2}\text{K}$$

5. Γ

$$\Gamma = \frac{(0/b)^2}{(0.04/1160)^2} \quad (\text{From Eq. (4.3)})$$

$$= \frac{(0.0816 \text{ m}^{1/2} / 2035 \text{ J/m}^2\text{s}^{1/2}\text{K})^2}{(0.04/1160)^2}$$

$$= 1.35$$

6. Maximum fictitious time, t_{\max}^* (hr)

$$t_{\max}^* = t_{\max} \times \Gamma \quad (\text{From Eq. (4.8)})$$

$$= 0.589 \text{ hr} \times 1.35$$

$$= 0.795 \text{ hr}$$

7. Maximum fire temperature, T_{\max} ($^{\circ}\text{C}$)

$$T_{\max} = 20 + 1325 (1 - 0.0324 e^{-0.2 t^*} -$$

$$0.204e^{-1.7t^*} - 0.472e^{-19t^*})$$

(From Eq. (4.1))

$$= 20 + 1325 (1 - 0.0324 e^{-0.2 \times 0.795 \text{ hr}} -$$

$$0.204e^{-1.7 \times 0.795 \text{ hr}} -$$

$$0.472e^{-19 \times 0.795 \text{ hr}})$$

$$= 909.4 \text{ }^{\circ}\text{C}$$

(iii) Decay Phase

At 1 hour fire duration:

1. Time to reach fire temperature, t , $t = 1 \text{ hr}$
(hr)

2. Fictitious time, t^* (hr)

$$t^* = t \times \Gamma$$

$$= 1 \text{ hr} \times 1.35$$

$$= 1.35 \text{ hr}$$

3. Decay temperature, T_{decay}

$$T_{\text{decay}} = T_{\text{max}} - 250 (3 - t^*_{\text{max}}) (t^* - t^*_{\text{max}})$$

(From Eq. (4.9))

$$= 909.4 \text{ }^{\circ}\text{C} - 250 (3 -$$

$$0.795 \text{ hr}) (1.35 \text{ hr} - 0.795 \text{ hr})$$

$$= 603.5 \text{ }^{\circ}\text{C}$$

APPENDIX D: Example Calculation of concrete temperature, T_c and steel reinforcement temperature, T_s in Classroom at 4 hours fire duration.

(i) Given Information:

-
- Time of fire duration, t (hr) = 4 hr
 - Fire temperature at 4 hours fire duration, T_{max} = 27 °C (Refer to Table 4.8)
 - Effective depth, d' (m) = 0.06
-

1. Temperature of steel reinforcement, $T_s = (1 - 0.0616 t^{-0.88}) T$ (From Eq. (4.10))

$$T_s = (1 - 0.0616 \times (4 \text{ hr})^{-0.88}) 27 \text{ °C}$$

$$= 26.51 \text{ °C}$$

2. Concrete temperature, T_c

$$T_c = (0.18 \ln \frac{t}{d'^2} - 0.81) T_s \text{ (From Eq. (4.11))}$$

$$= (0.18 \ln \frac{(4 \times 60) \text{ min}}{(0.06 \text{ m})^2} - 0.81) 26.51 \text{ °C}$$

$$= 31.53 \text{ °C}$$

APPENDIX E: Example Calculation of Moment Resistance, $M_{R,fi}$ at different fire duration of Beam No. 3 in Classroom.

(i) Given Information:

• Beam width, b	375 mm
• Beam effective depth, d	740 mm
• Concrete compressive strength, f_{ck}	24 MPa
• Reinforcement yield strength, f_{yk}	414 MPa
• Area of tension reinforcement, A_s	12880 mm ² (8H16)
• Area of compression reinforcement, A_s'	11340 mm ² (6H20)
• Bottom and side cover, d'	60 mm
• Total Fire Load, Q_{fi}	240.6 MJ/m ²
• Opening Factor, O	0.08163 m ^{1/2}

(ii) Part 1: Moment resistance at ambient condition, $M_{R,ambient}$

1. Stress block depth, x

$$\begin{aligned}
 x &= (A_s - A_s') * f_{yk} / (0.84 * f_{ck} * b) \\
 &= ((12880 - 11340) \text{ mm}^2 * 414 \text{ MPa}) / \\
 &\quad (0.84 * 24 \text{ MPa} * 375 \text{ mm}) \\
 &= 83.34 \text{ mm}
 \end{aligned}$$

2. Concrete compressive force, $F_{cc} = 0.567 f_{ck} * b * 0.8x$

$$F_{cc} = 0.567 * 24 \text{MPa} * 375 \text{mm} * 0.8 * 83.34 \text{mm}$$

$$= 340.23 \text{ kN}$$

3. Lever arm, Z

$$Z = d - (0.8x/2)$$

$$= 740 \text{mm} - ((0.8 * 83.34 \text{mm})/2)$$

$$= 706.66 \text{ mm}$$

4. Reinforcement tensile force, F_{sc}

$$F_{st} = 0.87 * f_{yk} * A_s'$$

$$= 0.87 * 414 \text{ MPa} * 11340 \text{ mm}^2$$

$$= 4694.76 \text{ kNm}$$

5. Lever arm, Z_l

$$Z_l = d - d'$$

$$= 800 \text{mm} - 60 \text{mm}$$

$$= 740 \text{ mm}$$

6. Moment resistance at ambient condition, $M_{R, \text{ambient}}$

$$M_{R, \text{ambient}} = (F_{cc} * Z) + (F_{sc} * Z_l)$$

$$= (340.23 \text{ kN} * 706.66 \text{mm}) + (4694.76 \text{kN} * 740 \text{mm})$$

$$= 3017.8 \text{ kNm}$$

(iii) Part 2: Moment resistance at fire condition, $M_{R,fi}$

-
- | | |
|--|--|
| 1. Reduced beam width, b_{fi} | $b_{fi} = d - d' - d'$ $= 375\text{mm} - 60\text{mm} - 60\text{mm}$ $= 255\text{mm}$ |
| 2. Reduced beam depth, d_{fi} | $d_{fi} = d$ $= 740$ |
| 3. Time to reach maximum fire temperature, t_{max} (hr) | $t_{max} = \frac{0.2 \times 10^{-3} \times Q_{fi,t}}{0}$ $= \frac{0.2 \times 10^{-3} \times 240.6}{0.08163}$ $= 0.59\text{hr}$ |
| 4. Maximum fire temperature, T_{max} (°C) | $T_{max} = 20 + 1325 (1 - 0.0324 e^{-0.2 t^*} - 0.204 e^{-1.7 t^*} - 0.472 e^{-19 t^*})$ $= 909.41 \text{ } ^\circ\text{C}$ |
| 5. Concrete surface temperature, T_s (°C) | $T_s = (1 - 0.0616 t_{max}^{-0.88}) T_{max}$ $= 820.3 \text{ } ^\circ\text{C}$ |
| 6. Concrete temperature, T_c (°C) | $T_c = (0.18 \ln \frac{t_{max}}{d'^2} - 0.81) T_s$ $= 693 \text{ } ^\circ\text{C}$ |
| 7. Concrete compressive strength reduction factor at T_{max} , $k_{fc,Tmax}$ | $0.3105 \text{ (Interpolation of Figure 2.9)}$ |

8. Concrete compressive strength, f_{ck}
- $$f_{ck} = f_{ck,20}^0 * k_{fc,Tmax}$$
- $$= 24 \text{ MPa} * 0.3105$$
- $$= 7.45 \text{ MPa}$$
9. Reinforcement yield strength reduction factor at T_{max} , $k_{fy,Tmax}$
- 0.1164 (Equation from Table 2.4)
10. Reinforcement yield strength, f_{yk}
- $$f_{yk} = f_{yk,20}^0 * k_{fy,Tmax}$$
- $$= 414 \text{ MPa} * 0.1164$$
- $$= 48.2 \text{ MPa}$$
11. Stress block depth, x
- $$x = ((A_s - A_s') * f_{yk}) / (0.84 * f_{ck} * b)$$
- $$= ((12880 - 11340) \text{ mm}^2 * 48.2 \text{ MPa}) /$$
- $$(0.84 * 7.45 \text{ MPa} * 255 \text{ mm})$$
- $$= 45.97 \text{ mm}$$
12. Concrete compressive force, F_{cc}
- $$F_{cc} = 0.567 f_{ck} * b * 0.8x$$
- $$= 0.567 * 7.45 \text{ MPa} * 255 \text{ mm} * 0.8 * 45.97 \text{ mm}$$
- $$= 39.61 \text{ kN}$$

13. Lever arm, Z
- $$Z = d - (0.8x/2)$$
- $$= 740\text{mm} - ((0.8 * 122.56\text{mm})/2)$$
- $$= 691 \text{ mm}$$
14. Reinforcement tensile force, F_{st}
- $$F_{st} = 0.87 * f_{yk} * A_s'$$
- $$= 0.87 * 48.2 \text{ MPa} * 11340 \text{ mm}^2$$
- $$= 475.53 \text{ kN}$$
15. Lever arm, Z_1
- $$Z_1 = d - d'$$
- $$= 800\text{mm} - 60\text{mm}$$
- $$= 740 \text{ mm}$$
16. Moment resistance at afire condition, $M_{R,fi}$
- $$M_{R,fi} = (F_{cc} * Z) + (F_{sc} * Z_1)$$
- $$= (39.61 \text{ kN} * 691 \text{ mm}) + (475.53 \text{ kN} * 740\text{mm})$$
- $$= 351.95 \text{ kNm}$$
-

(iv) Concrete compressive strength, f_{ck} and reinforcement yield strength, f_{yk} of classroom Beam 2 at different fire duration.

By following step 7 to step 10 in (iii) Part 2, the results are tabulated in Table below.

Fire Duration, R (hr)	Concrete Temperature (°C)	k f_{yk}	f_{yk} (MPa)	k f_{ck}	f_{ck} (MPa)
0.19	357.1	0.755	312.8	0.792	19.0
0.21	385.0	0.719	297.8	0.735	17.6
0.59	693.0	0.116	48.2	0.310	7.4
1	532.2	0.494	204.6	0.551	13.2
1.16	442.2	0.645	267.0	0.686	16.4
1.5	223.75	0.876	362.7	0.926	22.2
2	27.7	1	414	1	24
2.5	29.0	1	414	1	24
3	29.9	1	414	1	24
4	31.5	1	414	1	24

APPENDIX F: Table of concrete compressive strength, f_{ck} and reinforcement yield strength, f_{yk} of different fire room at different fire duration, R.

Fire Duration, R (hr)	Classroom		Office		Laboratory		Computer Room	
	f_{ck} (MPa)	f_{yk} (MPa)	f_{ck} (MPa)	f_{yk} (MPa)	f_{ck} (MPa)	f_{yk} (MPa)	f_{ck} (MPa)	f_{yk} (MPa)
0	24	414	24	414	24	414	24	414
1	13.24	204.63	19.1	252.42	24	414	24	414
1.5	22.23	362.77	13.19	203.31	24	414	24	414
2	24	414	13.01	198.46	24	414	24	414
2.5	24	414	13.21	203.72	24	414	24	414
3	24	414	13.64	215.42	24	414	24	414
4	24	414	14.96	251.21	24	414	24	414

APPENDIX G: Table of Concrete compressive strength, f_{ck} and reinforcement yield strength, f_{yk} of different fire room at different fire duration, R during continuous fire growth.

Fire Duration, R (hr)	Classroom		Office		Laboratory		Computer Room	
	f_{ck} (MPa)	f_{yk} (MPa)	f_{ck} (MPa)	f_{yk} (MPa)	f_{ck} (MPa)	f_{yk} (MPa)	f_{ck} (MPa)	f_{yk} (MPa)
0	24	414	24	414	24	414	24	414
1	22.9	377.35	23.9	413.4	22.8	373.4	22.9	376.4
1.5	20.9	340.6	23.2	386.8	20.6	335.3	20.8	339.4
2	19.2	312.1	22.4	366.0	18.9	305.6	19.2	310.7
2.5	17.9	240.0	21.4	349.3	17.2	239.2	17.7	239.8
3	16.1	237.9	20.6	335.4	15.4	237.1	15.9	237.7
4	13.2	204.0	19.3	312.7	12.4	182.3	13.0	198.9

APPENDIX H: FORM reliability analysis in classroom beam no 1 at 1 hour fire duration.

(i) Given Information:

-
- Area of compression reinforcement, A_{sn} = 12880 mm²
 - Area of tension reinforcement, $A_{s'n}$ = 11340 mm²
 - Beam width, b_n = 375 mm
 - Beam depth, d_n = 740 mm
 - Cover depth, d'_n = 60 mm

At 1 hour (Refer Appendix E):

- Concrete compressive strength, f_{ckn} = 22.94 MPa
- Reinforcement yield strength, f_{ykn} = 377.35 MPa

Note: X_n = nominal value ; X = probabilistic value.

(ii) gfun_z.m File:

1. Define limit state equation, $G(b, d, f_{ck}, f_{yk}, K_R, K_E)$
 $G(X_n)$

2. Define resistance equation. Resistance = $(F_{cc} + F_{sc}) K_R$

$$= (f_{ckn} b_n (0.8x + 0.87 f_{ykn} A_{s'n} - Z_1) K_R$$

$$\text{After substitute } x = \frac{(A_s - A_{s'}) f_{yk}}{0.85 f_{ck} b}$$

New Resistance equation become :

$$\text{Resistance} = ((821.82 f_{ykn} dn - 95575.16 \frac{f_{ykn} f_{ykn}}{f_{ckn} bn})$$

$$+ (9865.8 f_{ykn} dn - 591948 f_{ykn}) K_R$$

3. Define load equation.

$$\text{Load} = (F_{cc} + F_{sc}) K_E$$

$$= (f_{ck} b 0.8x Z + 0.87 f_{yk} A_s' Z_l) K_E$$

$$\text{After substitute } x = \frac{(A_{sn} - A_s' n) f_{ykn}}{0.85 f_{ckn} bn}$$

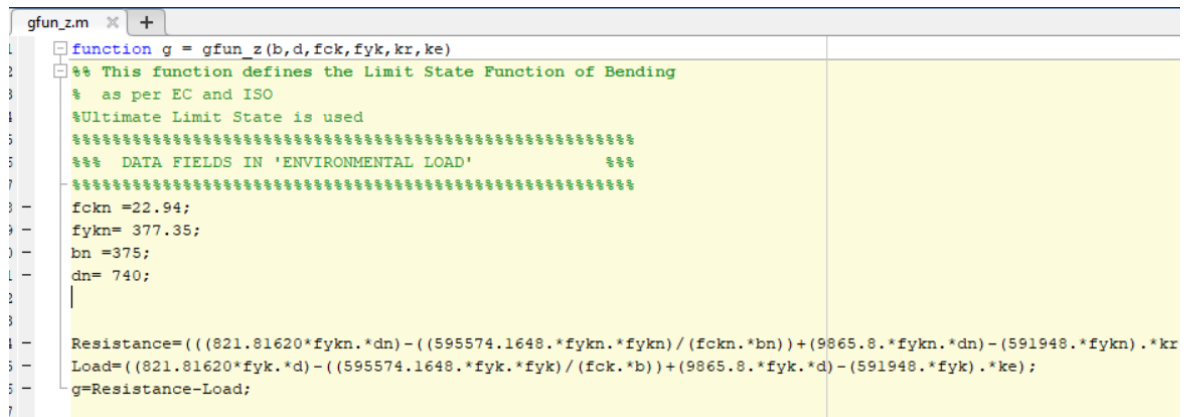
New Load equation become :

$$\text{Load} = ((821.82 f_{yk} d - 595575.16 \frac{f_{yk} f_{yk}}{f_{ck} b})$$

$$+ (9865.8 f_{yk} d - 591948 f_{yk}) K_E$$

4. Screenshot of gfun_z.m file in

MATLAB:



```

function g = gfun_z(b,d,fck,fyk,kr,ke)
% This function defines the Limit State Function of Bending
% as per EC and ISO
%Ultimate Limit State is used
%%%%%%%%%%%%%%%%%%%%%%%%%%%%%%%%%%%%%%%%%%%%%%%%%%%%%%%%%%%%%%%%%%%%%%%%%%%%%%
% DATA FIELDS IN 'ENVIRONMENTAL LOAD' %
%%%%%%%%%%%%%%%%%%%%%%%%%%%%%%%%%%%%%%%%%%%%%%%%%%%%%%%%%%%%%%%%%%%%%%%%%%%%%%
fckn = 22.94;
fykn = 377.35;
bn = 375;
dn = 740;

Resistance = ((821.81620*fykn.*dn) - ((595574.1648.*fykn.*fykn)/(fckn.*bn)) + (9865.8.*fykn.*dn) - (591948.*fykn).*kr
Load = ((821.81620*fyk.*d) - ((595574.1648.*fyk.*fyk)/(fck.*b)) + (9865.8.*fyk.*d) - (591948.*fyk).*ke);
g = Resistance - Load;

```

(iii) Inputfile_z.m File:

5. Define all random variables , X_n Probdata.name = 'b'
in load equation.

'd'

'f_{ck}'

'f_{yk}'

'f_{ck}'

'K_R'

'K_E'

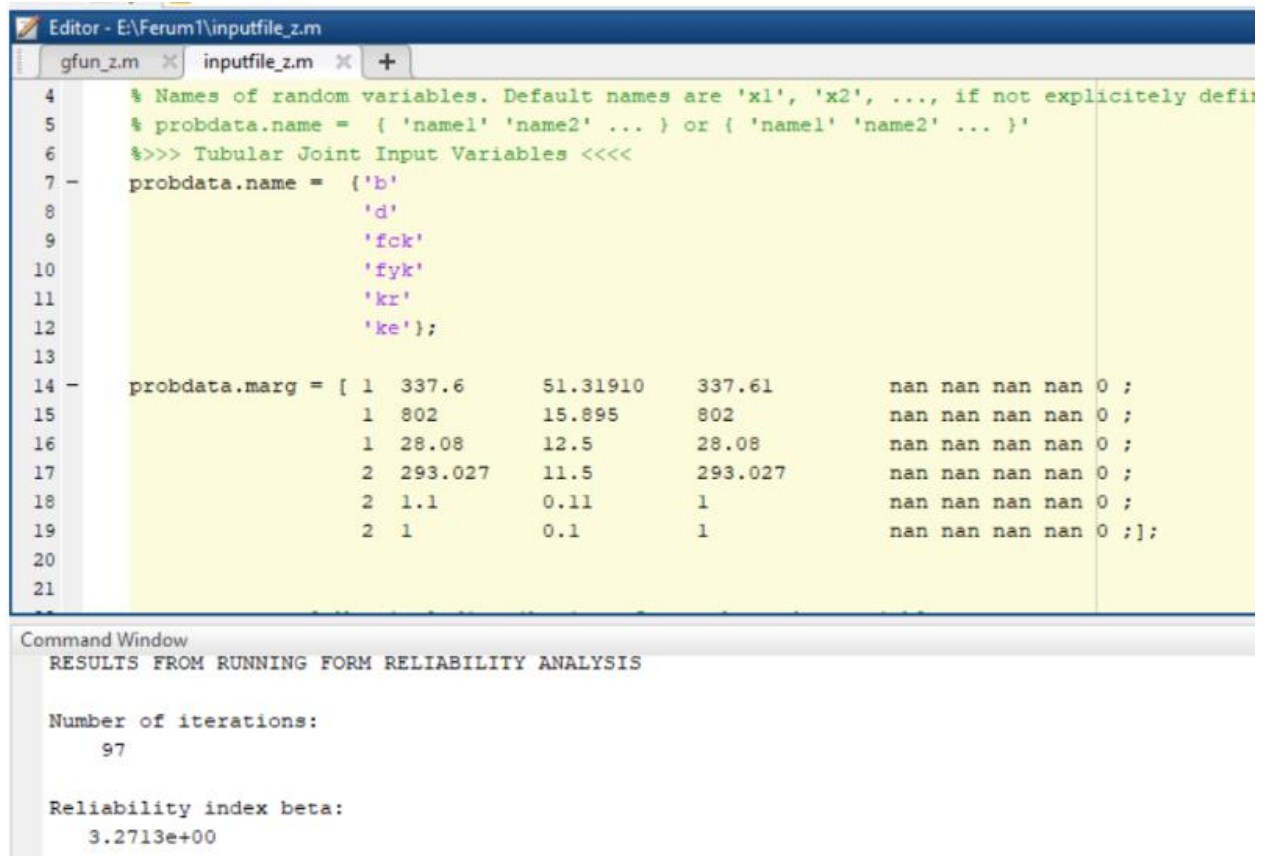
6. Define probabilistic data.
(in order of random variables
defined above.)

From left to right: distribution type, mean, μ ,
standard deviation, σ , mean, μ .

{				
2	28.83	659.7	28.83	
2	659.7	802	659.7	
2	28.08	12.5	28.08	
1	283.03	11.5	283.03	
2	1.1	0.11	1.1	
2	1	0.1	1	}

7. Run MATLAB FORM analysis
in inputfile_z.m

8. Screenshot of inputfile_z.m file in MATLAB:



The screenshot shows the MATLAB Editor window with the file 'inputfile_z.m' open. The script defines random variables and their correlations for a FORM reliability analysis. Below the script, the Command Window displays the results of the analysis.

```

4 % Names of random variables. Default names are 'x1', 'x2', ..., if not explicitly defini
5 % probdata.name = { 'name1' 'name2' ... } or { 'name1' 'name2' ... }'
6 %>>> Tubular Joint Input Variables <<<<
7 probdata.name = {'b'
8                  'd'
9                  'fck'
10                 'fyk'
11                 'kr'
12                 'ke'};
13
14 probdata.marg = [ 1  337.6      51.31910    337.61      nan nan nan nan 0 ;
15                  1  802        15.895       802        nan nan nan nan 0 ;
16                  1  28.08      12.5         28.08      nan nan nan nan 0 ;
17                  2  293.027    11.5         293.027    nan nan nan nan 0 ;
18                  2  1.1        0.11        1          nan nan nan nan 0 ;
19                  2  1          0.1         1          nan nan nan nan 0 ;];
20
21

```

Command Window

```

RESULTS FROM RUNNING FORM RELIABILITY ANALYSIS

Number of iterations:
    97

Reliability index beta:
    3.2713e+00

```

9. Derived reliability index, β value and results tabulated in
Table 4.16.

APPENDIX I: FOSM reliability analysis in classroom beam no 1 at 1 hour fire duration.

(i) Given Information:

-
- Area of compression reinforcement, A_{sn} = 12880 mm²
 - Area of tension reinforcement, $A_{s'n}$ = 11340 mm²
 - Beam width, b_n = 375 mm
 - Beam depth, d_n = 740 mm
 - Cover depth, d'_n = 60 mm

At 1 hour (Refer Appendix E):

- Concrete compressive strength, f_{ckn} = 22.94 MPa
- Reinforcement yield strength, f_{ykn} = 377.35 MPa

- Probabilistic data of random variables refer to Table 3.8:

Random Variables	Unit	Mean, μ	Standard Deviation, σ
b	mm	300	5
d	mm	650	5
f_{ck}	MPa	28.85	12.5
f_{yk}	MPa	293.03	11.5
K_R	-	1.1	0.11
K_E	-	1	0.1

1. Define limit state equation, $G(X_n)$ $G(b, d, f_{ck}, f_{yk}, K_R, K_E) = R(X) - L(X)$

2. Define resistance equation, $R(X)$

$$\text{Resistance} = F_{cc} + F_{sc}$$

$$= f_{ckn} b n 0.8 x Z + 0.87 f_{ykn} A_{s'n}$$

$$Z_1$$

$$\text{After substitute } x = \frac{(A_{sn} - A_{s'n}) f_{ykn}}{0.85 f_{ckn} b n}$$

New Resistance equation become :

$$\text{Resistance} = (821.82 f_{ykn} d n -$$

$$59575.16 \frac{f_{ykn} f_{ykn}}{f_{ckn} b n})$$

$$+ (9865.8 f_{ykn} d n - 591948 f_{ykn})$$

$$= (821.82 \times 377.35 \text{ MPa} \times 740 \text{ mm}) -$$

$$59575.16 \left(\frac{377.35 \text{ MPa} \times 377.35 \text{ MPa}}{22.94 \text{ MPa} \times 375 \text{ mm}} \right) +$$

$$(9865.8 \times 377.35 \text{ MPa} \times 740 \text{ mm}) -$$

$$(591948 \times 377.35 \text{ MPa})$$

$$= (2751.2 \text{ kNm}) K_R$$

3. Define mean of resistance equation, $\mu_R = (2751.2 \text{ kNm}) \mu_{KR}$

$$\mu_R$$

$$= 2751.2 \text{ kNm} \times 1.1$$

$$= 3026.32 \text{ kNm}$$

4. Define standard deviation
of resistance equation, σ_R

$$\begin{aligned}\sigma_R &= (2751.2 \text{ kNm}) \sigma_{KR} \\ &= 2751.2 \text{ kNm} \times 0.11 \\ &= 3026.32 \text{ kNm}\end{aligned}$$

5. Define load equation.

$$\begin{aligned}\text{Load} &= F_{cc} + F_{sc} \\ &= f_{ck} b 0.8x Z + 0.87 f_{yk} A_s' Z_1\end{aligned}$$

$$\text{After substitute } x = \frac{(A_s - A_s') f_{yk}}{0.85 f_{ck} b}$$

New Load equation become :

$$\begin{aligned}\text{Load} &= ((821.82 f_{yk} d - 595575.16 \frac{f_{yk} f_{yk}}{f_{ck} b}) \\ &\quad + (9865.8 f_{yk} d - 591948 f_{yk})) K_E\end{aligned}$$

6. Define mean of load equation,
 μ_L

$$\begin{aligned}\mu_L &= \\ &((821.82 f_{yk} d - 595575.16 \frac{f_{yk} f_{yk}}{f_{ck} b}) + \\ &(9865.8 f_{yk} d - 591948 f_{yk})) K_E \\ &= ((821.82 \times 293.03 \text{ MPa} \times 650 \text{ mm}) - \\ &(595575.16 \times \frac{293.03 \text{ MPa} \times 293.03 \text{ MPa}}{25.85 \text{ MPa} \times 300 \text{ mm}}) + \\ &(9865.8 \times 293.03 \text{ MPa} \times 650 \text{ mm}) - \\ &(591948 \times 293.03 \text{ MPa})) \times 1 \\ &= 1855.59 \text{ MPa}\end{aligned}$$

7. Define standard deviation
of load equation, σ_L

$$\sigma_L =$$

$$((821.82 f_{yk} d - 595575.16 \frac{f_{yk} f_{yk}}{f_{ck} b}) +$$

$$(9865.8 f_{yk} d - 591948 f_{yk})) K_E$$

$$= ((821.82 \times 11.5 \text{ MPa} \times 5 \text{ mm}) -$$

$$(595575.16 \times \frac{11.5 \text{ MPa} \times 11.5 \text{ MPa}}{12.5 \text{ MPa} \times 5 \text{ mm}}) +$$

$$(9865.8 \times 11.5 \text{ MPa} \times 5 \text{ mm}) -$$

$$(591948 \times 11.5 \text{ MPa})) \times 0.1$$

$$= -0.7453 \text{ MPa}$$

8. Reliability index,

$$\beta = \frac{\sum_{i=1}^n a_i \mu x_i}{\sqrt{\sum_{i=1}^n (a_i \sigma x_i)^2}}$$

$$\beta = \frac{\mu_R - \mu_L}{\sqrt{\sigma_R^2 + \sigma_L^2}}$$

$$= \frac{3026.32 \text{ kNm} - 1855.59 \text{ MPa}}{\sqrt{(302.63 \text{ kNm})^2 + (-0.7453 \text{ MPa})^2}}$$

$$= \frac{1170.73 \text{ MPa}}{\sqrt{91585.47 \text{ MPa}^2}}$$

$$= 3.85$$

REFERENCES

1. ACI 216. (1994). Guide for determining the fire endurance of concrete elements. Farmington Hills, Mich. American Concrete Institute.
2. ACI 318. (2011). Building code requirements for structural concrete (ACI 318-11). ACI Committee 318, Farmington Hills, MI, USA.
3. Buchanan, A. H. & Abu, A. K., 2017. *Structural Design For Fire Safety*. Second edition ed. Chichester: John Wiley & Sons, Ltd.
4. Balogh, T. and Vigh, L. (2016). Complex and comprehensive method for reliability calculation of structures under fire exposure. *Fire Safety Journal*, 86, pp.41-52.
5. Breitung, K. (1984). Asymptotic approximation for multi-normal Integrals. *Journal of Engineering Mechanics, ASCE*, 110(3), 357–366.
6. EC 1990. (2002). Eurocode 0: Basis of structural design. European Committee for Standardization CEN.
7. EC 1991-1-1. (2002). Eurocode 1: Actions on structures – Part 1-1: General actions – Densities, self-weight, imposed loads for buildings. European Committee for Standardization CEN.
8. EC 1991-1-2. (2002). Eurocode 1: Actions on structures – Part 1-2: General actions – Actions on structures exposed to fire. European Committee for Standardization CEN.
9. EC 1992-1-1. (2004). Eurocode 2: Design of concrete structures – Part 1-1: General rules and rules for buildings. European Committee for Standardization CEN, Brussels, Belgium.
10. EC 1992-1-2. (2004). Eurocode 2: Design of concrete structures—part 1-2: General rules—Structural fire design. European Committee for Standardization CEN.

11. Erdem, H. (2009). Nominal moment capacity of box reinforced concrete beams exposed to fire. *Turkish journal of engineering and environmental sciences* 33: 31–44.
12. Guo. Q. R. (2015) Structural reliability assessment under fire. Doctoral thesis, University of Michigan.
13. Halдар, A., and Mahadevan, S. (2000). Reliability assessment using stochastic finite element analysis, John Wiley and Sons, New York.
14. Hasofer, A. M. (2012). *Risk Analysis in Building Fire Safety Engineering*. Oxford: Routledge.
15. Holický, M., Sýkora, M. (2010). Stochastic models in analysis of structural reliability: Proc. Symp stochastic models in reliability engineering, life sciences and operation management. Beer Sheva, Israel.
16. ISO-834. (1975). Fire resistance tests elements of building construction part 1-9, *International Standards Organization*, Geneva.
17. JCSS. (2007). Probabilistic model code. The joint committee on structural safety.
18. Kodur, V. and Dwaikat, M. (2008). A numerical model for predicting the fire resistance of reinforced concrete beams. *Cement and Concrete Composites*, 30(5), pp.431-443.
19. Molken, T., Van Coile, R., Gernay, R. (2017). Assessment of damage and residual load bearing capacity of a concrete slab after fire: applied reliability-based methodology.
20. Sudret, B., Der Kiureghian, A. (2000). Stochastic finite element methods and reliability. *A state-of-the-art report*, Department of Civil & Environmental Engineering University of California, Berkeley.
21. Van Coile, R., Bisby, L. (2017). Optimum investment in structural fire safety: case-study on the applicability of deflection-based failure criteria. In applications of structural fire engineering (ASFE'17). Manchester.
22. Van Coile, R. (2015). Reliability-based decision making for concrete elements exposed to fire. Doctoral thesis, Ghent University.

23. Van Coile, R., Balomenos, G. and Pandey, M. (2018). *Efficient method for probabilistic fire safety engineering*. [online] Biblio.ugent.be. Available at: <https://biblio.ugent.be/publication/8039239> [Accessed 8 Jul. 2018].
24. Van Coile, R., Caspeelee, R., Taerwe, L. (2013). The mixed lognormal distribution for a more precise assessment of the reliability of concrete slabs exposed to fire. Proceedings of the 2013 European safety and reliability conference (ESREL). 29/0902/10, Amsterdam, Netherlands, 2693-2699.
25. Veljkovic, M., Dimova, S., Sousa, M., Nikolova, B., Poljanšek, M., Pinto, A., Weynand, K., Dubinã, D., Landolfo, R., Simões da Silva, L., Simões, R., Wald, W., Jaspert, J., Vila Real, P. and Gervásio, H. (2015). *Eurocodes, background & applications*. Luxembourg: Publications Office.